Rockefeller University
Digital Commons @ RU

Student Theses and Dissertations

2011

Spatial Control of CDC42 Activation Regulates Cell Width and Growth Zone Formation

Felice D. Kelly

Follow this and additional works at: http://digitalcommons.rockefeller.edu/student_theses_and_dissertations

Part of the Life Sciences Commons

Recommended Citation

Kelly, Felice D., "Spatial Control of CDC42 Activation Regulates Cell Width and Growth Zone Formation" (2011). *Student Theses and Dissertations.* Paper 130.

This Thesis is brought to you for free and open access by Digital Commons @ RU. It has been accepted for inclusion in Student Theses and Dissertations by an authorized administrator of Digital Commons @ RU. For more information, please contact mcsweej@mail.rockefeller.edu.

SPATIAL CONTROL OF CDC42 ACTIVATION REGULATES CELL WIDTH AND GROWTH ZONE FORMATION

A Thesis Presented to the Faculty of

The Rockefeller University

in Partial Fulfillment of the Requirements for

the Äegree of DoctÏr of PhilÏsophy

by

Felice D. Kelly

June 2011

© Copyright by Felice D. Kelly 2011

Spatial control of Cdc42 activation regulates cell width and growth zone formation

Felice D. Kelly, Ph.D.
The Rockefeller University 2011

The fission yeast *Schizosaccharomyces pombe* is a rod-shaped cell that grows by linear extension at the cell tips, with a nearly constant width throughout the cell cycle. This simple geometry makes it a good system to study the control of cellular dimensions. Here I used the width of the cell as a model for the control of growth zone size.

To identify genes that influence cell size I carried out a near-genome-wide screen for mutants wider than wild-type cells. I found eleven deletion mutants that were wider; seven of the deleted genes are implicated in the control of the small GTPase Cdc42. Further analyses showed two different pathways are involved: one is defined by the Cdc42 guanine-nucleotide exchange factor (GEF) Scd1 and the second by the GTPase activating protein (GAP) Rga4. Deletions of *rga4* and *scd1* had additive effects on cell width, and the proteins localized independently of one another, with Rga4 located at the cell sides and Scd1 at the cell tips. Delocalization and ectopic retargeting experiments showed that these localizations are crucial for Rga4's and Scd1's roles in determining cell width. I propose that the GAP Rga4 and the GEF Scd1 establish a gradient of activated Cdc42 at the cellular tip, and it is this gradient that determines cell growth zone size and thus cell width.

Cell wall removal generates round spheroplasts that can recover into normal rod-shaped cells, allowing the study of how a growth zone of a particular shape and

dimensions is formed. Spheroplasts initially have a disorganized cytoskeleton and depolarized growth zone proteins. During recovery, these components repolarize and form one, or in some cases two, new growth zones from the rounded spheroplast body. Regenerated new growth zones have the same width as wild-type rod-shaped cells, and their width is controlled by the same genes that determine the width of normal exponentially growing cells. Scd2, a scaffold protein that is normally localized to the growth zone, forms a polarized patch in the rounded spheroplast before cell shape becomes polarized, showing that a growth zone protein can self-organize independent of cell shape. Rga4 is initially randomly distributed along the round spheroplast membrane but is excluded from the de novo growth zone as growth begins. A stable patch of Scd2 forms before Rga4 is reorganized, suggesting that growth polarization may precede Rga4 exclusion. These results provide evidence that a cell's growth zone can form de novo with the correct dimensions and that the cell's rod shape is a cell-intrinsic, genetically controlled trait that does not depend on cell wall history.

These studies show that the spatial regulation of Cdc42 is a major determinant of cell width in exponentially growing cells, and influences the width of a growth zone formed do novo. Cdc42 is an essential regulator of growth that is conserved throughout eukaryotes, and so this paradigm of spatial regulation may be broadly applicable.

Acknowledgments:

I would like to thank my advisor, Paul Nurse, who has provided sage advice and exuded calm confidence throughout my time in his lab. Thank you for creating an atmosphere of support and freedom with ample space for me to develop as an independent scientist. I hope I have learned at least a fraction of what you have tried to teach me.

I would like to thank the members of my committee, Sandy Simon and Cori Bargmann, for their counsel and encouragement, both on the project and on my career. And to Pilar Pérez: Thank you for your musings on the intricacies of Rho GTPases, fission yeast, and Spanish wines. Thank you for coming so far for my defense. I am very fortunate to have a committee composed of scientists I so admire.

I cannot adequately acknowledge the members of the Nurse Lab. Your guidance, advice, and good company have made whatever good work I have done here better. Thanks especially to Jamie Moseley and Frank Neumann, my partners in cell biology, and Lee Kiang, who made it all much more fun.

To my parents, Jack and Kathleen Kelly: Thank you for giving me your curiosity about the world around us, and for your support throughout this long process, and for (almost) never asking me when I was finally going to finish school. Just so you know, if I'm lucky I'll never finish.

To my sister, Natalie Kelly: You have been an inspiration, a great roommate, and a model scientist. It's a pleasure to hang out with such a rock star.

To my coach, Tony Ruiz, and all my running partners, especially my fellow cell biologist Sarah Alaei: Thank you for helping me find balance and keep a sound body around my occasionally unsound mind.

To Benjamin Gutman: Thank you for you faith in me, and for being the best editor a girl could ever wish for.

Table of Contents

Acknowledgments ..... **iii**

Table of Contents ..... **v**

List of Figures ..... **vii**

List of Tables ..... **ix**

List of Abbreviations ..... **x**

Chapter 1: Introduction **1**
- Size and shape determination in biological systems 1
- How are the specific dimensions of a whole cell determined? 6
- The proteins that shape cells are well conserved 6
- Cellular symmetry breaking 12
- Persistently polarized growth 15
- Fission yeast growth patterns and the influence of the cytoskeleton 18
- Multiple interacting pathways influence fission yeast cell shape 24
- What controls growth zone size and de novo formation? 36

Chapter 2: Screening for width mutants and genetic interactions **37**
- Introduction 37
- Results 38
- Discussion 54

Chapter 3: Specific localizations of Cdc42 regulators are important for their roles in cell-width control **57**
- Introduction 57
- Results 58
- Discussion 80

Chapter 4: De novo growth zone formation from spheroplasts **84**
- Introduction 84
- Results 85
- Discussion 106

Chapter 5: Discussion **111**
- Activated Cdc42 localization directs growth potential 112
- Cdc42 activation organizes a new growth zone 117
- Domains of GAP inhibition and GEF activation may be broadly conserved 124
- Future directions 125
- Conclusion: Wide mutants and spheroplast studies illuminate different aspects of the same problem 130

Chapter 6: Materials and Methods **131**
- Near-genome-wide screen for width mutants 131

Genetic characterization of wide mutants and strain construction 132
Microscopy 134
Fusion protein construction 135
Other protocols 138
Spheroplast generation 138
Spheroplast imaging 139
Diploid generation and spore germination 140
Appendix 1: Stout screen data 144
Works Cited 157

List of Figures:

Figure 1.1: The Rho-GTPase cycle 11
Figure 1.2: Fission yeast vegetative growth cycle 19
Figure 1.3: Protein complexes at cell tips direct growth 34
Figure 2.1: Screening for width mutants 41
Figure 2.2: Genes that influence cell width 44
Figure 2.3: Wide mutants can polarize growth 45
Figure 2.4: At least two independent pathways act to control cell width 51
Figure 2.5: Scd1 and Scd2 influence cell width by the same pathway 53
Figure 3.1: Rga4 and Scd1/Scd2 localize independently 59
Figure 3.2: Scd1 and Scd2 are mutually dependent for localization 61
Figure 3.3: Scd1 and Scd2 depend on actin for their localization, although Rga4 does not 63
Figure 3.4: The deletion mutants *scd2Δ* and *scd1Δ* maintain polarized growth 65
Figure 3.5: Cdc42-GTP localization is altered in the *scd2Δ* mutant 67
Figure 3.6: Temperature-sensitive *pak1* allele shows reduced tip localization 69
Figure 3.7: Retargeting of Scd1 to the cell tips can complement *scd2Δ* 72
Figure 3.8 Targeting Scd1 to the cell tips rescues Pak1 localization in the *scd2Δ* mutant 74
Figure 3.9: Localization of Rga4 to the cell cortex is crucial for cell-width control 77
Figure 3.10: Partial disruption of actin increases cell width 79
Figure 4.1: Depolarized spheroplasts can re-form a normal growth zone 88
Figure 4.2: Microtubules are not required for growth zone formation, but they influence the angle of bipolar growth 90
Figure 4.3: Growth zone size is also influenced by cell size 93
Figure 4.4: Spheroplasts can recover with growth zones of wild-type width 95
Figure 4.5: Spore germination tubes are the same width as wild-type growth zones, and may be controlled by the same genes 97
Figure 4.6: Cdc42 regulators do not carry the memory of the growth zone through spheroplasting 99
Figure 4.7: Scd2 polarizes before cell shape changes 101

Figure 4.8: Rga4 is excluded as the growth zone forms.....103
Figure 4.9: Scd2 organizes into a patch before Rga4 is excluded.....105
Figure 5.1 Activated Cdc42 directs cellular growth potential.....116
Figure 5.2: Stochastic growth initiation organizes zones of growth activation and inhibition.....121

List of Tables:

Table 1.1: Orthologs of genes that interact with *cdc42* 31
Table 2.1: Widths of putative wide mutants grown in hydroxyurea 42
Table 2.2 Wide Mutant Correction by Sorbitol 48
Table 6.1 *Schizosaccharomyces pombe* strains used in this thesis 141

List of Abbreviations:

CRIB	Cdc42/Rac Interactive Binding
DIC	Differential Interference Contrast
DMSO	Dimethly Sulfoxide
EMM	Edinborough Minimal Media
EMM4S	Edinborough Minimal Media with Supplements
GAP	GTPase Activating Protein
GDP	Guanosine Diphosphate
GEF	Guanine Nucleotide Exchange Factor
GTP	Guanosine Triphosphate
GTPase	Guanine Triphosphatase
GZ	Growth Zone
HU	Hydroxyurea
LatA	Latrunculin A
LUT	Look-Up Table
MBC	Carbendazim
MT	Microtubules
OE	Over Expressed
PAK	p21 Activated Kinase
PAR	Partitioning defective
RDI	Rho-protein GDP Dissociation Inhibitor
SNARE	Soluble N-ethylmaleimide-sensitive fusion protein-attachment receptor
TBZ	thiabendazole
WT	Wild-Type
YE4S	Yeast Extract media with Supplements

Chapter 1: Introduction

Size and shape determination in biological systems

Cells come in many different shapes and sizes, but the mechanisms of shape and size determination are not well understood. In metazoans, cells with radically different morphologies are generated from the same embryonic cells with their shapes encoded by the same genome, and their characteristic morphologies are specified using a small set of polarity proteins. The complexity of multicellular eukaryotes makes it difficult to explain what governs their cell size and shape. Starting with relatively simple examples should make it easier to look for common mechanisms that underlie cellular morphology.

Macromolecular assemblies

The size of a single protein is determined by its primary sequence and post-translational modifications. The shape of a single protein is a product of primary sequence and folding, which can be influenced by other proteins. Predicting the shape of a single protein from primary sequence has been challenging (Dill *et al.*, 2008), but although it is neither simple nor perfectly predictable, we have a good understanding of how a protein's size and shape are established. With simple multi-protein structures we can also reasonably explain their size and shape—for example, the size and shape of a dimer will be the product of the two monomers and the interactions between them. Larger macromolecular assemblies become increasingly difficult to predict, but their sizes and shapes are basically the sum of

direct interactions between a small number of copies of the components. The eukaryotic ribosome is a large macromolecular protein-RNA complex made up of 79 proteins and four structural RNAs (Ben-Shem et al., 2010). The proper assembly of all of these components determines the size and shape of the ribosome, through a complex process that involves more than 200 non-ribosomal proteins (Kressler *et al.*, 2010). Despite that complexity, the resulting structure can be understood in terms of stable, direct molecular interactions established at the atomic level.

A molecular ruler—a protein that has the desired length of the overall structure—can specify size, and potentially shape (Rafelski and Marshall, 2008). The length of phage virus tails can be specified this way. In bacteriophage λ, the length of the tail is directly influenced by insertions or deletions in protein H (Katsura, 1987), and the stretched length of the H protein is predicted to be the same length as the phage tail (Katsura, 1990).

In a more complicated but related system, virus capsid shells assemble as three-dimensional structures specified simply by the interaction of repeating protein subunits. The bacteriophage P22 encodes a coat protein and a scaffold protein that will efficiently assemble a closed icosahedral shell from purified monomers, and if the P22 coat protein is in high concentration, it can even assemble shell-like structures without the scaffold protein (Fuller and King, 1982). The shape of virus shells is specified by the geometry of the coat and scaffold proteins, with the curvature of the virus particle controlled, in part, by the bonding of proteins to one another, and the need to assemble a closed structure. This can be easily imagined in two dimensions: If a chain is made of subunits assembled end-to-end, and the

subunits attach at a set angle, then eventually these subunits will form a closed polygon, and the diameter of that polygon and the number of subunits in the polygon will both be determined by the angle of attachment (Moody, 1999). Electron micrographs of bacteriophage revealed that they were symmetric structures, and mutational analysis revealed that one, or very few, proteins encoded the caspid wall (Botstein *et al.*, 1972). These observations led to a geometric model for caspid assembly in which identical subunits assembled into closed solids that resemble icosahedra, based on the formation of either hexamers or pentamers by the same coat subunit (Caspar and Klug, 1962; Moody, 1999). The molecular ruler of the phage tail, and the geometry of phage head assembly, use stable molecular interactions to encode the size of a biological object. But moving from macromolecular assembly to the morphology of the cell increases the scale of the problem by at least two orders of magnitude, and different solutions may apply.

Dynamic equilibriums can determine organelle size

Most large structures in the cell are not specified by stable direct molecular interaction, but instead depend on a dynamic balance between assembly and disassembly of components acting over longer distances. In a dynamic system the steady-state size of the structure can be determined by the point where the rates of assembly and disassembly become equal. The microtubules that form eukaryotic flagella undergo continuous growth and catastrophe at the distal tips. The microtubule subunits required for continued growth are transported along the length of the microtubules by a specialized protein complex, and the number of

these complexes on the flagellum is not influenced by its length (Marshall and Rosenbaum, 2001). The rate of transport to the tip of the microtubule depends on the length of the microtubule, but microtubule disassembly is not influenced by length (Marshall *et al.*, 2005). These two rates determine the steady-state length of the flagellum, though transport dynamics are altered in very short, regenerating flagella (Engel *et al.*, 2009).

The nucleus is a more complicated organelle, but its size is also influenced by a dynamic balance, here the balance between nuclear import and export. In budding yeast, nuclear size scales with the size of the cell independent of DNA content (Jorgensen *et al.*, 2007). This is also true in fission yeast, where the ratio between the size of the nucleus and the size of the cell is nearly invariant across a wide range of cell sizes. In multi-nucleated fission yeast cells with equal DNA content per nucleus, the size of each nucleus is influenced by the relative amount of cytoplasm surrounding it (Neumann and Nurse, 2007), implying that a local cytoplasmic factor may convey information about the size of the cell. The information from the surrounding cytoplasm is likely conveyed through a dynamic balance of nuclear import and export. When nuclei are reconstituted in egg extracts from *Xenopus laevis* and *Xenopus tropicalis*, the nuclear growth rates for each species reflect the relative sizes of the nuclei in early cleavage embryos—*X. laevis* has bigger nuclei, and in egg extracts *X. laevis* nuclei grow faster and have faster import rates (Levy and Heald, 2010). Increasing import rates by adding exogenous activated importin α to reconstituted *X. tropicalis* eggs increases nuclear size, while depleting importin α reduces nuclear import and nuclear size. One of the relevant substrates that

determine nuclear size is the nuclear lamin LB3; addition of recombinant LB3 can increase nuclear size, though addition of other importin α cargos does not. Many details remain to be investigated, but the dynamic balance between import and export that maintains the size of the nucleus could be a model for how other biological sizing mechanisms work.

The cell cycle controls overall cell volume

Organelles present examples of size determination, but they do not necessarily reflect how a cell's overall dimensions are determined. One of the best-understood controls of cell size is the control of the cell cycle. In fission yeast, total cell size is under the control of cell division cycle progression, as shown by the isolation of large and small mutants with cell-cycle defects (Russell and Nurse, 1986; Nurse, 1975). The control of the cell cycle affects the progression through DNA replication and cell division, but it was discovered through mutants that change cell length. When the cell cycle is advanced, as in a *wee1-TS* mutant, cells divide smaller. When the cell cycle is delayed, as in a *cdc25-TS* mutant, cells are elongated. The geometry of the cell feeds into the control of cell size through a tip-localized kinase, Pom1, which inhibits cell division through Wee1 until cells have reached a minimum length (Martin and Berthelot-Grosjean, 2009; Moseley et al., 2009). The tightly controlled size at division allowed the identification of mutants with altered cell-cycle timing, but these mutants do not generally have altered cell morphology. They do, however, offer a method for identifying genes that alter cellular dimensions: Choose a simple read-out of an easily measureable cellular trait with little variation,

and then look for mutants that alter that trait without other pleiotrophic defects. I have used this approach to isolate mutants with altered cell width.

How are the specific dimensions of a whole cell determined?

The examples presented here provide models for thinking about biological sizing, but they do not address the question of how a cell's shape is genetically encoded. Many cell types grow from a distinct growth zone, and the pattern of growth defines the shape of the cell. Thus, I set out to investigate how the size of the growth zone is genetically encoded, how proteins act to specify its size, and how it is established de novo. The genetic amenability, regular shape, and tip-localized growth zones of fission yeast made it a good system for this investigation. The proteins that mediate and direct growth are well conserved, and so findings in fission yeast may be of general importance.

To put this question in context, I will review basic conserved cellular growth mechanisms, a few well-described pathways that specify cell shape, and the proteins that contribute to cell growth in fission yeast.

The proteins that shape cells are well conserved

Though cell sizes, shapes, and functions are incredibly diverse, the structural components of the cell and the proteins that shape the cell are remarkably few and well conserved. These proteins are necessary for growth, and define the growth zones of polarized cells.

The cytoskeleton and exocytosis are necessary for cell shape and growth

Actin is a major component of eukaryotic cells' cytoskeletons and a prime example of the conservation in sequence and function across eukaryotes. At the sequence level, the Act1 protein of fission yeast and the human muscle actin protein ACTA1 have 89% sequence identity when aligned, though even the small differences have physiological consequences (Ti and Pollard, 2011). One reason for the high level of sequence conservation could be the interactions required between monomers for the assembly of actin structures (Galkin et al., 2010; Galkin et al., 2002). The functional conservation of actin is apparent from the structural conservation of several major proteins that interact with and regulate actin (Derivery and Gautreau, 2010; Paavilainen et al., 2004). The conservation between budding yeast, fission yeast, and mammals makes it possible to generalize about actin's function in growth from the budding yeast and fission yeast studies.

Cytoskeletal microtubules are also involved in determining cell shape in animal cells and fission yeast, though they are less important for cell shape in budding yeast. In animal cells microtubules provide cell structure and serve as tracks for long-range transport. Microtubules are dynamic, linear protein assemblies made up of repeating α/β tubulin heterodimers, and they transition rapidly between extension, catastrophe, and rescue. Like actin, the basic α- and β-tubulin subunits of microtubules are highly conserved throughout eukaryotes (Dutcher, 2001). The importance of microtubles is apparent in neurons, where they have been shown to play roles during axon formation, axon elongation, axon branching, and dendrite formation. The rapid elongation of axons depends on

microtubule elongation (Dutcher, 2001), and inhibition of microtubule nucleation by micro-injection with a γ-tubulin antibody inhibits axon formation (Ahmad *et al.*, 1994). Axons contain more stable microtubules than dendrites, and stabilization of microtubules causes a severed dendrite to regenerate as an axon (Gomis-Ruth *et al.*, 2008). The striking effects that microtubule alteration can have in neurons testify to their importance in determining cellular morphology.

The cytoskeleton and associated proteins provide the cell's structure, but exocytosis is necessary for growth. Exocytosis also occurs by conserved mechanisms, though there are many variations. Regulated exocytosis is the last step in the secretory pathway and occurs by an initial vesicle tethering followed by fusion of the vesicle with the plasma membrane. Tethering is mediated by the evolutionarily conserved eight-protein exocyst complex, which was initially described for its essential role in budding yeast exocytosis (TerBush and Novick, 1995), and then found as a membrane complex in mammalian cells (Hsu et al., 1996; Ting et al., 1995). Membrane fusion is mediated by pairs of SNARE proteins that can bring the vesicle membrane and plasma membrane very close, and induce fusion (Weber *et al.*, 1998; Zwilling *et al.*, 2007). In yeast, exocyst mutants also disrupt the assembly of the SNARE complex, linking the localization of these two steps (Grote *et al.*, 2000).

Rho GTPases are conserved molecular switches

Rho GTPases play conserved roles in the cellular morphologies of diverse eukaryotes. Among the most important and well conserved are Rac, Rho, and Cdc42.

These small G-proteins can act as molecular switches, transitioning between an active GTP-bound state that interacts with effector proteins, and an inactive GDP-bound state. A representation of the Rho GTPase cycle is shown in Figure 1.1. Rho proteins have intrinsic GTPase activity and can hydrolyze GTP to GDP, but this hydrolysis is usually inefficient. It is promoted when the Rho protein binds to a GTPase-activating protein (GAP). After GTP is hydrolyzed to GDP, reactivation is stimulated by binding to a guanine-nucleotide exchange factor (GEF), which facilitates the release of GDP. Since the cellular concentration of GTP is higher than that of GDP, the Rho protein will usually rebind GTP and return to its active state. GTPases are often regulated by multiple nonexclusive GAPs and GEFs. Rho guanine-nucleotide dissociation inhibitors (GDIs) also negatively regulate GTPases by maintaining them in a GDP-bound state and preventing their membrane association. (Perez and Rincon, 2010)

Rho GTPases have diverse functions in cell morphology

Within one organism, metazoan cells can have many different morphologies, and Rho GTPases act as molecular switches to coordinately regulate effectors that specify those morphologies. The first indications of the importance of Rho GTPases in mammalian cells came from the effects of recombinant, purified, constitutively activated proteins in fibroblasts. Micro-injection of activated RhoA induced the formation of stress fibers and focal adhesions (Ridley and Hall, 1992), injection of activated Rac1 induced the formation of lamellipodia (Ridley *et al.*, 1992), and injection of activated Cdc42 induced the formation of filopodia (Nobes and Hall, 1995). These experiments indicated that different Rho GTPases have distinct but interacting contributions to cell morphology,

and that many of these effects change the organization of the actin cytoskeleton. Those observations have been borne out in many different systems, but neurons again provide an example of the complexity of growth regulation.

Neurons are highly polarized cells, and several different Rho GTPases contribute to their morphology and development. As axons form, CDC42 and RAC1 promote neurite growth through the formation of lamellipodia and filopodia, while RhoA mediates growth-cone collapse (Iden and Collard, 2008; Kozma et al., 1997). Experiments in *Drosophila melanogaster* showed that tissue-specific expression of dominant negative and constitutively active forms of the fly homolog of Rac1 in neurons caused major axonal outgrowth defects (Luo *et al.*, 1994). Cdc42 and RhoA are rapidly activated when the dendritic spines of rat pyramidal neurons are stimulated, which causes an increase in dendritic spine volume that is largely inhibited if Cdc42 activation is blocked (Murakoshi *et al.*, 2011). As in many other polarized eukaryotic cells, neuronal morphology is determined by the coordinated regulation of Rho GTPases.

Figure 1.1

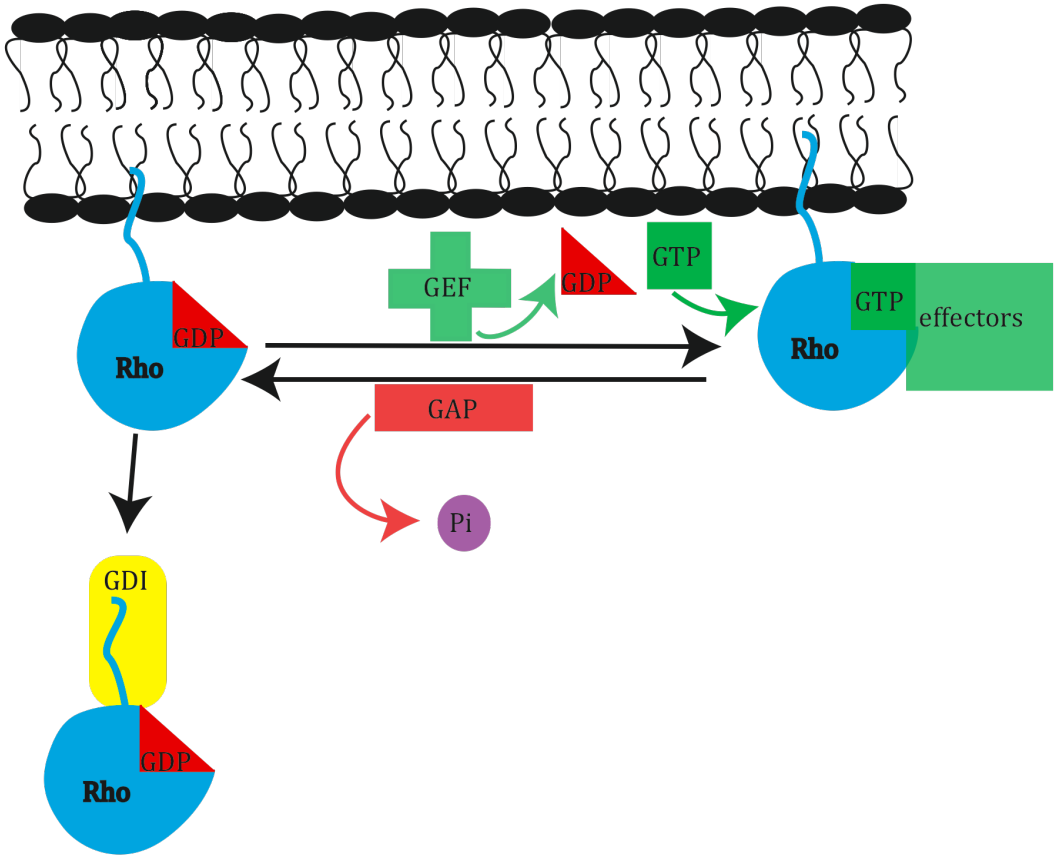

Figure 1.1: The Rho GTPase cycle. Rho GTPases are regulated by cellular location and GTP/GDP-bound state. GDIs extract Rho GTPases from the membrane, rendering them functionally inactive. In the membrane, Rho GTPases are inactive when bound to GDP. A GEF catalyzes the release of GDP, which enables its replacement by GTP. The GTP-bound Rho protein can then interact with downstream effectors. GAP binding to the Rho GTPase catalyzes the hydrolysis of GTP to GDP, rendering the GTPase inactive.

Cellular symmetry breaking

The most basic cell shape is a sphere that grows uniformly. To generate any complex morphology, symmetrical cells must begin polarized growth, which can be initiated by an outside cue or through spontaneous symmetry breaking. Once a cell is asymmetric additional mechanisms act to continue polarized growth at specific cellular dimensions.

Sperm entry provides a cue for asymmetric development in worm eggs

The initial establishment of an organism's polarity in development is necessary for all other patterning events. In the *Caenorhabditis elegans* zygote, the initial cue for polarization comes from the entry of the sperm. This cue directs a system that specifies the first asymmetric cell division, which is a prerequisite for subsequent cell-fate determinations (Nance and Zallen, 2011). Partitioning defective (PAR) mutants that improperly position the initial division plane have defined a system of seven genes that are essential for establishing the anterior/posterior axis of the developing worm. Some of the proteins encoded by these genes localize differentially in the zygote. PAR-1 and PAR-2 localize to the posterior end of the cell, where fertilization has taken place, whereas PAR-3, PAR-6, and the atypical protein kinase C PKC-3 localize to the anterior end. The differential segregation of these proteins is initiated by polarized actin-myosin contractility.

After fertilization the whole cortex of the cell has shallow cortical contractions driven by actin and myosin. As polarity is initiated, these contractions

become polarized, with the anterior cortex continuing to contract while the posterior cortex becomes quiescent (Hird and White, 1993; Munro *et al.*, 2004). The polarization of contractility is regulated by non-uniform RHO-1 activation, which is set up by the posterior exclusion of the Rho-GEF ECT-2 by the sperm centrosome (Motegi and Sugimoto, 2006; Munro et al., 2004) and the anterior localization of the sperm-provided pool of the Rho-GAP CYK-4 (Jenkins *et al.*, 2006). The segregation of PAR proteins into different domains and the subsequent downstream effects on division depend on CDC-42—when CDC-42 is partially depleted by RNAi, the first cell division is symmetric, the posterior PAR protein PAR-2 is uniformly distributed on the cell cortex, and the anterior PAR proteins are incorrectly localized after the first division (Gotta *et al.*, 2001).

Stochastic activation of Cdc42 can establish polarity in budding yeast

Budding yeast cells grow isotropically after division and then transition to polarized growth at the end of G1 (Snyder *et al.*, 1991). This transition depends on cell-cycle signals. Freshly budded cells grow isotropically until the GEF Cdc24 is released from the nucleus, stimulating polarized growth to form a new bud (Shimada *et al.*, 2000). In wild-type cells the location is predetermined—the new bud will form adjacent to the previous bud site. The selection of the bud site is influenced by the Ras homolog Rsr1 and the GAP Rga1. Cells that lack the protein Rsr1 will bud at randomly selected locations (Bender and Pringle, 1989; Chant and Herskowitz, 1991), and cells without Rga1 will reuse the same bud site (Tong *et al.*, 2007). When the bud site is randomly selected the cell must transition from a

homogenous distribution of growth to a focused point of growth without a preexisting cue. Some controversy remains over the exact mechanisms that cells use to organize the bud site (Irazoqui *et al.*, 2003; Slaughter *et al.*, 2009a), and this symmetry-breaking event can occur in either an actin-independent or an actin-dependent way. In both mechanisms, the stochastic activation of Cdc42 is important.

In the experiments that led to the actin-independent model, freshly budded cells that do not have the normal bud-site landmarks are isolated by elutriation, and activated Cdc42 forms a defined cap with or without actin and microtubules. But this polarization depends on the scaffold Bem1 and requires the GTPase cycling of Cdc42 (Irazoqui *et al.*, 2003). Later experiments showed that Bem1's role in symmetry breaking is to nucleate a complex that contains the GEF Cdc24, the PAK kinase STE20, and Cdc42 (Kozubowski *et al.*, 2008). The components of the complex form a positive feedback loop where the complex activates more Cdc42 nearby, which leads to the formation of more complexes, and ultimately to the formation of a stable patch of polarized Cdc42.

The actin-dependant mechanism for symmetry breaking was described for the polarization of an over-expressed and constitutively active version of Cdc42 in cells arrested in G1. The over-expressed activated Cdc42 is originally spread throughout the cell membrane and then stochastically forms polarized, stable protein caps. The formation of these caps depends on actin-cable-based polarized transport, and was modeled as a positive feedback loop. In this model spontaneous actin-cable nucleation or a slight perturbation of the distribution of activated Cdc42 would result in more actin cables transporting more activated Cdc42 to that

location, and the formation of a stable cap (Wedlich-Soldner *et al.*, 2003). Both mechanisms may have a role in symmetry breaking, though the scaffold-dependent model is based on observations made in a less perturbed experimental system. The redundant actin-dependent and scaffold-dependent mechanisms that initiate symmetry breaking in bud-site-selection mutants are evidence that multiple pathways are acting in a normal cell to reinforce and stabilize polarized growth.

These symmetry-breaking systems provide mechanisms for the initial establishment of polarity, but they do not address the question of how to specify growth zone size. Symmetry breaking is necessary for the formation of a defined growth zone, but the size and shape of that growth zone may be independently determined.

Persistently polarized growth

Fungal hyphae and the pollen tubes of plants are stably polarized cells that grow long distances and retain a near-constant width during growth. The models for how this long-distance, stable growth is accomplished may shed light on the control of growth zone size.

Growth zone size is determined by the Spitzenkörper in hyphal fungi

The filamentous fungus *Ashbya gossypii* grows multi-nucleated hyphae with persistent tip localization of growth regulatory proteins, such as a formin, Bni1 (Schmitz *et al.*, 2006) and a PAK kinase, Cla4 (Ayad-Durieux *et al.*, 2000). But unlike fission yeast, these cells also contain a specialized vesicle supply center known as the Spitzenkörper, which forms in fast-growing, but not slow-growing, hyphae (Kohli *et al.*, 2008). By comparing fast- and slow-growing hyphae, Kohli *et al.* showed that the Spitzenkörper may be necessary to supply vesicles only when the tip is growing rapidly and so is quickly incorporating material. As the rate of hyphal growth increases, the diameter of the hyphae increase, and the localizations of several polarity proteins switch from an even cortical cap to a concentrated Spitzenkörper. This switch in growth mode may influence the width of the tip of the cell.

The pathogenic yeast *Candida albicans* can grow as a yeast form that resembles budding yeast, as a more elongated pseudo-hyphal form, and as a true hyphal form that grows from a persistently polarized tip (Sudbery *et al.*, 2004). The hyphal growth mode has parallel cell sides and a rounded cell tip where growth is localized, like the fission yeast growth pattern. When *Candida* is growing in the hyphal form, growth is driven by the Spitzenkörper, but the Spitzenkörper is not present in the yeast or psuedohyphal form (Crampin *et al.*, 2005), which may indicate that the Spitzenkörper is generally a hyphal-specific structure.

The tip growth of hyphae has been extensively modeled. The hyphoid model explains the morphology and width of the cell tip by invoking the vesicle-supply-

center role of the Spitzenkörper (Reynaga-Pena *et al.*, 1997). In this model, the Spitzenkörper continually sheds vesicles randomly in all directions. It is proposed that these vesicles are not targeted to any location—when they hit the cortex, they cause the cell to grow at that location. Thus, the position of the Spitzenkörper determines where growth takes place, and therefore determines the shape of the cell. For a long, straight hypha to form, the Spitzenkörper must continuously move towards the tip. This model is supported by studies in which the Spitzenkörper is disrupted or displaced. For example, in *Candida albicans* the width of the hypha is correlated with the distance of the Spitzenkörper from the tip of the cell. As the Spitzenkörper moves further from the apex of the cell tip, the area where vesicles hit the cell tip becomes more diffuse, and the tip becomes wider (Crampin *et al.*, 2005).

Growth in the pollen tube is driven by an ion gradient

Pollen tubes are another type of highly polarized cylindrical cell that grows by cell-wall addition at the cell tip. Tip growth depends on two major elements: a steep gradient of intracellular calcium (Pierson *et al.*, 1994) and actin-dependant polarized delivery (Vidali *et al.*, 2001). The high levels of tip-localized calcium may act to direct growth to the cell tip, since disruption of the calcium gradient causes pollen tube tips to swell, and local calcium gradient alteration can cause pollen tubes to bend and turn (Malho *et al.*, 1995). Fission yeast cells can grow in media without exogenously added calcium ions (Carnero *et al.*, 2000), so growth probably does not depend on the generation of a calcium gradient. But ion gradients form,

and will respond to, an electric field and the direction of fission yeast tip growth can be altered by the application of an electric field (Minc and Chang, 2010). This reorientation may be due to induced spatial changes in intracellular pH that redirect growth.

In hyphal fungi and pollen tubes, the study of growth control has historically been driven by physiological observations and investigations of conditions that alter growth patterns. These observations, and the well-developed models that are derived from them, can guide our investigations in yeast, which will focus more directly on the genes and proteins that determine the size of the growth zone.

Fission yeast growth patterns and the influence of the cytoskeleton

Fission yeast morphology and growth throughout the cell cycle

Fission yeast cells are walled and have a regular rod shape that, in the vegetative growth cycle, increases in volume by length extension at the cell tips. The width of the cell is approximately 4 microns throughout the cell cycle, while the length of the cell increases from 7 microns just after division to 14 microns just before division. After division, cells begin growth at one end of the cell before transitioning to bipolar growth once a minimal cell size has been reached. Bipolar growth then continues until cell division, when length extension stops and the growth machinery is concentrated in the center of the cell to form the septum and new cell wall (Figure 1.2, reviewed in (Hayles and Nurse, 2001)).

Figure 1.2

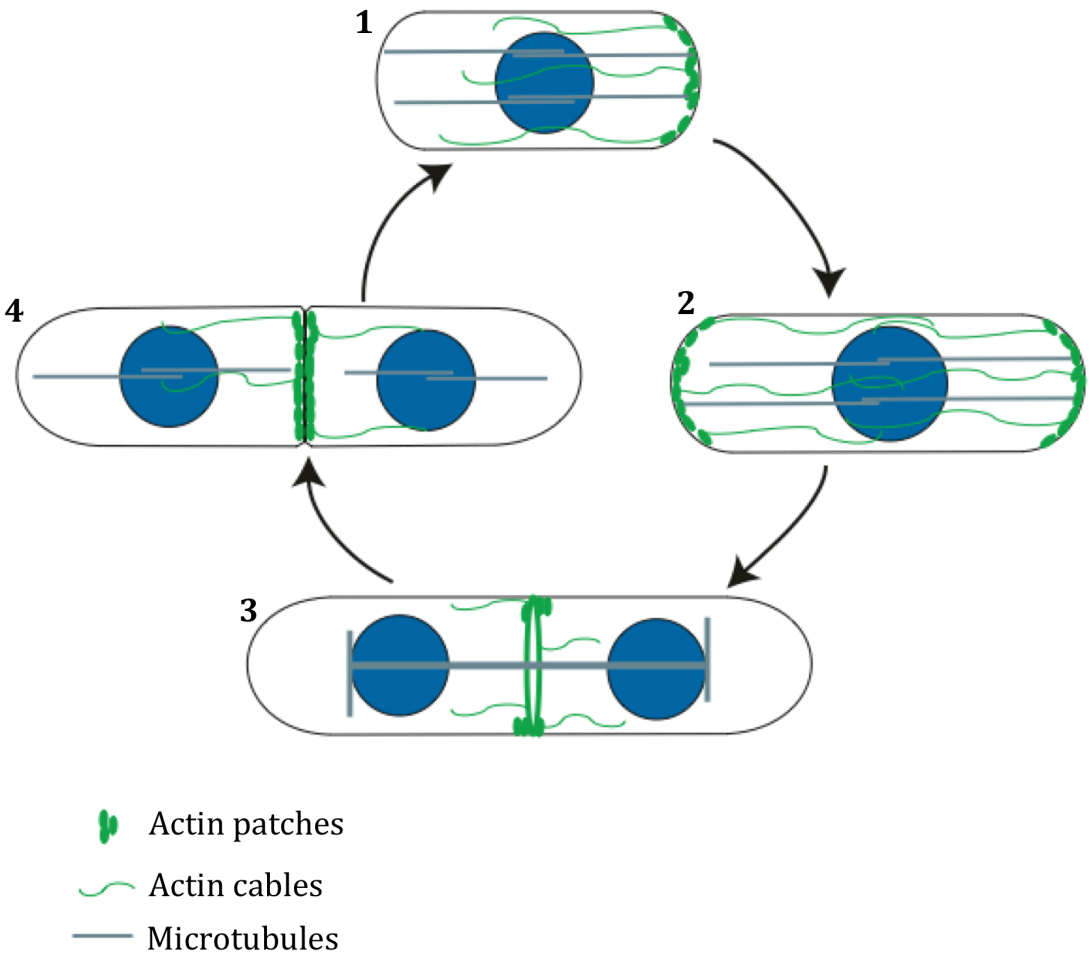

Figure 1.2: Fission yeast vegetative growth cycle. As cells proceed through the cell cycle, growth occurs at different locations. **1.** In a newly born cell, growth is monopolar, and actin patches and cables are localized to one tip of the cell. **2.** Coincident with G2, cells begin to grow at both ends of the cell. **3.** In mitosis, microtubules form a spindle that mediates nuclear division. The cell is divided by constriction of an actin-myosin ring. **4.** Once ring constriction is complete, growth and actin patches relocate to the cell center to build the septum and new cell walls. For this figure, actin localization is modeled on personal observations and Arai *et al.*, 2002; microtubule organization is modeled on personal observations and Vogel *et al.*, 2007.

In addition to mitotic growth and division, fission yeast can undergo a sexual meiotic cycle. In nutrient-limited conditions, cells of opposite mating types produce and respond to pheromone gradients, forming directed growths toward one another called shmoos (Niccoli and Nurse, 2002). These growths then fuse to form a diploid cell, which goes through one round of meiotic DNA synthesis, recombination, and two rounds of meiotic division. After the second meiotic division the four nuclei are segregated into four round spores, each surrounded by a newly synthesized spore membrane and stress-resistant cell wall. Chitin is an important component of the spore wall, though it is not a major component of the wall of vegetatively growing cells (Arellano *et al.*, 2000). When nutrients are available these spores can germinate, forming a new rod-shaped cell from a round spore.

The cell wall is required to shape the cell

A polysaccharide wall that protects against osmotic and mechanical stresses constantly surrounds the vegetatively growing cell. The major structural components of the fission yeast cell wall are (1-3)β-D-glucan, which makes up about half of the polysaccharides of the cell wall, and (1-3)α-D-glucan, which makes up about one-third of the polysaccharides of the cell wall (Bush *et al.*, 1974). Non-structural galactomannan accounts for about one-tenth of cell wall polysaccharides. Galactomannan can be linked to proteins to form glycoproteins (Ballou and Ballou, 1995).

Regulated production of the cell wall is essential to fission yeast survival. (1-3)β-D-glucan is made by an enzyme complex, the core of which is formed by the essential proteins Cps1/Bgs1, Bgs3, and Bgs4 (Cortes et al., 2005; Ishiguro et al., 1997; Martin et al., 2003). The catalytic subunit of (1-3)α-D-glucan synthase is encoded by the essential gene *mok1* (Hochstenbach *et al.*, 1998). After polysaccharide synthesis these components of the cell wall must undergo further processing to construct a branched, cross-linked, stable structure. Deletion of the (1,3) β -glucanosyl-transferase *gas1* reduces branching and crosslinking of (1-3)β-D-glucan within the cell wall, and renders cells dependent on osmotic stabilization (de Medina-Redondo *et al.*, 2010). The wall defines the shape of the cell, and when the wall is removed yeast cells either explode from internal turgor pressure or, when they are osmotically stabilized, become spherical (Diamond and Rose, 1970; Necas, 1971; Osumi, 1998).

The same turgor pressure that can cause cells to lyse can also drive cell growth by providing a force that favors cell expansion. But internal turgor pressure, generated by an osmotic gradient across the plasma membrane, is isotropic, while growth is directed. Growth from this uniform force can be specifically localized if the compliance of the cell wall is non-uniform (Harold, 1990). In fission yeast, new cell-wall components and enzymes that modify the cell wall are delivered to a specific growth zone. That directed delivery could specify areas of local compliance with the uniform force of turgor pressure. Thus, to determine how a yeast cell specifies its shape we must determine, in part, how compliance is localized.

Actin and microtubules are important for fission yeast cell shape

In both fission and budding yeast, actin is required for several different modes of growth, and I will discuss data from both systems where the mechanisms appear to be common to both yeasts. Actin patches have been shown to be sites of endocytosis in budding yeast, fission yeast, and mammalian cells (Galletta and Cooper, 2009). Actin labeling in budding yeast originally identified patches as puncta associated with the cell cortex at sites of growth and cables as filamentous structures that stretched through the cytoplasm (Adams and Pringle, 1984). Investigations in fission yeast showed similar actin structures, and also noted a equatorial ring associated with division (Marks *et al.*, 1986). In fission yeast, endocytosis co-localizes with growth throughout the cell cycle (Gachet and Hyams, 2005), and may play a role in membrane remodeling or cell wall synthesis. Since the initial identification of actin patches, many proteins that localize to actin patches have been characterized, and their disruption is often associated with endocytic defects (Moseley and Goode, 2006).

Studies of the dynamic recruitment and movement of actin-patch components have constructed a detailed picture of how these patches assemble and disappear from the cortex through endocytosis (Kaksonen *et al.*, 2003; Kaksonen *et al.*, 2005; Sirotkin *et al.*, 2005; Sirotkin *et al.*, 2010). Protein assemblies form that are nonmotile and contain several patch proteins including clathrin, but not actin. Then polymerized actin appears, forming an actin patch, and the patch begins to move slowly at the cortex with a small movement into the cell that corresponds to vesicle

invagination. Finally, membrane fission occurs and patches move quickly into the cell, apparently along actin cables (Galletta and Cooper, 2009). The cortical and internalized actin patches are associated with endocytic vesicles marked with the lipophilic dye FM4-64, an observation that directly links actin patches and cables to endocytosis (Huckaba *et al.*, 2004).

Yeast cells use actin cables to organize and polarize growth. Formins, such as the fission yeast For3 and the budding yeast Bni1, are recruited to sites of polarized growth and nucleate the assembly of actin cables composed of bundles of parallel actin filaments (Evangelista et al., 2002; Feierbach and Chang, 2001; Kamasaki et al., 2005). The actin cables then form tracks for myosin V mediated vesicle transport towards the cell tips (Motegi *et al.*, 2001; Schott *et al.*, 2002). In budding yeast it has been demonstrated that the vesicles transported on actin cables contain enzymes that contribute to cell growth, such as glucan synthase (Utsugi *et al.*, 2002).

Microtubules are more important for interphase cell growth in fission yeast than in budding yeast (Chang and Martin, 2009), since both actin and microtubules influence the rod shape of fission yeast (Hayles and Nurse, 2001). During interphase, fission yeast microtubules are organized into three to five bundles that each span over half the length of the cell, and overlap in the cell center. The microtubule bundles are parallel to one another, and can self-organize in the absence of the nucleus-associated microtubule-organizing center (Carazo-Salas and Nurse, 2006). Disruptions of the microtubule cytoskeleton can lead to bent and branched cells that retain polarized, but mislocalized, growth (Sawin and Snaith, 2004). These cells are often monopolar and do not go through the stereotypical

transition to bipolar growth. Microtubule organization is affected by cell shape, as is apparent from the arrangement of microtubules in rounded morphology mutants (Qyang et al., 2002; Verde et al., 1995). This has made it difficult to determine to whether microtubules actually control cell shape or simply respond to and reinforce cell shape. This issue has been partially addressed by experiments that manipulated cell shape by physical constraint. To do this cells were bent into a C-shape in polymer molds, and the microtubules repeatedly hit the sides of the cell rather than following the bend of the C-shaped cell. At the sites where the microtubules contacted the cortex, new growth zones eventually arose, demonstrating that microtubules can direct cell growth (Minc et al., 2009a; Terenna et al., 2008).

Multiple interacting pathways influence fission yeast cell shape

The Tea1 complex positions the growth zone

The interphase microtuble array is required for the cell-tip localization of a set of proteins that influence growth patterns. These proteins, Tea1, Tea4, Mod5, Tea3, Bud6, and Tip1/Noc1, form a complex at cell tips (Brunner and Nurse, 2000; Martin et al., 2005; Mata and Nurse, 1997; Snaith and Sawin, 2003). Tea1 is the original member of this complex, identified by a distinctive phenotype: In a *tea1Δ* mutant, cells often form bent or T-shapes, especially when re-initiating growth after starvation (Mata and Nurse, 1997; Sawin and Snaith, 2004), and so Tea1 has been proposed to be important for establishing new sites of cell growth. In addition, the proteins of the Tea1 complex are important for the initiation of bipolar growth—

deletion of *tea1, mod5,* and *tea3* increases the proportion of monopolar cells in the population, though the severity of the phenotype varies (Glynn *et al.*, 2001; Snaith *et al.*, 2005). Once a growth site at the cell tip is established, this complex, and microtubules, are dispensible for continued growth (Sawin and Snaith, 2004).

The Tea1 complex mediates some of its effects through regulating the interphase microtubule array. Tip1 is found at the tips of microtubules and at cell tips in growing cells. It is required for Tea1 localization to microtubule tips, and it mediates Tea1's delivery to cell ends through interactions with Mal3 and Tip2 (Bieling et al., 2007; Brunner and Nurse, 2000; Busch and Brunner, 2004). The protein complex Tip1-Tip2-Mal3 is required for the assembly of a normal microtubule array, and microtubules are shortened in *tip1Δ*, *tip2Δ*, and *mal3Δ* cells due to increased rates of catastrophe when microtubules encounter the cortex near the cell center (Browning *et al.*, 2000; Busch and Brunner, 2004). This complex may regulate microtubule length by preventing catastrophe while Tip1 is at the microtubule tips. When microtubules reach the cell tips, Tip1 and Tea1 remain at the cell cortex anchored by Mod5, and then microtubules are more likely to undergo catastrophe (Piel and Tran, 2009; Snaith and Sawin, 2003).

Two of the proteins that binds Tea1 at cell tips, Tea4 and Bud6, also interact with the formin For3, and those interactions are important for the initiation of bipolar growth (Glynn *et al.*, 2001; Martin *et al.*, 2005). Tea4 is primarily required for the bipolar recruitment of For3 to the second growing cell tip, while Bud6 participates in its activation by relieving For3's autoinhibition (Martin *et al.*, 2007).

The monopolar phenotype of Tea1-complex mutants may be due to the loss of For3 recruitment to the new end of the cell.

Rho1 and Rho2 control cell wall synthesis

The conserved Rho GTPases Rho1 and Rho2 contribute to cell morphology by activating cell wall synthesis. Rho1 is an essential gene that localizes to sites of active growth. Its primary role is the regulation of cell wall synthesis by activating the (1,3)β -D-glucan synthase complex (Arellano *et al.*, 1996). Rho1 is regulated by several different GEFs during the fission yeast life cycle. Rgf1 activates Rho1 during polarized growth (Garcia *et al.*, 2006), Rgf3 activates Rho1 during cytokinesis (Tajadura *et al.*, 2004), and Rgf2 plays an essential role in Rho1 activation during sporulation and has a role in polarized growth that is partially redundant with Rgf1 (Garcia *et al.*, 2009). If Rho1 is depleted, cells lyse during cytokinesis due to a weakening of the cell wall (Arellano *et al.*, 1997). Rho1 is also regulated by three GAPs. Disrupting the major GAP, Rga1, causes cells to grow a thickened cell wall due to the overactivation of Rho1 (Nakano *et al.*, 2001). Rga5 regulates cell integrity and cytokinesis (Calonge *et al.*, 2003). Rga8 also acts as a Rho1 GAP, but plays a more minor role, regulated by the Cdc42 effector Pak1 (Yang *et al.*, 2003).

Though it is not essential, Rho2 also regulates cell-wall synthesis, and *rho2Δ* mutants are rounded and hypersensitive to (1,3)β-D-glucan synthase inhibition (Hirata *et al.*, 1998). Overexpression of Rho2 causes cells to grow a thicker cell wall that contains a higher proportion of (1,3)α-D-glucan, which implicated Rho2 in the positive regulation of α-glucan synthase. Rho2-GTP interacts with the protein kinase

C homologs Pkc1 and Pkc2, and activates the α-glucan synthase Mok1 through Pkc2 (Calonge *et al.*, 2000). One of the regulators of Rho2, the GAP Rga2, influences the width of the cell. When Rga2 is overexpressed cells are shorter and broader, accumulate excess cell wall, and eventually lyse. In *rga2Δ* mutants, cells are longer and thinner, but it is unclear whether the loss of an element of Rho2 regulation is responsible for that change in morphology (Villar-Tajadura *et al.*, 2008).

Cdc42 directs polarized growth through multiple effectors

Cdc42 regulates cell growth in parallel to Rho1 and Rho2. The protein is essential for fission yeast growth, and its depletion results in small dense cells that can neither grow vegetatively nor mate (Miller and Johnson, 1994). Cdc42 is localized to the growing cell tips, the cell center during division, and the endomembranes of the cell (Merla and Johnson, 2000; Rincon *et al.*, 2007). Its localization to membranes is likely mediated by prenylation: Cdc42 is geranylgeranylated on a conserved motif in the C-terminus in budding yeast (Ziman *et al.*, 1993) and other organisms (Roberts *et al.*, 2008). Its activation is regulated by two partially redundant GEFs whose roles are revealed by their deletion mutants: Scd1 is primarily involved in polarized growth, and Gef1 is primarily involved in septum formation and initiation of bipolar growth (Coll *et al.*, 2003; Hirota *et al.*, 2003). Both of these GEFs localize to cell tips and the septum (Hirota *et al.*, 2003), and their partial redundancy is demonstrated by the synthetic lethality of *gef1Δ scd1Δ* mutants (Coll *et al.*, 2003). Only one GAP for Cdc42 has been reported, and deletion of that GAP, Rga4, results in wide cells, though it has a relatively minor

effect on total Cdc42 activation. Rga4 localizes to cell sides, and its overexpression causes cells to grow a narrower tip (Das *et al.*, 2007; Tatebe *et al.*, 2008). I also found this gene in my study, and its role in cell-width determination will be discussed in more detail in Chapters 2 and 3. Rga6 may also act as a GAP for Cdc42, and there is evidence that these two GAPs are partially redundant (P.Perez, unpublished data).

Cdc42 controls growth polarization through the activation of several different effectors. Since the protein structure of Cdc42 is highly conserved, as are the effectors, some of their roles have been inferred, in part, from experiments in budding yeast. Cdc42 regulates directed transport in interphase through the fission yeast formin For3, which is required for the formation of actin cables. For3 is autoinhibited by the intramolecular interaction of N- and C-terminal domains of the protein, which is relieved by binding activated Cdc42, the Cdc42-binding protein Pob1 (Rincon *et al.*, 2009), and the actin-binding protein Bud6 (Feierbach *et al.*, 2004). For3 mutants that cannot self-interact, and so do not autoinhibit, form more actin cables, and mutant alleles of Cdc42 that do not interact with For3 have a reduction in actin cables (Martin *et al.*, 2007). In addition, Cdc42 and Pob1 contribute to For3's localization to cell tips (Rincon *et al.*, 2009).

Cdc42 controls the activation of the essential kinase Pak1, which is also known as Shk1 or Orb2 (Marcus et al., 1995; Ottilie et al., 1995). This kinase may be one of the key Cdc42 effectors in fission yeast, since the lethal phenotypes of *cdc42Δ* and *pak1Δ* mutants are very similar. Pak1 is essential for growth; *pak1Δ* spores divide a couple of times and arrest as small, round cells, and overexpression of Pak1

can partially suppress the defects of cells expressing dominant-negative Cdc42 (Marcus et al., 1995). Partial-loss-of-function mutants of Pak1 have defects in bipolar growth, actin polarization, and microtubule organization (Qyang et al., 2002; Sawin et al., 1999). Like other PAK kinases, Pak1 is a multi-domain protein. It has a C-terminal kinase domain, and an N-terminal regulatory region that binds activated Cdc42 via a CRIB domain and also interacts with a scaffold protein, Scd2 (Chang *et al.*, 1999; Endo *et al.*, 2003). Pak1 is autoinhibited by an intramolecular interaction where the CRIB domain binds the kinase domain. This autoinhibition is relieved when the CRIB domain binds Cdc42-GTP, releasing the kinase domain and activating the kinase (Tu and Wigler, 1999). As a main effector of Cdc42, Pak1 itself is likely to have multiple downstream effectors, and it plays roles in cytokinesis and tip growth. Pak1 is one of the kinases that phosphorylates the class I myosin Myo1, which is essential for its role in fluid-phase endocytosis, though not for its role in actin localization or overall cell morphology and growth (Attanapola *et al.*, 2009). Pak1 localizes to the actomyosin ring and phosphorylates the myosin regulatory light chain, delaying cytokinesis until nuclear segregation is complete (Loo and Balasubramanian, 2008). Tea1 is phosphorylated by Pak1, which may link Cdc42 activation to Tea1 regulation (Kim *et al.*, 2003). Pak1 is negatively regulated by the essential kinase Skb15 (Kim *et al.*, 2001), and is capable of autophosphorylation (Ottilie *et al.*, 1995). A closely related kinase, Pak2, plays only a minor role in growth regulation but, if overexpressed, can compensate for the loss of Pak1 function (Yang *et al.*, 1998)

Cdc42 also regulates the conserved protein complex known as the exocyst, which directs membrane, protein, and cell wall addition by exocytosis. Because many of the components and regulatory functions are conserved between budding yeast and fission yeast, and the exocyst has been better characterized in budding yeast, I will describe some of the evidence for Cdc42 regulation of exocytosis in budding yeast. Genetic screens for secretion mutants revealed that several small GTPases control different aspects of exocytosis. Cdc42 controls exocytosis during the polarized growth of the early bud, as seen in a temperature-sensitive *cdc42* mutant that accumulates vesicles at the restrictive temperature without disruption of actin polarization (Adamo *et al.*, 2001). The location of the exocyst is not disrupted in this mutant, so in this case activation of the exocyst may be important. But Cdc42p is involved in the localization of other exocyst components: direct Cdc42p binding influences the localization of the exocyst component Sec3p (Zhang *et al.*, 2008), and the Cdc42-interacting scaffold Bem1p directly binds the exocyst activating protein Sec15p, and mediates its localization to the bud (France *et al.*, 2006). Genetic data suggests that another exocyst component, Exo70p, may also be a downstream effector of Cdc42p (Wu *et al.*, 2010).

Table 1.1:

S. pombe	*S. cerevisiae*	Protein function
cdc42	*CDC42*	small GTPase
scd1	*CDC24*	GEF
scd2	*BEM1*	scaffold
pak1	*STE20, CLA4*	PAK kinase
for3	*BNI1*	formin

Table 1.1: Orthologs of genes that interact with *cdc42*. Orthologs identified using YOGY application, Inparanoid ortholog identification (Penkett *et al.*, 2006). Please note that the orthologous members of the exocyst complex have the same name in *S. cerevisiae* and *S. pombe*.

In fission yeast Cdc42 also regulates the localization of the exocyst. The temperature-sensitive mutant *cdc42-1625* disrupts the cell-tip localization of the exocyst components Sec8 and Sec15 (Bendezu and Martin, 2011). The cell-tip localization of the exocyst component Sec8 also depends on the essential Cdc42-binding protein Pob1 (Nakano *et al.*, 2011). As mentioned above, Pob1 also binds to and regulates the formin For3, but actin-cable-based transport of secretory vesicles and polarized localization of the exocyst form two largely independent pathways for polarized growth (Bendezu and Martin, 2011). Though many details of how exocytosis is regulated in fission yeast remain unknown, it is clear that Cdc42 activation localizes exocytosis to the cell tip, and that the exocyst is a potentially important set of effectors.

Other Rho GTPases have specialized roles in exocytosis

In fission yeast, exocytosis is also regulated by two other Rho proteins, Rho3 and Rho4. The roles of these two proteins demonstrate specific regulation of exocytosis. Rho3 was isolated as a suppressor of a temperature-sensitive mutant of the exocyst component Sec8 (Wang *et al.*, 2003). This GTPase is essential only at high temperatures, when vesicles accumulate within the *rho3Δ* mutant. Rho3 interacts physically and genetically with For3, and so may play a role in coordinating polarized transport and exocytosis (Nakano *et al.*, 2002). Rho4 also influences secretion, but it has a very specific role—the major defect of *rho4Δ* mutants is the formation of multiseptated cells (Santos *et al.*, 2003), which can be suppressed by overexpression of the glucanases Eng1 and Ang1 (Santos *et al.*, 2005). This GTPase is specifically important after cell division, for the secretion of the enzymes that degrade the septum to allow the two daughter cells to separate completely.

Orb6 regulates cell separation and polarized growth

The conserved NDR-kinase Orb6 is an essential protein with roles in cytokinesis and polarized growth. Orb6 loss-of-function mutants are round and divide at a smaller size, while Orb6 overexpression causes cells to be delayed in G2 and divide at a larger size (Verde *et al.*, 1998). Orb6 localizes to growing cell tips and to the cell center, and it physically and genetically interacts in a complex with Mob2, Mor2, Nak1, and Pmo25, proteins involved in cell-cycle regulation and polarized

growth. Pmo25 and Nak1 localize to cell ends during polarized growth, but to the spindle pole body during early mitosis and anaphase. Orb6 is activated by Pmo25 and Nak1, which could link Orb6's growth regulation to the cell cycle (Kanai *et al.*, 2005). Orb6 also regulates the localization of the Cdc42 GEF Gef1 to cell tips, which is one of the mechanisms restricting the activation of Cdc42 (Das *et al.*, 2009).

Ras1 regulates mating and morphology through spatially separated pathways

Fission yeast has one Ras G-protein, Ras1, which stimulates effector proteins in two different pathways. The deletion mutant *ras1Δ* is sterile and rounded, but these two phenotypes are separable. Ras1 activates the kinase Byr2 to mediate pheromone signaling in the mating pathway, and loss of this activation makes cells sterile but does not affect cell shape (Wang *et al.*, 1991). Ras1 plays a role in cell shape through its activation of the Cdc42 GEF Scd1. Deleting Scd1 causes morphology defects, but cells can still respond to pheromone signaling (Chang *et al.*, 1994). Thus, Ras1 can activate two separate pathways that have nonredundant functions (Papadaki *et al.*, 2002). These two pathways are kept separate through differential localization to two different cell membranes, the plasma membrane for pheromone signaling and the endomembrane for Scd1 activation leading to normal cell morphology (Onken *et al.*, 2006). Ras1 is localized to those two membranes through post-translational lipid addition. Farnesylation is required for localization to either membrane, and a reversible palmitoyl addition mediates the localization to the plasma membrane. A mutant allele of Ras1 that cannot be palmitoylated restores normal cell morphology, but not pheromone signaling and mating.

Figure 1.3

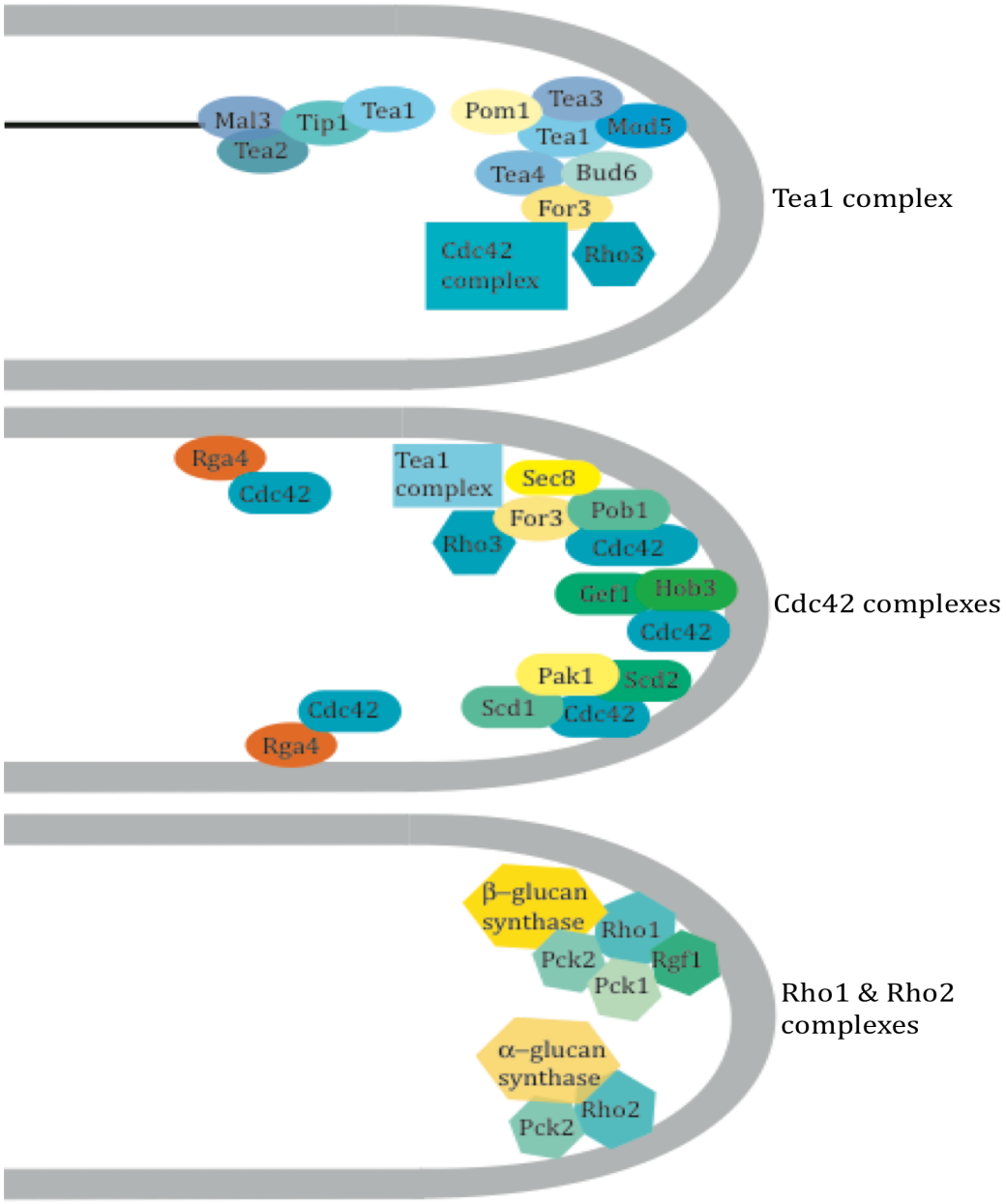

Figure 1.3: Protein complexes at cell tips direct growth. These diagrams of tip-localized proteins do not show all of the regulators; see text for details. Cdc42 in particular is present in multiple complexes that may regulate different effectors. Positive regulators are shown in green, negative regulator in red, and known effectors in yellow. For the GTPases, the GTP-bound form promotes growth at the cell tip.

Morphology pathways interact to shape the cell

Although I have described the above proteins in separate pathways, there is crosstalk between the pathways. One source of crosstalk is that the shape of the cell also influences proteins that direct growth. For example, mutants that are round almost always have defects in microtubule organization (Mendoza et al., 2005; Verde et al., 1995), but it is difficult to determine whether that is due to microtubules responding to the cell shape, or due to an active role for the mutated gene in microtubule regulation. When a cell forms a supernumerary growth zone, due to microtubule disruption or gene deletion, the proteins that activate growth, such as Pak1, Rho1, and Rho2, are localized to these new growth zones (Arellano et al., 1997; Castagnetti et al., 2007; Hirata et al., 1998; Qyang et al., 2002). The *tea1Δ* mutant forms these T-shaped cells, which would also indicate that Tea1 acts upstream of the growth-activation proteins that localize to the new tip. But Pak1 also phosphorylates Tea1 (Kim *et al.*, 2003), which would imply that Tea1 acts downstream of Pak1. Pak1 also phosphorylates Rga8, a GAP of Rho1 (Yang *et al.*, 2003). This could reduce the GAP activity of Rga8, thus promoting Rho1 activation and cell-wall production in response to the activation of Cdc42. As described above, the main formin involved in tip growth, For3, is regulated by the Tea1-complex-member Tea4, activated Cdc42, Bud6, and potentially Rho3. These interactions between pathways can complicate the interpretation of deletion phenotypes, and reflect the intricate regulation of cell morphology.

What controls growth zone size and de novo formation?

These findings on fission yeast growth and morphology have been informative about how growth occurs and how the location of the growth zone is determined. The mechanisms of growth and growth positioning form the framework for the experiments described in this thesis. But the published work tells us little about how the size of the growth zone is determined. As described above, the determination of cellular dimensions on the level of the whole cell is not well understood in any cell type. The body of work describing fission yeast growth, and the proteins that influence growth, combined with the cells' regular shape and genetic amenability, allowed me to use fission yeast to approach this basic biological question: How is the size of a cell's growth zone determined?

The study of short and long mutants in fission yeast provided a genetic key to understanding the cell cycle. Bent and T-shaped cells led to better understanding of growth zone positioning and microtubule dynamics and assembly within the context of the cell. The width of the fission yeast cell is very regular, and so I decided to use cell width as a model for the general control of cellular dimensions. To investigate how the size of the fission yeast growth zone is determined I used three different experimental approaches. The first was a genetic screen for deletion mutants that altered the width of normally growing cells. Using the results of that screen I then characterized the genetic interactions and specific protein localizations in selected mutants that were wider than wild-type cells. Finally, I used the reestablishment of the growth zone from depolarized cells to investigate how the cellular dimensions are established de novo.

Chapter 2: Screening for width mutants and genetic interactions

Introduction:

Although the transition to polarized growth has been studied extensively, much less work has been done on the determinants of the size and shape of the subsequent polarized growth zones. The fission yeast cell provides a useful model for investigating this problem because it has well-defined polarized tip growth zones where the size and shape of the growth zone is stably maintained. The cell is rod-shaped and grows by length extension at the cell tips where actin patches, glucan synthases, and endocytosis are concentrated. Throughout the growth cycle, cells maintain a near-constant width of about four microns (Hayles and Nurse, 2001).

The genetic control of this near-constant cell width has only recently begun to be explored. Two mutants that are still polarized but have altered cell widths have been described: a deletion of the GAP *rga4,* which increases the diameter of the cell by 10% (Das et al., 2007), and a deletion of the GAP *rga2*, which decreases the diameter of the cell by 9% (Villar-Tajadura et al., 2008). These mutants demonstrate that specific genes can influence cell width, and they implicate small GTPases as key factors in cell-width control. They have relatively small phenotypic effects and so would be difficult to identify using traditional genetic screens. Both mutants were identified because of their homology to known GAPs and were then subsequently found to have altered cell widths.

The development of a whole-genome gene deletion collection (Kim et al., 2010) allows the systematic examination of mutant strains to identify genes that determine cell width. To achieve this, I performed a non-biased visual screen of a subset of a near-genome-wide collection of the viable gene deletions. I screened for mutants that were wider or narrower than wild-type cells, and found eleven wide mutants, seven of which are implicated in the regulation of the small GTPase Cdc42. I did not find any mutants that were thinner than wild-type, despite specifically tailoring part of the screen to try to find them. I conducted epistasis analysis with selected wide mutants to determine how the genes that change width interact with one another.

Results:

Screening for width mutants

To identify genes that affect cell width when deleted, a subset of the whole-genome gene-deletion collection was used to conduct an unbiased genetic screen for viable width mutants (Figure2.1A). The viable haploid deletion mutants available at the time of the screen covered 85% of the haploid deletion library (Kim et al., 2010). These deletions were constructed as heterozygous diploids that were induced to sporulate, and the mutant spores were then selected by drug resistance.

A primary screen was carried out by observing morphology phenotypes in microcolonies on plates during spore germination and initial cell divisions (Jacqueline Hayles, manuscript in preparation), and identified a group of 97 viable mutants as candidates for increased cell width and 41 candidates for decreased cell

width. These candidates included mutants that were wide, irregular in shape, or almost completely depolarized. To distinguish between unpolarized spherical mutants and polarized mutants with a wider growth zone, I elongated cells by blocking cell-cycle progression, but not growth, with the ribonucleotide-reductase inhibitor hydroxyurea (HU) (Sazer and Sherwood, 1990), and measured the width of each polarized mutant near the tip of the cell (Figure 2.1B). Wild-type cells, when arrested in HU for five hours, widened slightly, from an average of 3.9μM to an average of 4.1μM, so mutants grown in HU were compared to wild-type cells grown in HU. The widths measured in the secondary screen can be found in Table 2.1, and are graphed in Figure 2.2A. Images of the putative wide mutants can be found in Appendix 1. Because the objective of this screen was to isolate mutants with a specific phenotype—normal polarity but abnormal width—mutants that had other phenotypic defects, such as a grossly irregular shape, were excluded but will be described in a separate manuscript (Jacqueline Hayles, manuscript in preparation). One morphology mutant, *tea1Δ*, was previously noted to be wide (Foethke *et al.*, 2009), but was not found to be wide in this screen (Table 2.1), perhaps due to differences in measurement protocol given that Foethkke et al. measured cells by tubulin fluorescence, not by cell shape in brightfield images.

The primary screen also identified 41 viable long mutants that might have been thinner than wild-type. The screen for thin mutants was based on the idea that a mutant that was thinner that wild-type would also be longer than wild-type, if there was no cell cycle disruption and overall cell volume was maintained. Secondary screening for thin mutants identified nine putative mutants, but upon

regrowth and remeasuring in the tertiary screen none of them was less that 3.5μM in average diameter (10% thinner than wild-type), so this category of thinner mutants was not pursued further.

Wide mutants are enriched for regulators of the small GTPase Cdc42

Using a cutoff of >4.6 μM (0.5μM wider than wild-type cells), I identified 26 wide mutants for rescreening by measuring exponentially growing cells. The tertiary screen identified eleven mutants that were at least 10% wider than wild-type cells in both hydroxyurea and exponential growth (Figure 2.2B). Three criteria were used to exclude mutants that were wide in the secondary screen from the final group of wide mutants: some mutant strains were sickly and grew very poorly in exponential culture, ten mutant strains that were wide in the initial measurement in hydroxyurea were not wide in exponential culture, and two of the deletion mutants proved to be diploid. The large class of mutants that were wide when blocked in the cell cycle, but not in exponential growth, may indicate that the width of the cell can be reset during cell division. This group could be interesting for further study.

Figure 2.1:

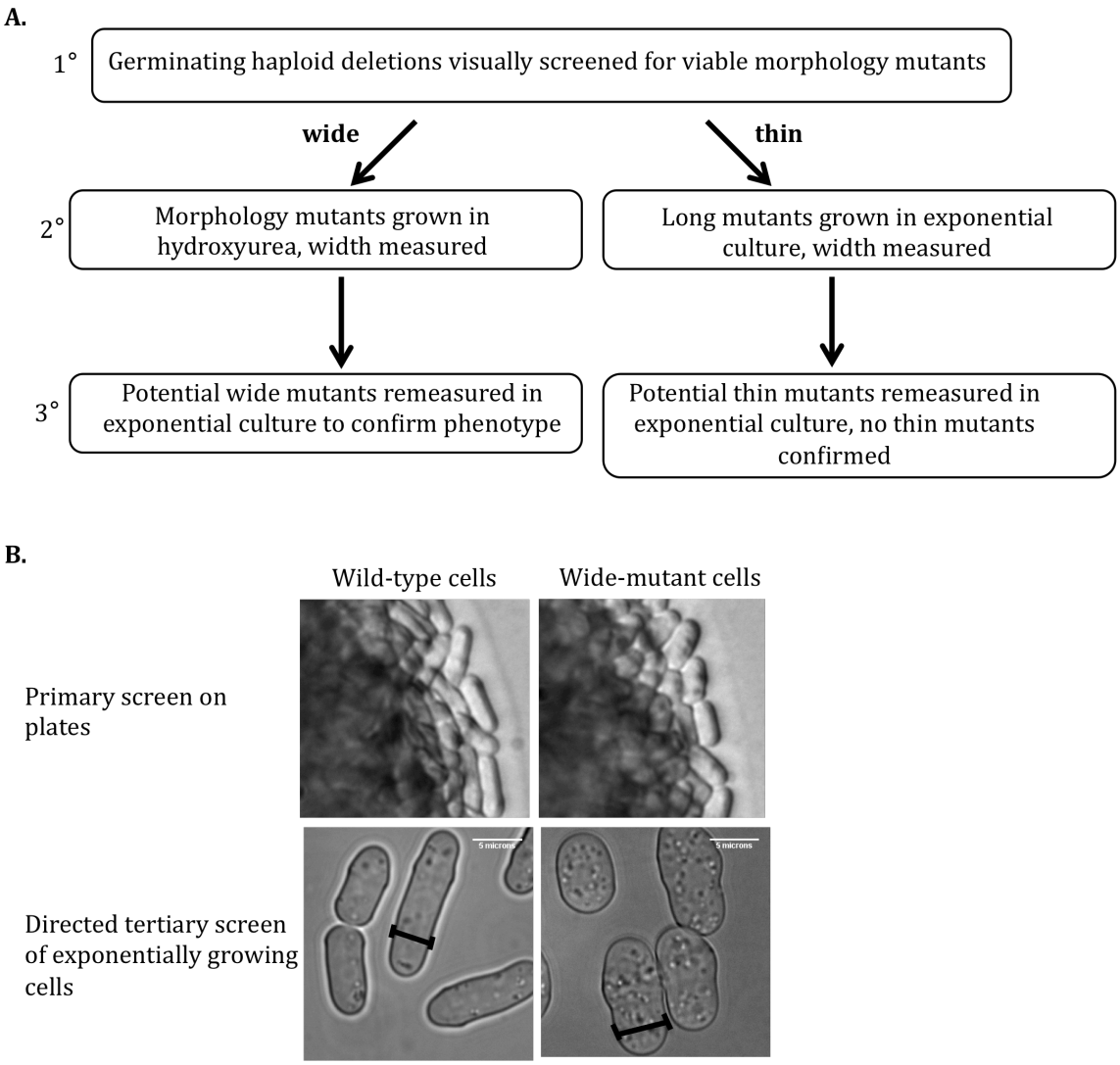

Figure 2.1: Screening for width mutants. A. Three-step screen for wide and thin deletion mutants. Potential wide mutants were grown for 5 hours in hydroxyurea to elongate cells and differentiate between round and wide cells. **B.** An example of cells of wild-type width and a wide mutant (*scd2Δ*) in the primary and tertiary screens. The black lines indicate where the width would be measured on each of these cells, near the cell tip. The scale bars in the lower panels are 5 microns.

Table 2.1:

gene deleted	average width, microns	SD
trm112	3.73	0.18
mal3	3.73	0.27
tea1	3.92	0.30
tea2	3.92	0.29
gyp10	3.93	0.26
pmc5	3.95	0.26
pep3	3.99	0.23
clp1	3.99	0.19
SPAP27G11.06c	4.02	0.24
spn3	4.02	0.30
SPCC794.11c	4.03	0.26
wee1	4.04	0.22
SPAC8C9.11	4.05	0.22
SPAC1F5.05c	4.05	0.21
rgs1	4.05	0.23
SPAC513.06c	4.05	0.20
set3	4.08	0.20
SPAC637.06	4.08	0.33
pom1	4.09	0.34
gps2	4.10	0.30
alg5	4.11	0.27
SPBC119.12	4.11	0.32
SPAC23H4.17c	4.12	0.26
alp14	4.12	0.25
chr3/cfh1	4.13	0.26
SPAC1B2.02c*	4.13	0.16
SPCC1919.15	4.15	0.25
SPCC584.11c	4.16	0.40
sce3	4.16	0.21
WT	4.17	0.27
SPCC4F11.03c	4.18	0.27
SPBC16H5.08c	4.18	0.24
SPAC1071.04c	4.20	0.25
SPBC27.02c	4.21	0.29
cap1	4.21	0.27
alg6	4.22	0.33
vps45	4.25	0.29
ubr1	4.26	0.25
SPBC9B6.07	4.26	0.28
brl1	4.26	0.29
for3	4.27	0.28
alm1	4.28	0.35
SPAC11E3.05*	4.29	0.23
SPAC7D4.12c	4.29	0.25
meu29	4.29	0.36
SPAC1071.02*	4.29	0.23
atp10*	4.29	0.23
SPAC227.01c	4.29	0.26
SPAC607.04	4.30	0.38
SPBC4F6.12	4.31	0.37

gene deleted	average width, microns	SD
pek1	4.32	0.32
SPAC11E3.05	4.33	0.25
SPAC3H1.11	4.34	0.26
SPAC2G11.07c	4.35	0.34
SPAC323.05c	4.35	0.26
SPAC1006.03c	4.36	0.32
alp13	4.39	0.32
pdt1	4.39	0.28
sec14/spo20	4.39	0.28
ogm1	4.40	0.34
sat1	4.41	0.46
iws1	4.41	0.43
rdi1	4.41	0.27
SPAC1071.06	4.44	0.36
SPBC30B4.04c	4.45	0.37
rdr1	4.46	0.52
SPAC1782.05	4.46	0.55
par1	4.49	0.33
SPBC8D2.17	4.49	0.30
rga6	4.51	0.30
SPCC63.02c	4.53	0.40
SPBC3E7.15c	4.53	0.44
pub1	4.55	0.33
SPAP27G11.06c	4.58	0.31
SPAC959.04c	4.54	0.24
pab1	4.60	0.28
scd1- partial deletion	4.60	0.62
pmp1	4.62	0.43
SPAC13G6.10C	4.65	0.29
cpp1^	4.70	0.49
SPBC30B4.03c	4.72	0.39
spy1/mpr1	4.72	0.35
SPAC824.02	4.78	0.28
ral2	4.78	0.32
SPAC1F5.05c	4.79	0.34
kin1	4.81	0.53
pmr1	4.82	0.45
myo52	4.94	0.42
asp1	4.96	0.41
rga4	4.99	0.40
efc25	5.00	0.37
myo1	5.01	0.51
yak4	5.05	0.43
SPAC821.05	5.10	0.33
ras1	5.16	0.37
SPBC31F10.10c	5.48	0.86
scd2	5.50	0.36
cta4*	5.65	0.35
scd1	5.73	0.56

Table 2.1: Widths of putative wide mutants grown in hydroxyurea. Average cell width and standard deviation after 5 hours' growth in hydroxyurea. Mutants marked with an asterisk (*) grow only in YE4S media; those with a caret (^) are temperature-sensitive and grow better at 25°C than at 32°C.

Seven of the eleven genes identified in the tertiary screen (*scd1*, *scd2*, *rga4*, *ras1*, *cpp1*, *ral2*, and *efc25*) are linked to the regulation of the small GTPase Cdc42 (Figure 2.2C). Scd1 is the main GEF for Cdc42 (Chang et al., 1994; Fukui and Yamamoto, 1988), and binds Cdc42 in a complex with the scaffold Scd2 (Chang et al., 1999). Ras1 acts upstream of Scd1, presumably in its activation (Chang et al., 1994), and the Ras1 activity related to cell morphology is regulated by Efc25 (Papadaki et al., 2002; Tratner et al., 1997) and Ral2 (Fukui et al., 1989). Ras1 is probably farnesylated by Cpp1 (Yang et al., 2000). Rga4 is a predicted GAP that can affect the activation state of Cdc42 (Das et al., 2007; Tatebe et al., 2008). Our near-genome-wide screen for width mutants was not biased towards genes in any particular genetic pathway, and so the fact that seven of the eleven wide mutants are missing genes involved in Cdc42 regulation suggests that this pathway is a major mechanism for the determination of cell width.

Among the final group of eleven mutants, six (*scd1Δ*, *scd2Δ*, *ral2Δ, efc25Δ, ras1Δ, cpp1Δ*) had been previously described as spherical, implying they were depolarized (Chang et al., 1994; Fukui and Yamamoto, 1988; Tratner et al., 1997; Yang et al., 2000), but I found that these mutants were actually polarized and wide, as revealed by growth in hydroxyurea. The deletions *scd1Δ* and *scd2Δ* are two examples of wide mutants that may look round in exponential culture, but are clearly polarized when cells are elongated by growth in hydroxyurea (Figure 2.3). All of the wide mutants were able to polarize growth and none were spherical. It has been theorized that a spherical fission yeast would not be viable because the cell uses its rod shape to organize the division plane (Ge *et al.*, 2005).

Figure 2.2:

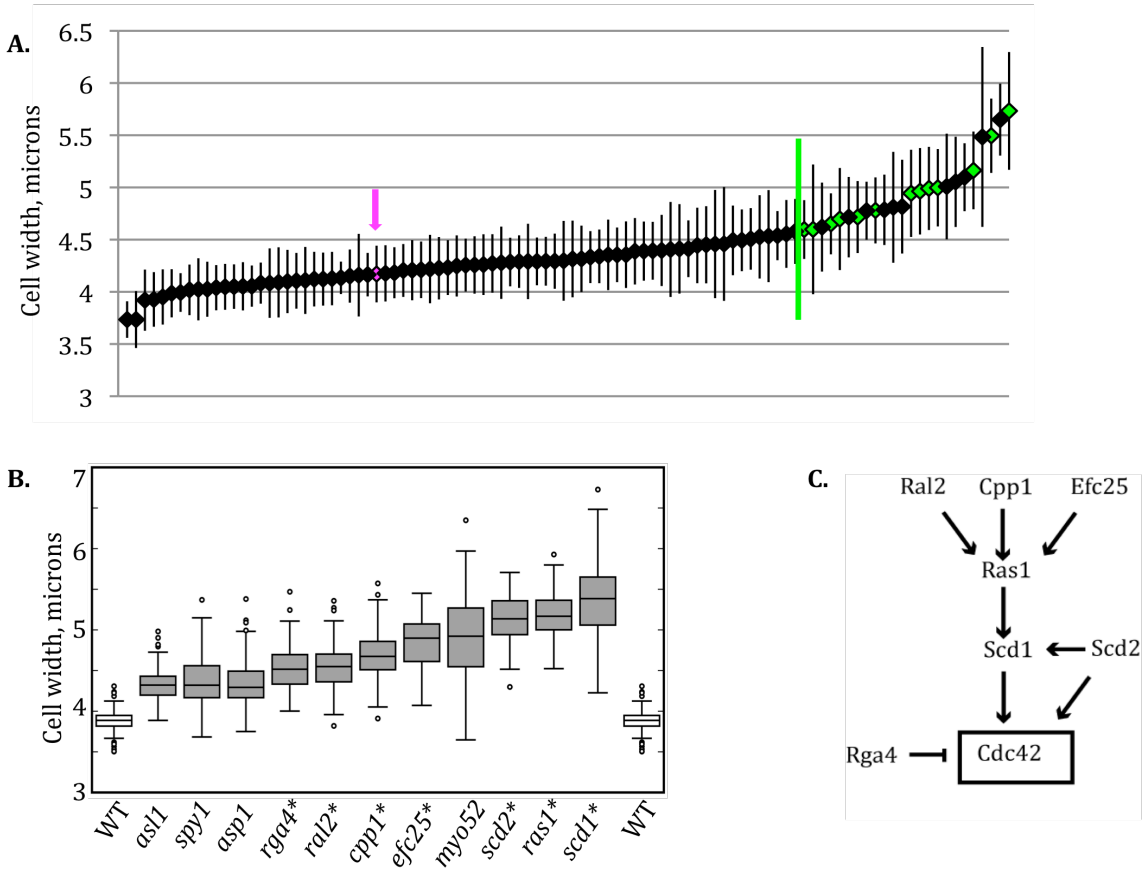

Figure 2.2: Genes that influence cell width. **A.** Average widths of 97 deletion mutants grown in HU are plotted in ascending order; error bars represent one standard deviation. Magenta arrow and magenta diamond indicate wild-type. Green line indicates the cutoff for mutants selected for tertiary screening. Green diamonds indicate mutants that were ultimately found to be wide. At least 40 cells were measured for each strain. **B.** Box-and-whiskers plot of the cell widths of wild-type and eleven deletion mutants isolated from the gene deletion collection. At least 100 exponentially growing cells were measured for each strain. Boxes indicate one quartile of the distribution in each direction. Asterisks indicate genes implicated in Cdc42 regulation. All mutant widths are significantly different from wild-type by Student's T-test with $p < .0001$. **C.** Of the eleven deletion mutants identified, seven have been implicated in the control of Cdc42 (see text). Arrows indicate positive regulation; T indicates negative regulation.

Figure 2.3:

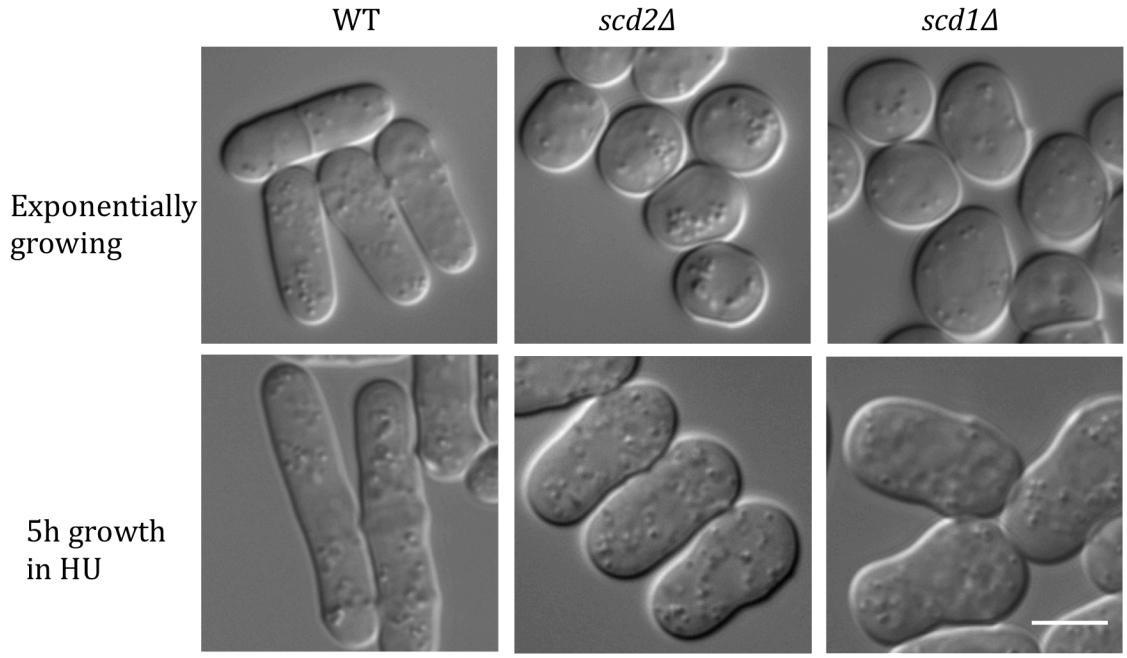

Figure 2.3: Wide mutants can polarize growth. Both *scd1Δ* and *scd2Δ* have been previously described as round or rounded, but their wide, polarized growth pattern is apparent when they are grown for 5 hours in hydoxyurea. DIC images; scale bar represents 5 microns.

Wide mutants not predicted to influence Cdc42 regulation

Four mutants were identified that are not directly connected to the control of Cdc42: *myo52Δ*, *spy1Δ, asp1Δ,* and *asl1Δ*. Myo52 is a type V myosin, one of two in fission yeast, and has been described as rounded (Motegi *et al.*, 2001; Win *et al.*, 2001). Type V myosins are generally involved in directed vesicle transport along actin cables (Titus, 1997), and directed transport is important for polarized cell growth, so *myo52Δ* may be wide due to a defect in the delivery of either materials important for cell wall growth or other proteins that regulate cell width.

Spy1, also known as Mpr1, is a phosphorelay protein that is involved in transducing the signals for oxidative stress. The deletion mutant was previously noted for its short cell length and ovoid shape, and due to the cells' reduced length at division the protein was thought to advance the cell cycle (Aoyama *et al.*, 2000). But our screen casts doubt on this conclusion: Because the deletion mutant is both shorter and wider than wild-type, it may have a normal cell volume at division. Asp1 was originally identified as a high-copy suppressor of a temperature-sensitive mutation in the actin regulatory protein Arp3 (Feoktistova *et al.*, 1999). At that time its molecular function was not known, but it has since been identified as an inositol pyrophosphate synthase that phosphorylates inositol hexakisphosphate to generate diphosphoinositol pentakisphosphate and bis-diphosphoinositol tetrakisphosphate (Mulugu *et al.*, 2007). These high-energy inositol derivatives can act as signaling molecules. Asp1 has also been shown to regulate the switch between single-cell and invasive filamentous growth (Pohlmann and Fleig, 2010). Asl1 has not been characterized beyond predictions of function based on homology as a putative

adhesin (Linder and Gustafsson, 2008), and its covalent binding to the cell wall (de Groot *et al.*, 2007).

Most of the wide mutants are not fully corrected by growth in an osmotic stabilizer

I investigated whether the changes in cell width could be due to defects in the cell wall. Fungal cells, like plant cells, maintain an osmotic differential with the surrounding liquid, which results in a constant internal turgor pressure. If a weakened cell wall did not withstand the internal osmotic pressure, the cell would swell, making it wider. Some morphology mutants with defects in cell wall composition can be rescued by the addition of 1.2M sorbitol to the media, which decreases the relative internal pressure in the cell by increasing the external osmolarity (Ribas et al., 1991). Therefore I compared the width of each mutant grown for two generations in media supplemented with 1.2M sorbitol to the width of wild-type cells grown in media supplemented with 1.2M sorbitol. But only one of the wide mutants, *asl1Δ*, was corrected to wild-type width by addition of sorbitol (Table 2.2). Our results suggest that this deletion affects either cell wall integrity or turgor pressure. Deletion of *ras1*, which alters cell wall composition (Harmouch et al., 1995), showed a partial correction, and the largest change in cell width, after addition of sorbitol. But the mutant phenotype could not be completely rescued by sorbitol, so Ras1 may have both cell-wall-dependent and cell-wall-independent effects on width. Since ten of our original eleven wide deletion mutants are not completely rescued by addition of sorbitol, they likely play roles in directly determining the size of the polarized growth zone.

Table 2.2:

	Width in EMM4S, µM	% WT width in EMM4S	Width in EMM4S +1.2M sorbitol, µM	% WT Width in EMM4S + 1.2M Sorbitol	% Change in 1.2M Sorbitol
wild-type	3.88	100	3.81	100	-3
als1Δ	4.35	112	3.90	102	-11
spy1Δ	4.35	112	4.50	118	3
asp1Δ	4.35	112	4.57	120	5
rga4Δ	4.53	117	4.18	110	-8
ral2Δ	4.54	117	4.54	119	0
cpp1Δ	4.70	121	4.40	115	-6
efc25Δ	4.85	125	4.41	115	-10
myo52Δ	4.89	126	5.36	141	10
scd2Δ	5.12	131	4.70	123	-9
ras1Δ	5.19	133	4.48	118	-14
scd1Δ	5.85	150	5.28	139	-10

Table 2.2 Wide Mutant Correction by Sorbitol. Cells were grown in EMM4S or EMM4S + 1.2M sorbitol for at least two generations. The % WT Width compares the width of the mutant strain grown in sorbitol to the width of the wild-type strain grown in sorbitol. The % Change in Sorbitol compares the width of each strain grown in EMM4S + 1.2M sorbitol to the width of that strain grown in EMM4S.

At least two independent pathways act to control cell width.

Deletions of a Cdc42 GEF (Scd1) and its scaffold (Scd2), which are predicted to reduce cellular levels of Cdc42-GTP, and deletion of a Cdc42 GAP (Rga4), which is predicted to increase cellular levels of Cdc42-GTP, all produced wider cells. This apparently paradoxical result could be explained if the GEF and GAP operated independently, perhaps separated either in space or time. I tested these possibilities through genetic epistasis analysis here, and an analysis of localization and retargeting that is described in the next chapter.

Epistasis analysis predicts that proteins that function in parallel independent pathways should have additive genetic interactions, while proteins that function together, either in a linear pathway or in a complex, should not. To test the genetic relationships of the GEF, GAP, and scaffold, I made double mutants and measured their widths (Figure 2.4A). When both the GAP Rga4 and the scaffold Scd2 were deleted, the cells were still polarized but wider than either of the single mutants (Figure 2.4A, B). Similarly, the *scd1Δ rga4Δ* strain, lacking both the GEF and the GAP, was wider than any single mutant, supporting the hypothesis that the GEF and GAP work in parallel to control width (Figure 2.4A, B).

In fission yeast there is another Cdc42 GEF, Gef1, that acts primarily in septum formation but also has a partially overlapping function with Scd1, as evidenced by the synthetic lethality of these two deletions (Coll et al., 2003). The deletion mutant *gef1Δ* does not have an increased cell width (exponential cell width = 3.83μM ±0.25), but like *scd1Δ,* it is additive with *rga4Δ* (Figure 2.4A, B). This

additive interaction may occur because Gef1 is also involved in the activation of Cdc42 at cell tips, although it plays a more minor role than Scd1. Gef1 is mislocalized to cell sides in *orb6* loss-of-function mutants, which results in the loss of cell polarity due to Cdc42 activation, and subsequent growth, on the cell sides (Das et al., 2009), so Gef1 is clearly capable of directing cell growth. The result shows that an *rga4Δ* mutant has an increased sensitivity to the loss of GEF activity, since *gef1Δ* has no effect on cell width on its own, but exacerbates the *rga4Δ* phenotype.

Figure 2.4

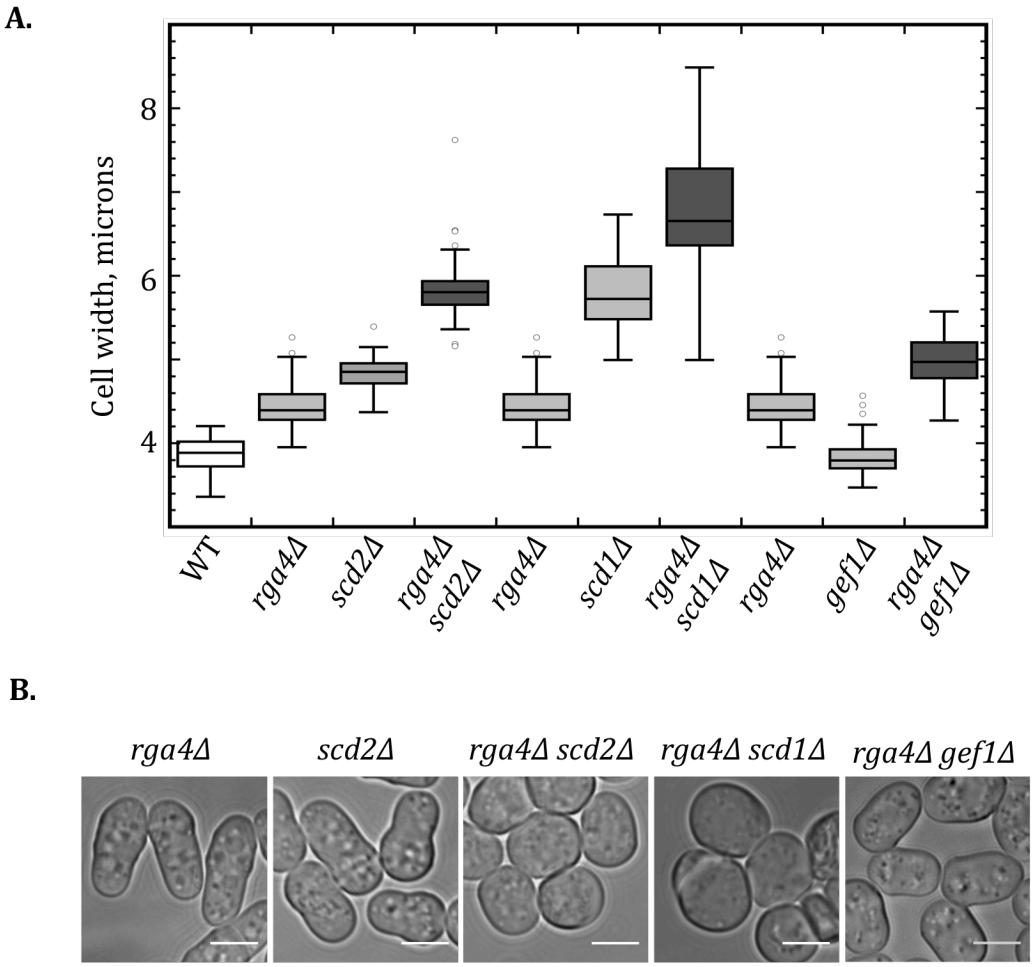

Figure 2.4: At least two independent pathways act to control cell width.

A. Double mutants *scd2Δ rga4Δ*, *scd1Δ rga4Δ,* and *gef1Δ rga4Δ* are additive. Box-and-whiskers plot. At least 50 cells were measured for each genotype. All differences are statistically significant by a Student's T-test with p <.0001

B. Exponentially growing cells, brightfield; scale bars represent 5 microns.

Scd1 and Scd2 influence cell width by the same pathway

In contrast to the additive interactions with *rga4Δ*, double-mutant *scd1Δ scd2Δ* cells, with both the GEF and the scaffold deleted, resembled *scd1Δ* alone (Figure 2.5A, B). Scd2 contains multiple protein-protein interaction domains, including two tandem SH3 domains, a PX domain, and a PB1 domain (Chang *et al.*, 1994; Ponting, 1996). Scd2 is known to bind Scd1, Cdc42, and an essential downstream kinase called Pak1 (Endo et al., 2003; Wheatley and Rittinger, 2005), so the primary effect of deleting *scd2* may be the disruption of this complex (Endo et al., 2003). If localization of Scd1 to the complex is essential to its formation or function then a non-additive genetic interaction would be expected between *scd1Δ* and *scd2Δ*.

Many mutants in the Cdc42 activation pathway have mating defects because the pathway is also involved cell conjugation (Papadaki et al., 2002; Pruyne and Bretscher, 2000). To further explore the genetic interactions between the wide mutants further, I used a wide deletion mutant that acts upstream of Cdc42 activation, through Ras1, but does not have a mating defect (Onken *et al.*, 2006). I crossed this mutant, *efc25Δ*, with three of the four non-Cdc42 mutants and assessed their phenotypes by eye. All of the double mutants were viable, and were wider than either single mutant (Figure 2.5C). The fourth non-Cdc42 mutant, *spy1Δ*, was difficult to cross in our hands, and I did not pursue it further.

Figure 2.5

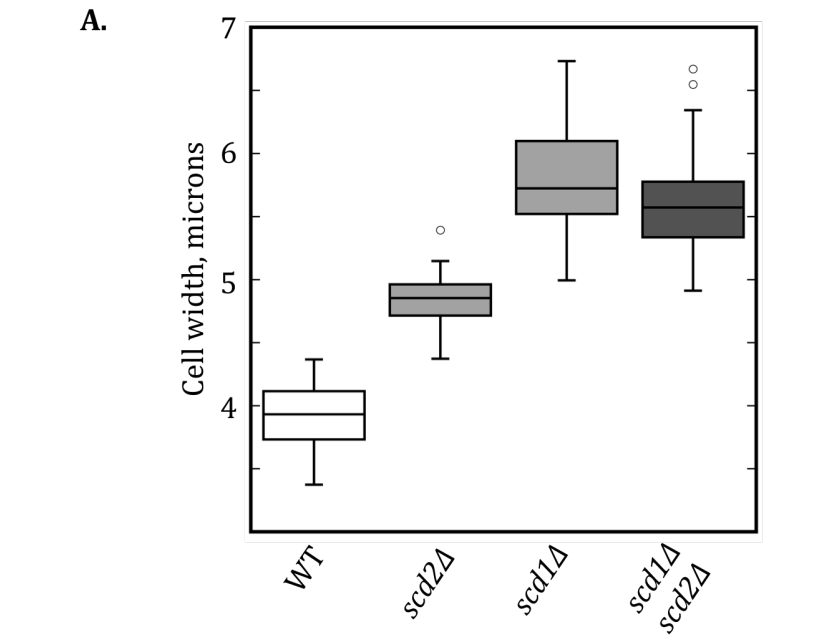

C.

Double mutant	Additive phenotype?
efc25Δ asp1Δ	+
efc25Δ asl1Δ	++
efc25Δ myo52Δ	+

Figure 2.5: Scd1 and Scd2 influence cell width by the same pathway. A. *scd1Δ* and *scd2Δ* are not additive. Box-and-whiskers plot. Cells for this analysis were grown in hydroxyurea for 5 hours to elongate cells and aid width measurements. At least 50 cells were measured for each genotype. **B.** Cells grown for 5 hours in hydroxyurea, brightfield; scale bar represents 5 microns. **C.** Width phenotypes of selected double mutants assessed on plates.

Discussion:

Cell width control is distinct from growth polarization.

Cell width in fission yeast is determined in a two-stage process. Polarization is the first stage, and is an on-off switch—either growth is polarized or it is not. The second stage is the determination of the size of the growth zone, and this near-genome-wide screen was designed to identify the genes important for this second stage. In a polarized cell with a normal cell wall, the size of the tip-localized growth zone will determine the width of the cell, and so I screened for polarized mutants that are wider than wild-type, but not fully corrected by an osmotic stabilization. Even the widest mutants I have identified can polarize growth, as shown through cell elongation when grown in hydroxyurea.

Thin mutants may be less common and less extreme than wide mutants

The screen was designed to screen for wide and thin mutants, but with our cutoff of at least a 10% change in width, I found only wide mutants. Thinner growth zones are possible—cells tips are reduced in diameter when Rga4 is overexpressed (Das *et al.*, 2007), and cells are not obviously growth impaired. A thin mutant is also possible, as shown by *rga2Δ*, which is 89% of wild-type width (Villar-Tajadura *et al.*, 2008). When our screen was conducted, this gene was not in the original pool of mutants, so it would not have been identified in this screen. I did not identify any other thin mutants, although the screen was deliberately designed to capture them. To ensure that we were able to isolate viable thin mutants, if they existed, I screened

41 mutants that were originally characterized as elongated, reasoning that a cell that was slightly narrower but retained normal cell volume would be noticeably longer. It is possible that wild-type cells are near their minimum width. An analysis of nuclear volume found that the average nucleus ranges between 2.3 and 3μM in width during the cell cycle (Neumann and Nurse, 2007), and for nuclear centering by microtubules the nucleus must be able to move within the cell (Tran *et al.*, 2001). Perhaps mutants narrower than the normal width of the nucleus would not be viable. Finally, the minimum width of the cell could be set by a redundant set of inputs, and the phenotype would not be observed very often in this type of single-gene-deletion screen.

Multiple genetic pathways are involved in setting cell width

The epistasis analysis here shows multiple additive interactions between wide mutants, which implies multiple pathway inputs into cell width determination. Among genes that influence Cdc42 activation, the double mutants *rga4Δ scd1Δ*, *rga4Δ gef1Δ,* and *rga4Δ scd2Δ* all showed additive genetic interactions, with the double mutant wider than either single mutant. These genes are all predicted to act through control of Cdc42, but Rga4 may regulate the GTP-to-GDP transition independent of the other three genes, all of which stimulate the exchange of GDP for GTP to activate Cdc42. Our limited analysis of the non-Cdc42 mutants showed that most were additive with a representative mutant from the Cdc42 activation pathway, *efc25Δ*, which supports the idea that they may act outside of Cdc42 regulation, affecting the width of the cell through different means. Additional

epistasis analysis would be necessary to confirm that they were not acting through Rga4's regulation of Cdc42.

The Cdc42 regulatory network controls polarization and growth zone size

Of the genes found in this screen, seven of eleven are involved in the control of Cdc42 activation, establishing its importance in determining growth zone size. Cdc42 has been previously shown to be important in growth polarization, but this study provides an additional role for the regulatory network. In fission yeast, *cdc42* is essential, and spores that lack the gene cannot form germination tubes, because they cannot polarize growth (Miller and Johnson, 1994). In addition, mutations in the essential kinase Orb6 lead to the mislocalization of Cdc42 to cell sides (Das et al., 2009), and render cells round (Verde *et al.*, 1998).

Directed cell growth is a spatially organized process, and to understand better how these mutants might influence growth localization, I fluorescently tagged them and observed their localization in different genetic contexts. The results of those experiments are discussed in the next chapter.

Chapter 3: Specific localizations of Cdc42 regulators are important for their roles in cell-width control

Introduction:

GTPase-regulating GEFs and GAPs are known to regulate Cdc42 spatially to direct cell growth. In budding yeast, the Cdc42 GAP Rga1 localizes to the old bud site and blocks the renewal of budding there. This causes the new bud to form near the site of the old bud, but not at the same spot (Tong *et al.*, 2007). In *C. elegans* development, at the single-cell stage, the GAP CHIN-1 is required for the polarized distribution of Cdc42 on the membrane, and CHIN-1 is localized to the end of the embryo opposite activated Cdc42 (Kumfer et al., 2010). In each these, and many other, cases, the localizations of the regulators are thought to be important to spatially restricted Cdc42 activation.

In *S. pombe*, the deletion mutants *scd1Δ* and *rga4Δ* are both wider than wild-type cells, even though they are predicted to have opposite effects on the activity of Cdc42. Our previous epistasis results suggested that the GEF Scd1 and the GAP Rga4 operate independently, because the double mutant *scd1Δ rga4Δ* has an additive cell-width phenotype. This may be partly explained if the GEF and GAP operate in different places in the cell, as suggested by previous studies of the proteins' localizations: Overexpressed Scd1-GFP and Scd2-GFP localize to growing cell tips (Hirota et al., 2003; Sawin et al., 1999), while Rga4-GFP forms puncta at the cell cortex and is excluded from the cell tips (Das et al., 2007; Tatebe et al., 2008).

Based on localization and function, we hypothesized that these two sets of regulators were acting to control Cdc42 independently and that their spatially separated localizations were important for cell-width determination. I tested these possibilities through genetic analyses of the determinants of localization, disruption of the cytoskeleton, and protein retargeting.

Results:

Rga4 and Scd1/Scd2 localize independently

If Rga4 and Scd1/Scd2 act in parallel pathways controlling width, and if their cellular localizations are important to their functions, then their localizations should be independent of one another. To test this I determined the localizations of Scd1, Scd2, and Rga4 by triple-GFP-tagging the proteins in the endogenous genomic locations in wild-type and mutant cells. The cell width and growth rate for each tagged strain did not differ significantly from those for the wild-type strain, demonstrating that the fusion proteins are functional. These will be referred to as GFP-tagged or -3GFP for the remainder of the study. Rga4-3GFP was primarily localized to the cell sides in wild-type, *scd1Δ*, and *scd2Δ* cells (Figure 3.1A). This was particularly apparent for *scd1Δ* Rga4-3GFP when the cells are elongated by growth in hydroxyurea. Neither Scd1-3GFP nor Scd2-3GFP depended on Rga4 for their localization, as they were unchanged in the *rga4Δ* strain, localizing to the wider cell ends (Figure 3.1B).

Figure 3.1:

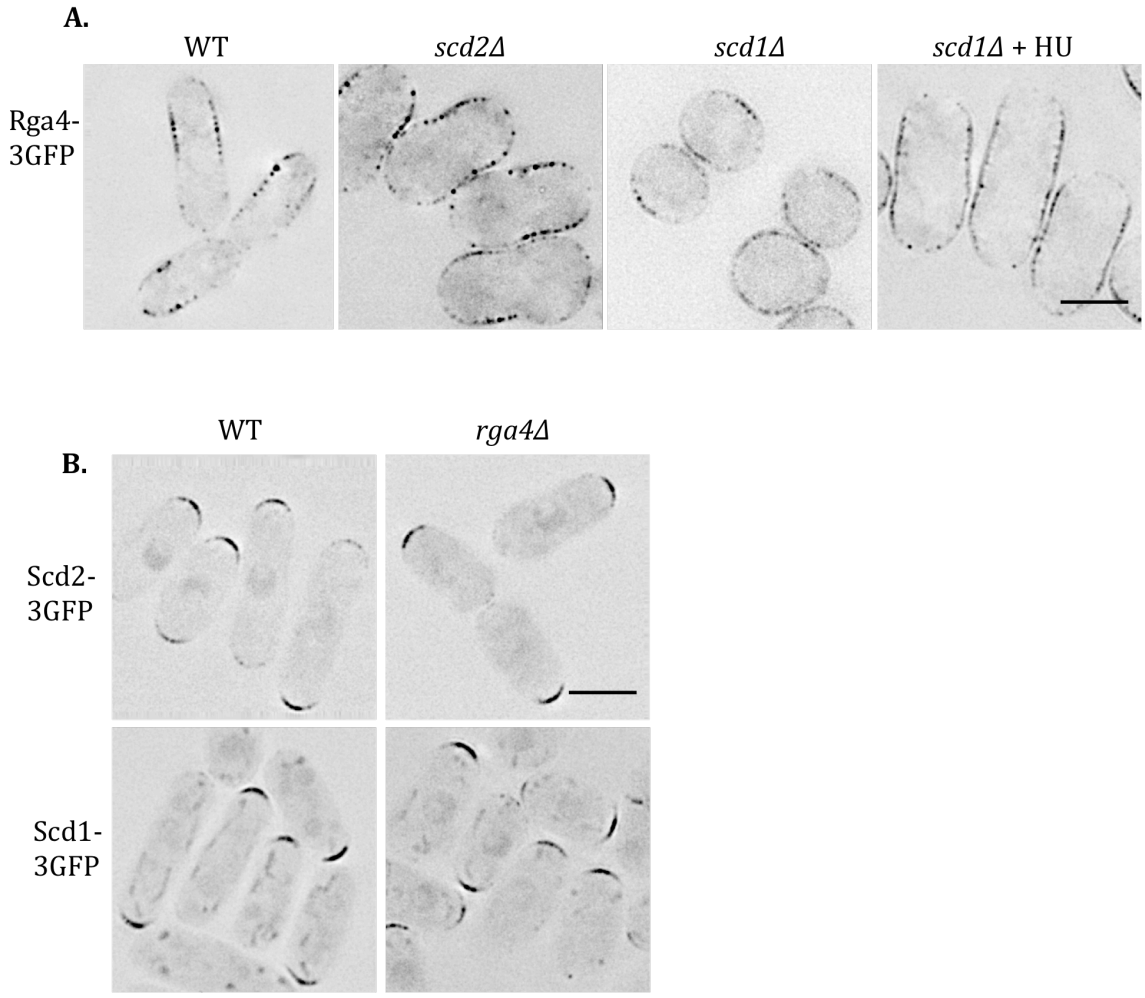

Figure 3.1: Rga4 and Scd1/Scd2 localize independently. A. Rga4-3GFP does not require Scd1 or Scd2 for localization to cell sides. **B.** Neither Scd1-3GFP nor Scd2-3GFP is dependant on Rga4 for localization to cell tips. Images for all are representative, deconvolved, look-up table (LUT) inverted, single focal planes. Scale bars represent 5 microns. Unless marked, cells were in exponential growth at the time of imaging. *scd1Δ* is also shown after growth for 5 hours in HU to elongate the cells.

This comports with the genetic epistasis experiments, which suggested that Rga4 acts in a separate pathway from Scd1 and Scd2. It also helps resolve the apparent paradox that deletion of both positive and negative regulators of Cdc42 can increase cell width. This happens because the two proteins act independently in different locations.

The deletions of *scd1* and *scd2* were not additive. To see if this was because Scd2 was required for the localization of Scd1, I GFP-tagged the endogenous Scd1 in wild-type and *scd2Δ* cells. In wild-type cells, Scd1-GFP localized to the growing cell ends, as has been reported for the over-expressed protein (Hirota et al., 2003). In the *scd2Δ* mutant, the cell-end localization of Scd1-GFP was lost, and most of the protein was found in the cytoplasm and nucleus (Figure 3.2A), indicating that Scd2 is required for the localization of Scd1-GFP. If Scd2 directed the localization of Scd1, then its localization to growing cell tips should be independent of Scd1. But I found that Scd2-3GFP is poorly localized to the cell tips in *scd1Δ*, both in exponentially growing cells and in cells elongated by growth in hydroxyurea (Figure 3.2B). These results show that the GEF Scd1 and the scaffold Scd2 are mutually dependent for localization. It had been previously suggested that Scd2 acts upstream of Scd1, since Scd2 overexpression could not rescue a *scd1Δ* mutant (Chang et al., 1994). But our results indicate that the genetic relationship is not that simple—there is at least a mutual dependence for localization, perhaps through a positive a feedback loop in the activation of Cdc42 and recruitment of the complex, as in budding yeast (Wedlich-Soldner et al., 2003).

Figure 3.2:

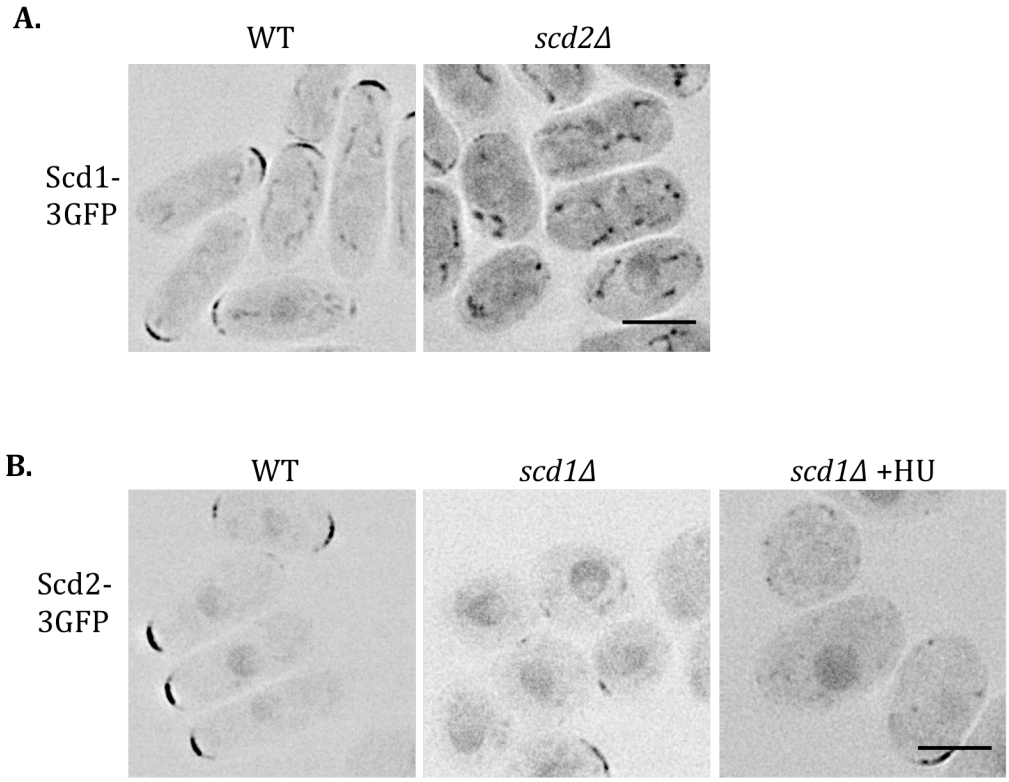

Figure 3.2: Scd1 and Scd2 are mutually dependent for localization. A. Scd1-3GFP is lost from the cell tips in *scd2Δ* cells. **B.** Scd2-3GFP is mislocalized in *scd1Δ*. Images for all are representative, deconvolved, LUT inverted, single focal planes. Scale bars represent 5 microns. Unless marked, cells were in exponential growth at the time of imaging. *scd1Δ* is also shown after growth for 5 hours in HU to elongate the cells.

Scd1 and Scd2 depend on actin for localization, although Rga4 does not.

One source of codependence for localization would be delivery or maintenance by the same cytoskeletal elements that might be disrupted in both mutants. To test the role of actin and microtubules in the localization of these proteins, I incubated cells in either 50μg/mL carbendazim (MBC) to inhibit microtubule polymerization or 100μM Latrunculin A (LatA) to depolymerize actin. After 30 minutes of growth in MBC, both Scd1-3GFP and Scd2-3GFP were still localized to cell tips (Figure 3.3A). In contrast, after treatment with 100μM LatA Scd1-3GFP became diffuse throughout the cytoplasm within 10 minutes. Scd2-3GFP moved away from the cell tips within 30 minutes after LatA addition, but it still seemed to be associated with the cell cortex and still formed patches (Figure 3.3A). It was previously reported that Scd2-GFP localization is disrupted after treatment with thiabendazole (TBZ) and LatA, but the broader spectrum of defects associated with TBZ made these experiments more difficult to interpret (Sawin and Snaith, 2004). Our results indicate that, in addition to being mutually dependent, both Scd1-3GFP and Scd2-3GFP depend on actin, although not microtubules, for their localization.

In contrast, Rga4-3GFP localization is not affected by treatment with LatA (Das et al., 2007), treatment with MBC to depolymerize microtubules, or even treatment with both at the same time, at least within this timescale (Figure 3.3B). These drugs may not completely destroy the cytoskeleton, but they certainly disrupt its normal arrangement, and yet they have no apparent effect on Rga4 localization.

Figure 3.3:

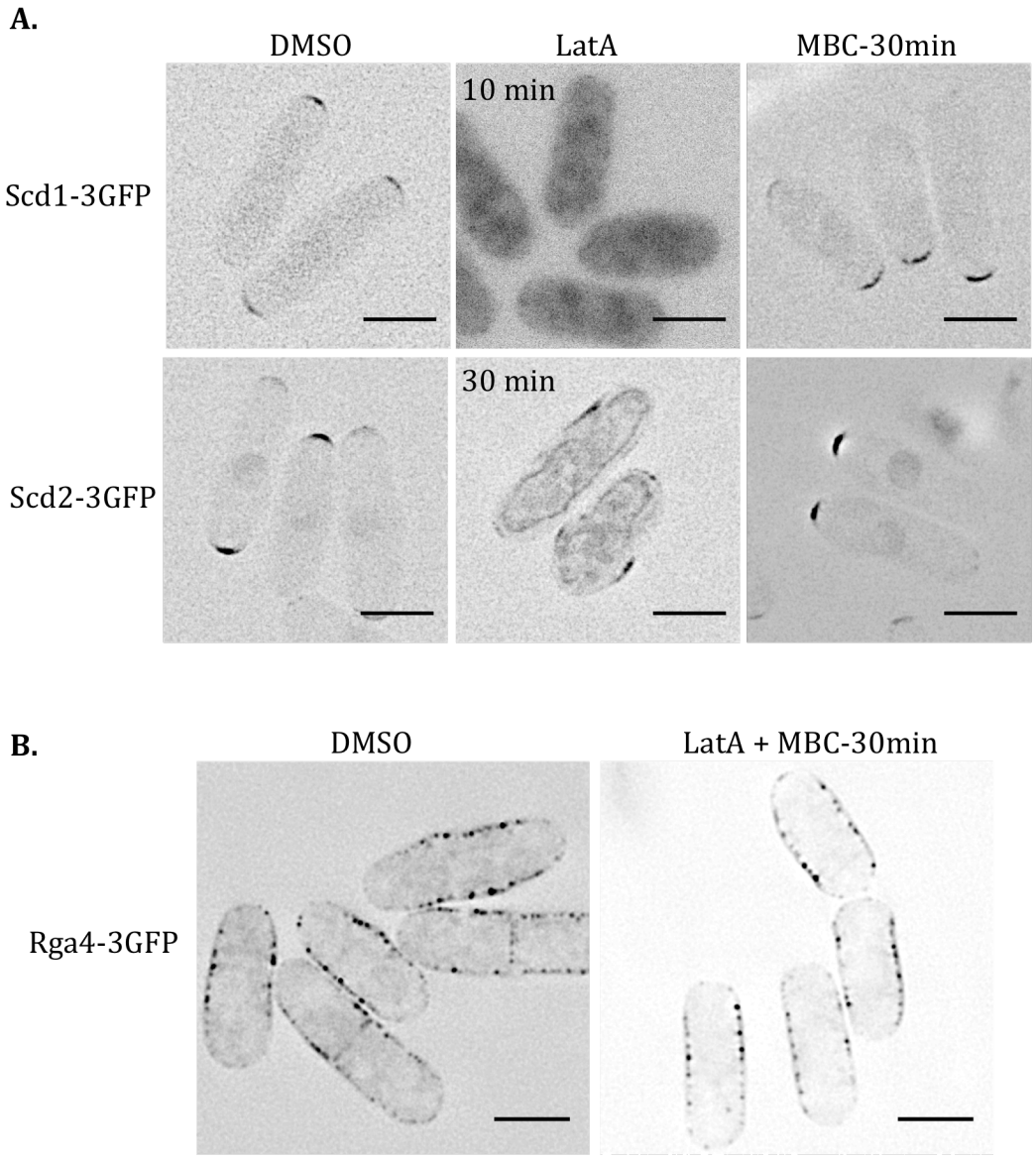

Figure 3.3: Scd1 and Scd2 depend on actin for their localization, although Rga4 does not. **A.** Scd1-3GFP and Scd2-3GFP in DMSO, 100µM Latrunculin A to depolymerize actin, or 50µg/mL carbendazim (MBC) to inhibit microtubule polymerization. Images are LUT inverted, deconvolved, single focal planes. **B.** Rga4-3GFP in DMSO or 100µM Latrunculin A and 50µg/mL MBC. Images are representative, LUT inverted, deconvolved sums of the fluorescence across the middle 1.2 microns of the cell. Scale bars represent 5 microns.

The deletion mutants scd2Δ and scd1Δ maintain polarized growth

Scd1 is the major Cdc42 GEF in fission yeast, and Cdc42 is an essential gene required for polarized growth. As mentioned earlier, growth in HU (Figure 2.3) indicated that *scd1Δ* and *scd2Δ* cells are polarized and are not spherical. To confirm that these cells were polarized I carried out three sets of experiments. First, the polysaccharide stain Blankophor, which selectively stains newly added cell wall, stained each of these mutants more brightly at the cell tip (Figure 3.4A). Second, when these mutants were grown in HU, actin patches, here marked by fluorescently labeled phalloidin, were enriched at the cell tips (Figure 3.4B). This result also shows that actin organization is not grossly disrupted in either mutant. Third, a GFP-tagged CRIB domain, previously shown to be a marker for activated Cdc42 (Tatebe et al., 2008), was located at the cell tips in both *scd2Δ* and *scd1Δ*, although it was less concentrated there than in wild-type cells (Figure 3.4C).

Cdc42-GTP distribution is altered in the scd2Δ mutant.

Although we are studying the extreme end of the distribution of cell widths among the deletion mutants, these cells are still polarized. Because polarity is maintained, it is expected that growth protein localization may be altered rather than completely disrupted.

Figure 3.4:

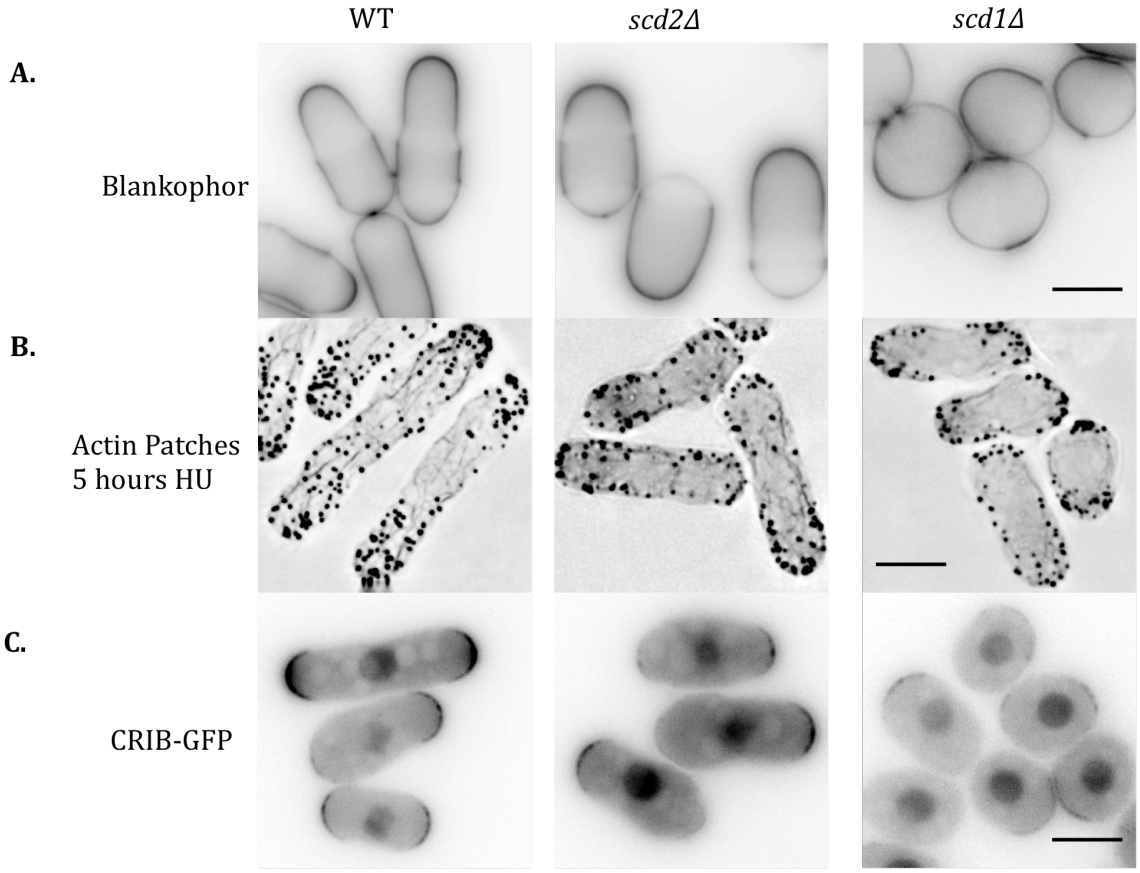

Figure 3.4: The deletion mutants *scd2Δ* and *scd1Δ* maintain polarized growth. **A.** Blankophor staining of exponentially growing cells shows brighter staining at the cell tips. Images are LUT inverted, single focal planes. **B.** Alexa Fluor 488 Phalloidin stained cells grown in HU for 5 hours to elongate the cells. Images are deconvolved, inverted maximum projections of the full cell width. **C.** CRIB-GFP. Images are single, inverted, focal planes. Scale bars represent 5 microns.

As shown in Figure 3.4, the Cdc42-GTP marker CRIB-GFP is still enriched at the cell tips in the *scd1Δ* and *scd2Δ* mutants, but the distribution is altered. Though the protein is not depolarized, an alteration of the distribution of activated Cdc42 could make cells wider. To quantify that alteration, I analyzed the distribution of CRIB-GFP at the cell tip in wild-type and *scd2Δ* cells by drawing a continuous line, five pixels wide, beginning at the center of the cell tip and measuring the average fluorescence intensity along that line. I did 50 line scans, like those illustrated by the white lines in Figure 3.5A, for each genotype. The line scans of CRIB-GFP at the tip of the cell revealed that the *scd2Δ* mutant has a lower peak fluorescence than wild-type cells (Figure 3.5B).

The localization of Rga4-3GFP to cell sides suggested that it might act as a boundary element to restrict the spread of Cdc42-GTP. To investigate this possibility, I analyzed the distribution of CRIB-GFP in *rga4Δ* cells. It has been previously shown that *rga4Δ* does not disrupt overall CRIB-GFP localization to cell tips (Tatebe et al., 2008), but I used linescans to investigate whether there was a quantitative difference in the distribution of Cdc42 within the cell tip in this mutant. The localization of CRIB-GFP in the *rga4Δ* mutant is generally similar to the wild-type distribution. There is some increase in the intensity of CRIB-GFP at the distal portion of the cell tip (between 2.0 and 3.5 microns away from the center of the cell tip) in the *rga4Δ* mutant, which is consistent with boundary-element activity, but this increase is rather small (Figure 3.5C).

Figure 3.5:

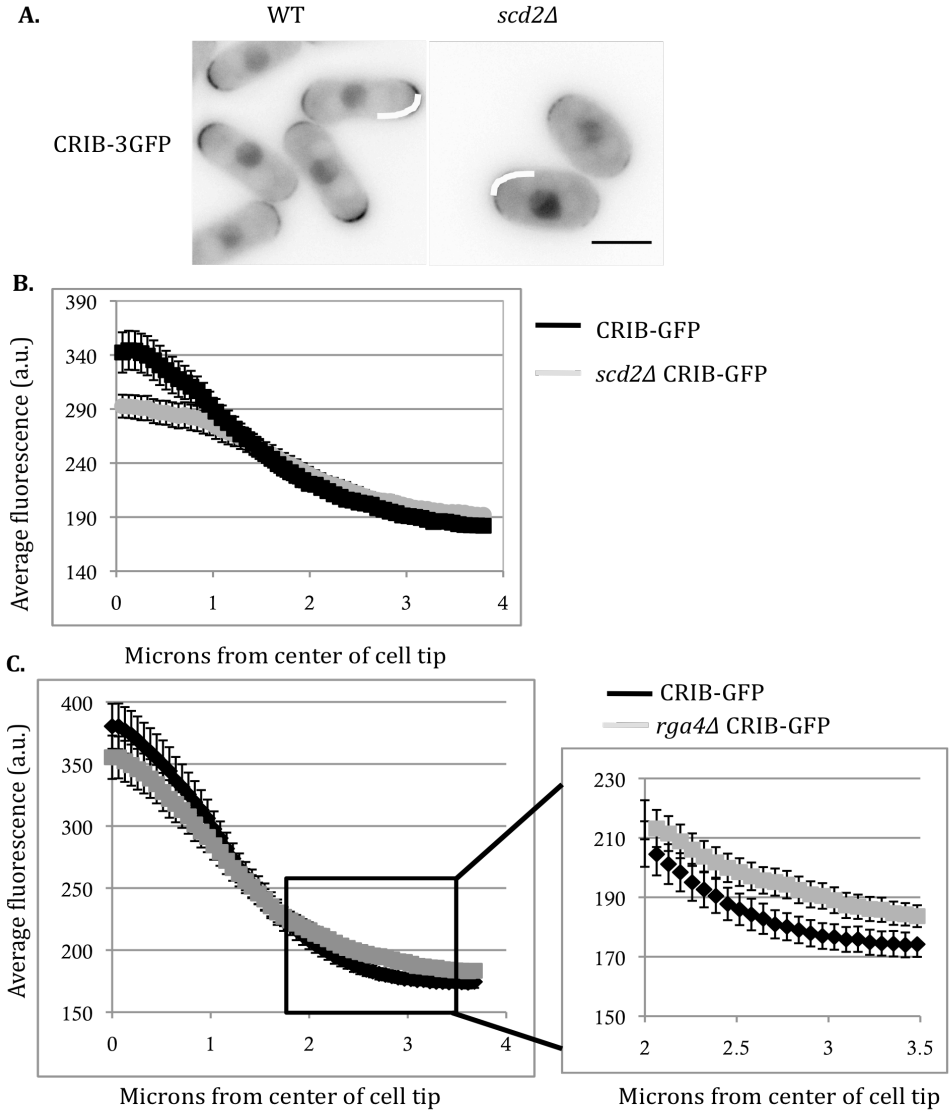

Figure 3.5: Cdc42-GTP localization is altered in the *scd2Δ* mutant. A. CRIB-GFP, white lines indicate line scans. Images are single focal planes displayed with inverted look-up tables. **B.** Line scan quantification of the distribution of CRIB-GFP in wild-type and *scd2Δ* genetic backgrounds. **C.** Line scan quantification of the distribution of CRIB-GFP in wild-type and *rga4Δ* genetic backgrounds; inset zooms in on the small change at the edge of the cell tip. Line scans were done on half tips, aligned by the cell center. Plots show the average intensity of line scans along the cell tip. Each line is the average of 50 line scans (from 25 cell tips) of each genotype. Error bars represent 95% confidence intervals. Scale bar represents 5 microns.

An essential polarity kinase is also required for proper width control

In fission yeast, many downstream effectors of Cdc42 have been predicted based on homology, but have not been experimentally verified. One of these predicted effectors that has been shown to bind activated Cdc42 is the essential protein kinase Pak1/Shk1 (Endo *et al.*, 2003). The gene *pak1* was initially identified as the temperature-sensitive mutant *orb2-34* in a screen for conditionally depolarized mutants (Verde *et al.*, 1995). I will refer to this allele as *pak1-TS*. As noted in the original description, the *pak1-TS* mutant does not become spherical upon temperature shift—it is still polarized but is wider. The sole mutation in the temperature sensitive allele is a single nucleotide change that changes amino acid 517 from glycine to glutamic acid (Figure 3.6 A). This residue is near the DFG motif that is nearly invariant in protein kinases of many different families. The DFG triplet helps orient the γ-phosphate of ATP for transfer by the kinase (Hanks and Hunter, 1995). In many kinases, including the budding yeast homolog Ste20, the glycine that is mutated in *pak1-TS* is also conserved.

To investigate how this mutation might increase cell width I GFP-tagged the temperature-sensitive mutant. The GFP tagged Pak1-TS was still localized to cell tips, but that localization was weaker at the restrictive temperature of 36.5°C, when compared to wild-type Pak1-GFP at the same temperature (Figure 3.6B). The reduction in fluorescence at cell tips could be due to a change in protein localization or reduced protein levels.

Figure 3.6

A.

pak1: TCA CTT CAA GGA GAT ATT AAA CTT ACC GAT TTT GGG
pak1-TS: TCA CTT CAA G**A**A GAT ATT AAA CTT ACC GAT TTT GGG

Pak1: S L Q G D I K L T D F G
Pak1-TS: S L Q **E** D I K L T D F G

B.

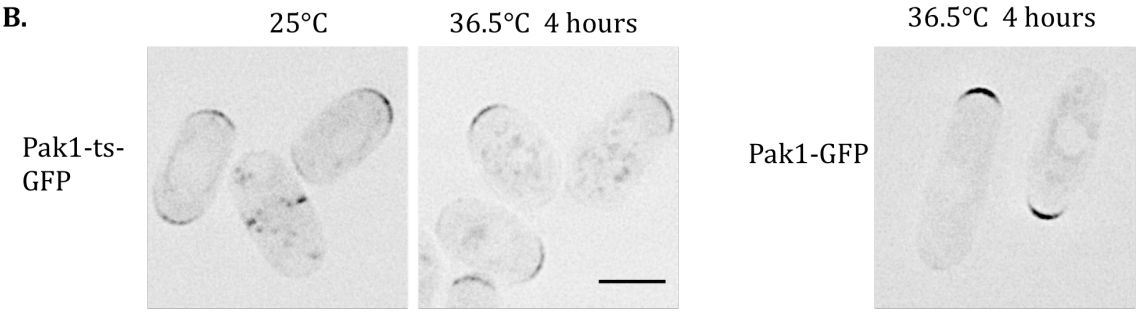

Figure 3.6: Temperature-sensitive *pak1* allele shows reduced tip localization. **A.** Nucleotide and amino acid sequencing of the temperature-sensitive allele *pak1-TS*. Nucleotides 1540-1575 are displayed; the nucleotide in red is the single mutation found in the sequence. Amino acids 514-525 are displayed; the amino acid in red is altered in the temperature-sensitive protein. The grey box contains the conserved DFG triplet. **B.** Localization of Pak1-TS-GFP at the permissive and restrictive temperatures. The wild-type Pak1-GFP is shown at right for comparison. All images are displayed with the same look-up tables. Images are deconvolved, inverted single planes shown with inverted look-up tables. Scale bar represents 5 microns.

Scd1 localization to cell tips is crucial for proper control of cell width.

The genetically independent, mutually exclusive localizations of Rga4 and Scd1 led us to hypothesize that these proteins establish spatially separate domains that determine the width of the cell. If these domains of Cdc42 activation and inhibition are important, then the localization of Scd1 to the cell tip and Rga4 to the cell sides will be necessary for their functions in determining cell width. I tested this model by disrupting and then restoring the localizations of Scd1 and Rga4.

Scd2 is necessary for the localization of Scd1-3GFP (Figure 3.2A) and is thought to act as a scaffold stabilizing the interaction between Scd1 and Cdc42, as well as between Cdc42 and downstream effectors, including the essential kinase Pak1 (Endo et al., 2003). If the primary function of Scd2 is to localize Scd1, then the mislocalization of Scd1 in *scd2Δ* cells could be responsible for the increase in the width of this mutant. To test whether the localization of Scd1 is important for the control of cell width, I added an extra protein domain to target Scd1 to the cell tips in *scd2Δ*. I fused the N-terminal targeting domain of For3, which is sufficient for cell-tip localization (Martin and Chang, 2006), to Scd1 under an inducible promoter. This fusion protein, where the For3N domain replaces Scd2 as a tip-targeted membrane tether, localized to the cell tips even in the *scd2Δ* strain, while the induced Scd1-GFP was located diffusely in the cytoplasm and in the nucleus (Figure 3.7A). For3N-Scd1-GFP complemented the cell-width phenotype of *scd2Δ*, but Scd1-GFP did not (Figure 3.7B). Induced overexpression of For3N alone did not affect the width of the *scd2Δ* mutant (data not shown). The effect of the fusion protein is not due to increased

protein levels, because For3N-Scd1 was not expressed at higher levels than Scd1-GFP (Figure 3.7C). At no point during the course of induction did Scd1 complement the width phenotype of *scd2Δ*. Therefore tip-localized Scd1 acts at the tip of the cell to set the normal width of the cell, whether it is localized there by Scd2 or by an artificial fusion with For3N.

In budding yeast, the deletion of the Cdc42-scaffold homolog of Scd2, Bem1p, can be complemented by a fusion of the GEF to a downstream kinase (Kozubowski et al., 2008). Numerous fusion proteins in that study showed that the connection between the GEF and the kinase was an essential part of the function of the scaffold Bem1. In our case, however, I have rescued the width defect of *scd2Δ* simply by restoring the localization of the GEF Scd1 to the cell tips, without restoring the interaction of Scd1 with the homologous essential kinase Pak1.

Targeting Scd1 to the cell tips rescues Pak1 localization in the scd2Δ mutant

The essential effector kinase Pak1 binds activated Cdc42 , Scd2, and Scd1 to form a quaternary complex. The interaction with activated Cdc42 is via a CRIB domain, the same type of domain that has been used as a sensor for activated Cdc42. To test how well the targeting of Scd1 to the cell tip restored the functional interactions with effectors I analyzed the localization of Pak1-mCherry in wild-type cells, the *scd2Δ* mutant, and *scd2Δ* mutant with the overexpressed For3N-Scd1-GFP and Scd1-GFP constructs (Figure 3.8).

Figure 3.7:

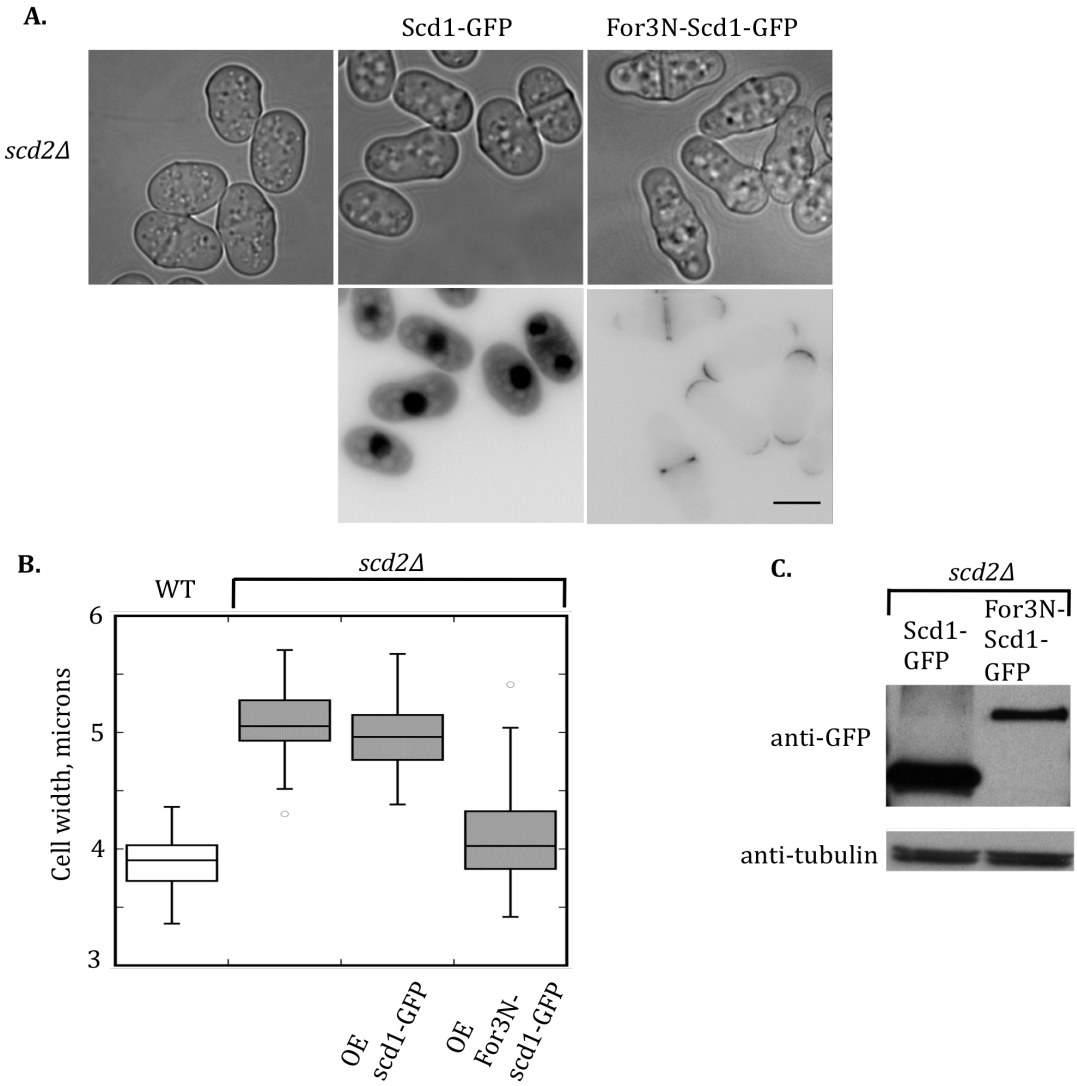

Figure 3.7: Retargeting of Scd1 to the cell tips can complement *scd2Δ*.

A. Brightfield and fluorescent images of *scd2Δ* cells, expressing Scd1-GFP and For3N-Scd1-GFP as indicated, induced from the *nmt41* promoter for 15 hours. Images are single focal planes, with inverted look-up table for the fluorescent proteins. **B.** Box-and-whiskers plot of cell width in the same strains, under the same expression conditions. **C.** Western blot of whole-cell extracts from *scd2Δ* cells induced for 15 hours expressing either Scd1-GFP or For3N-Scd1-GFP under control of the *nmt41* promoter. Protein levels were assayed by blotting against GFP. Anti-tubulin from the same lanes is included as a loading control.

The localization of Pak1 to cell tips is greatly reduced in the *scd2Δ* mutant, and the change in localization between wild-type and the mutant is greater than for CRIB-GFP (Figure 3.8 A, B). This is not surprising, because the *scd2Δ* mutant disrupts all three interactions that localize Pak1 to the cell tip—Scd2 is deleted, Scd1 is not localized to the cell tip, and the peak of Cdc42 activation at the cell tip is reduced. Expression of For3N-Scd1-GFP restored the peak of Pak1-mCherry localization at the cell tip and the rapid decline in fluorescence from the center of the cell tip (Figure 3.8 A, C). This is as would be expected from its correction of the cell-width defect of the *scd2Δ* mutant. Expression of Scd1-GFP has a much weaker effect on the localization of Pak1-mCherry to the cell tip, though there is some localized increase in Pak1-mCherry (Figure 3.8A, C). Expression of Scd1 alone does not rescue the cell-width defect of *scd2Δ* (Figure 3.7). This could be due to a number of differences between the distributions of Pak1 in these two mutants. The absolute level of Pak1 at the tip is still lower in the *scd2Δ* OE-Scd1 background, and there may be a threshold for growth activation. The distribution of Pak1 is also much flatter in the *scd2Δ* OE-Scd1 strain, and the rate of decline away from the cell tip could be more important than the peak level. As shown in the Western in Figure 3.7, Scd1 is also expressed at a higher level than For3N-Scd1 under the same expression conditions, which may further complicate the interpretation. To isolate the effect of the fusion proteins on Pak1 localization I normalized the Pak1-mCherry values in Figure 3.8C by subtracting the Pak1-mCherry *scd2Δ* fluorescence level from both line scans.

Figure 3.8

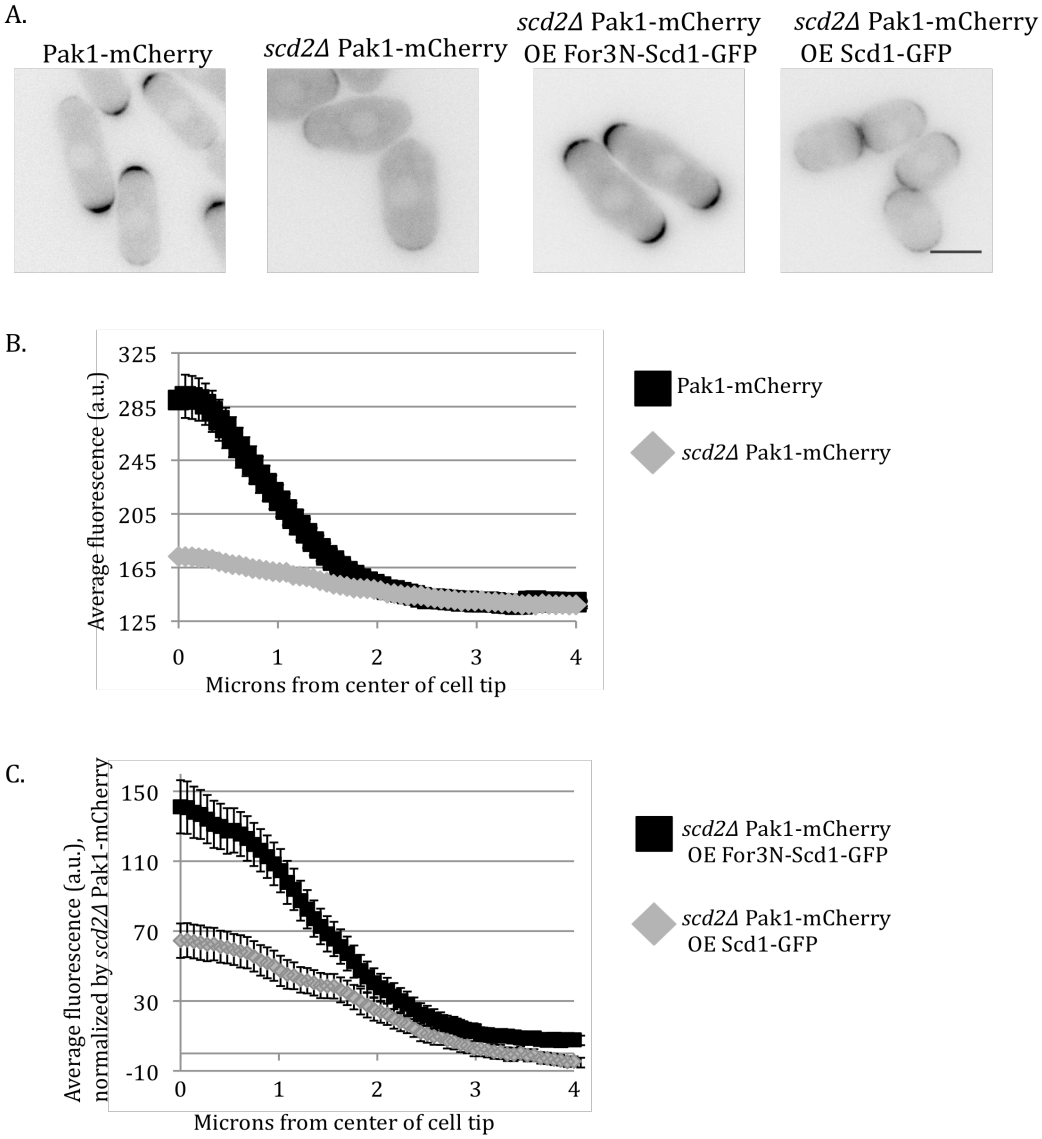

Figure 3.8 Targeting Scd1 to the cell tips rescues Pak1 localization in the *scd2Δ* mutant. A. Pak1-mCherry, in the indicated genetic backgrounds, with indicated fusion proteins expressed for 15h. Images are LUT inverted, single focal planes. **B.** Line scan quantification of the distribution of Pak1-mCherry in wild-type and *scd2Δ* genetic backgrounds. **C.** Line scan quantification of the distribution of Pak1-mCherry in *scd2Δ* with either Scd1-GFP or For3N-Scd1-GFP expressed for 15h from the *nmt41* promoter. Both scans are normalized to the *scd2Δ* baseline by subtraction. Line scans were done as in Figure 3.5. Scale bar represents 5 microns.

Localization of Rga4 to the cell cortex is crucial for cell-width control

To assess the importance of localization for the function of Rga4, I sought to alter its localization. I initially constructed fusion proteins using the full-length Rga4, but the fusion proteins CRIB-Rga4 and For3N-Rga4 still localized to the cell sides rather than the cell tips (data not shown). Since the full-length protein was resistant to retargeting, I took another approach. To parallel the loss of Scd1 localization in *scd2Δ*, I expressed an alternative version of Rga4 that localizes to the cytoplasm (Figure 3.9A, (Tatebe et al., 2008)). This cytoplasmic Rga4 (cytoRga4) has an internal deletion of 138 amino acids. When a GFP tag was added to these residues, they localized evenly throughout the membrane, with no evidence of exclusion from the cell tips (Figure 3.9D), so this mediates localization to the cell periphery.

CytoRga4 only partially rescued the *rga4Δ* phenotype when expressed either under the endogenous *rga4* promoter or at higher levels under the inducible *nmt41* promoter (Figure 3.9B). When overexpressed, cytoRga4-GFP also formed aggregates in some cells, usually one or two per cell, but when cytoRga4 was expressed as the sole copy from the endogeous promoter it did not form aggregates, and the cells were still wider than wild-type cells (Figure 3.9 A, B).

This inability of cytoRga4 to correct the deletion phenotype fully could be due to mislocalization or impaired protein function. To test if mislocalization was the primary defect, I relocalized cytoRga4 back to the cell sides by fusion with the cortically localized protein Blt1 (Moseley et al., 2009). Blt1-cytoRga4-GFP localized

throughout the cell periphery, including to the cell sides and cell tips (Figure 3.9A). Despite this broader localization, Blt1-Rga4-GFP fully corrected the width phenotype of *rga4Δ* (Figure 3.9B). When Rga4 is overexpressed, it makes cells thinner (Das et al., 2007), so differences in expression level could potentially cause differential effects on cell width, but the cytoRga4 is expressed at higher levels than Blt1-cytoRga4, as measured by Western blot (Figure 3.9C). When Blt1 was expressed alone, it slightly increased the width of *rga4Δ* cells (data not shown), so the Blt1 component is unlikely to be responsible for the decrease in cell width caused by the fusion protein. I conclude that the localization of Rga4 to the cell cortex is important for its function and, like Scd1, Rga4 cannot influence the width of the cell unless it is localized to the cell membrane.

Figure 3.9:

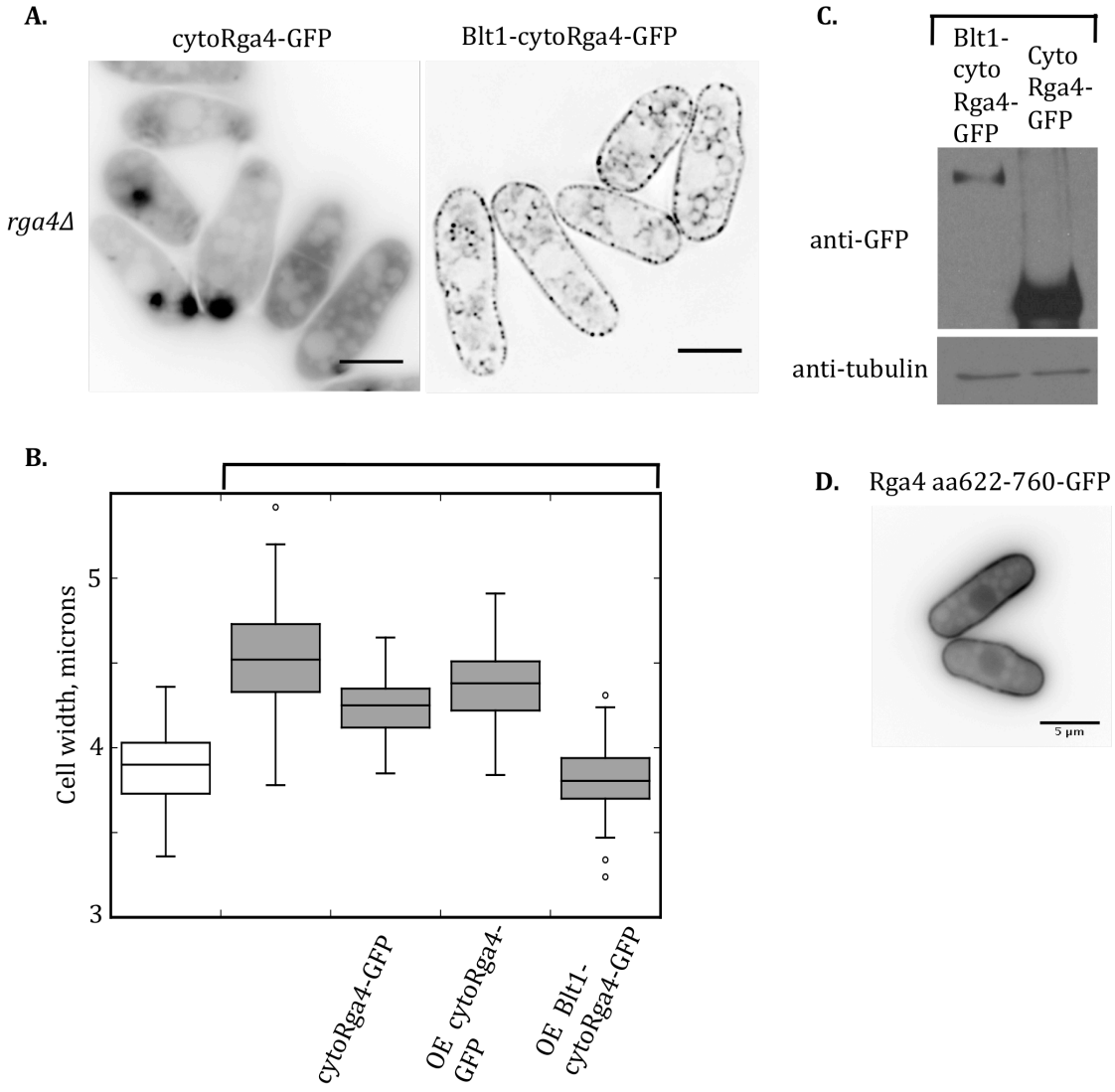

Figure 3.9: Localization of Rga4 to the cell cortex is crucial for cell-width control. A. Fluorescence images of GFP-tagged Rga4-derived proteins as indicated. All images are deconvolved single planes, with inverted LUTs. **B.** Cell widths of the indicated strains. Only the wild-type strain retains Rga4 in the endogenous location. **C.** Whole-cell extracts from *rga4Δ* cells induced for 18 hours expressing either Blt1-cytoRga4-GFP or cytoRga4-GFP under control of the *nmt41* promoter. **D.** Putative targeting domain of Rga4, aa622-760, tagged with GFP. Protein is expressed constitutively from a plasmid under the nmt41 promoter. Image is an inverted single plane. All scale bars represent 5 microns.

Partial disruption of actin increases cell width.

In fission yeast, Cdc42 influences actin cable polarization, and severe actin cable defects are evident in temperature-sensitive mutants of Cdc42 that disrupt the cell-tip localization of For3 (Martin et al., 2007; Rincon et al., 2009). To investigate whether actin organization affects cell width, I treated cells with a range of concentrations of the actin depolymerizing drug Latrunculin A (LatA). At a concentration of 10μM LatA, which is tenfold less than what is used to depolymerize actin completely, actin cables were depolymerized but there were no visible effects on the more resistant actin patches as shown by staining with phalloidin (Figure 3.10A). Higher levels of LatA blocked growth, but at a concentration of 10μM cells continued exponential growth for about two hours (Figure 3.10B). Within one hour of 10μM LatA addition, cells became 0.5 micron wider (Figure 3.10C). Deleting the major *S. pombe* formin *for3* (Feierbach and Chang, 2001) increases the width of the cell only slightly, with a width in exponential culture of 4.1 micron ±0.25, compared with 3.9 micron ±0.15 for wild-type cells. Although Scd1 and Scd2 were delocalized upon complete depolymerization of actin (Figure 3.3A), their localizations appear to be unchanged in 10μM LatA (Figure 3.10D). Therefore low-level LatA affected the width of the cell without disrupting the localization of these Cdc42 regulators. To see if there might be a resultant change in Cdc42 activation, I looked at the localization of CRIB-GFP in 10μM LatA. Because CRIB-GFP still localized to cell tips after one hour in 10μM LatA (Figure 3.10D), I conclude that while actin polymerization is important for the control of cell width, it either has a subtle effect on protein localization or acts downstream of Cdc42.

Figure 3.10:

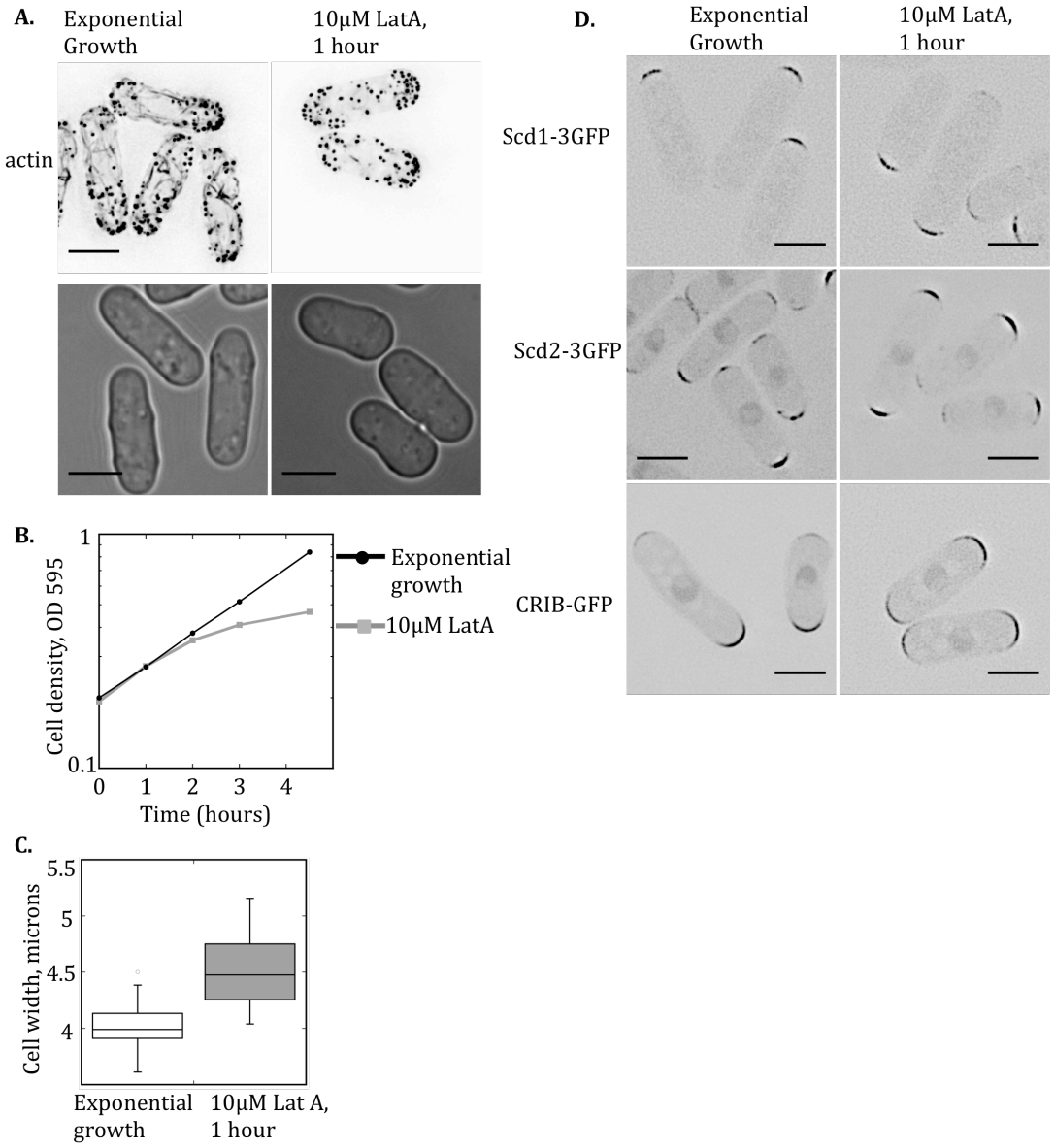

Figure 3.10: Partial disruption of actin increases cell width A. Cells treated with 10μM LatA have reduced actin cables while retaining polarized actin patches, as shown by Alexa Fluor 488 phalloidin staining of growing cells. **B.** In 10μM LatA, cells continue to grow normally for about two hours. **C.** Cell width is increased after one hour of growth in 10μM LatA. 50 cells measured for each condition, $p<.001$. **D.** Low-level LatA does not affect the localization of Scd1-3GFP, Scd2-3GFP, or CRIB-GFP. Images are deconvolved, inverted, single focal planes. Scale bars represent 5 microns.

Discussion:

Rga4 localizes to cell sides independent of actin, microtubules, Scd1, and Scd2

Many proteins involved in growth organization in fission yeast localize to the cell tips. In contrast, the protein Rga4, which is predicted to regulate growth negatively through its deactivation of Cdc42, localizes to cell sides. The cellular factors that direct this unusual localization are unknown. Here I showed that the protein did not depend on either the actin or microtubule cytoskeletons for localization, at least in the short term. Nor was it influenced by the deletion of two other Cdc42 regulators, Scd1 and Scd2. Rga4's localization to cell sides is quite stable, and fusion of the full-length protein to domains that localized to other areas in the cell did not change the localization of the fusion protein.

There is one published account of an alteration of Rga4 localization—deletion of an internal domain of the protein renders the protein diffuse in the cytoplasm (Tatebe *et al.*, 2008). This internal domain does not mediate cell side localization—when it was GFP-tagged, the fusion protein localized evenly throughout the membrane, with no evidence of exclusion from the cell tips. Thus it is likely that this domain mediates localization to the cell cortex, but other parts or functions of the protein are responsible for the specific localization to cell sides.

Scd1 and Scd2 depend on one another and on actin for localization to cell tips

The GEF Scd1 and the scaffold Scd2 localize to cell tips, where they activate Cdc42. Our genetic analyses show that they are mutually dependant for that localization: Scd1-3GFP is diffuse in the cytoplasm in the *scd2Δ* mutant, and Scd2-3GFP is lost from the cell tips in the *scd1Δ* mutant (Figure 3.2). Both proteins also depend on an intact cytoskeleton for their localization: When cells are treated with high levels of LatA, the localization of both proteins is disrupted (Figure 3.3). If the basic organization of actin within the cell were disrupted in both mutants, and both Scd1 and Scd2 depended on actin for their localization, it would explain their codependancy and their epistatic relationship. But the overall organization of the actin cytoskeleton seems to be maintained in both deletions, so their mutual dependance is not due to major actin disruption in both mutants (Figure 3.4).

The proteins' mutual dependence for localization could be explained by a cooperative system, where Scd1, stabilized by Scd2, activates Cdc42, which then stabilizes the complex, leading to an accumulation of both Scd1 and Scd2. This would be similar to the interaction between the homologous budding yeast scaffold protein Bem1p and GEF Cdc24p. Binding of Bem1p to Cdc24p is necessary for the localization of Cdc24p, but not directly required for the localization of Bem1p, since a mutant version of Bem1p that does not interact with Cdc24p can still localize to the bud neck and the bud cortex (Butty et al., 2002). But Bem1p's localization depends on Cdc42p activation, and our results do not allow us to determine whether the loss of Scd2 from the tips of *scd1Δ* cells is due to the reduced levels of

Cdc42-GTP or due to a direct interaction between Scd1 and Scd2 that is lost. I have shown that both *scd1Δ* and *scd2Δ* do not concentrate Cdc42-GTP at the site of growth as well as wild-type (Figure 3.5), and this shared phenotype may account for the increase in cell width in both mutants.

The distribution of activated Cdc42 may direct cell width

I propose that that even when the basic shape of the cell is normal and polarized, the spatial control of Cdc42 affects the width of the polarized growth zone. Using CRIB-GFP as a marker for activated Cdc42, I have quantitatively shown that there is a gradient of activation, with maximum activation near the center of the cell tip. Deletion of either the GEF *scd1* or the scaffold *scd2* reduces the peak of Cdc42 activation, and makes cells wider. Scd1, Scd2, and Cdc42 form a complex at the cell tip (Endo et al., 2003), and this complex may act to concentrate and focus growth by stabilizing activated Cdc42. When the complex is disrupted by deletion of *scd1* or *scd2*, I propose that Cdc42 can be activated at the cell tip but the activation is not as well focused, as evidenced by the localization of the CRIB-GFP in *scd2Δ* and *scd1Δ*, both of which have a shallower gradient (Figures 3.4 C & 3.5 B). This model is described in detail in the discussion.

Retargeting Scd1 to the cell tips in an *scd2Δ* mutant restores the wild-type cell width and restores the localization of Pak1. Since Pak1 localization to the cell tips is mediated by binding Cdc42-GTP via a CRIB domain, the restoration of Scd1 to cell tips probably also restores the tip-localized activation of Cdc42.

Actin-based positive feedback may play a role in Cdc42 recruitment to the cell end.

Many of the same genes are involved in growth polarization in budding yeast and cell-width control in fission yeast, although they act at different steps in the polarized growth process. In budding yeast, Cdc42p polarization is involved in the switch from isotropic to polarized growth. The initial polarization is strengthened by a positive feedback loop that results from Cdc42 recruitment of the activating PAK/scaffold/GEF complex (Kozubowski et al., 2008). This feedback is not normally essential for growth polarization, but it becomes essential when the bud-site-selection landmark protein Rsr1 is absent (Irazoqui et al., 2003).

Our results indicate a role for actin polarization in determining the width of the fission yeast cell. Actin is essential for normal cell growth (Ishijima et al., 1999), but has not previously been shown to be involved in cell-width control. I found that addition of 10μM LatA caused cells to increase in width, with major actin cable defects evident by phalloidin staining. Since deletion of the fission yeast formin *for3* is viable and causes only a slight increase in cell width, treatment with 10μM LatA probably leads to a more severe actin disruption. Activated Cdc42 is still localized to the cell tips when cells are grown in low-level LatA (Figure 3.10D), so the effect on cell width is not due to disruption of Cdc42. Higher doses of LatA disrupt both Scd1 and Scd2 localization (Figure 3.3A). The high-level LatA disruption of growth and Cdc42 localization (Bendezu and Martin, 2010) could occur via disruption of delivery and recruitment of Scd1 and Scd2, but the low-level LatA effect on cell width could be acting by additional mechanisms involving a downstream component.

Chapter 4: De novo growth zone formation from fission yeast spheroplasts

Introduction:

Fission yeast exhibits a constant cylindrical shape, and a near-constant cell width, throughout the normal vegetative cell cycle. This consistent cell shape has been instrumental in exploring cell-shape determination. But persistent polarization throughout the cell cycle and near-constant cell width make it difficult to determine which of the many proteins that influence cell growth are primarily responsible for organizing the shape of the cell. It is also difficult to determine what role the cell wall plays in organizing the cytoskeleton and determining protein localization. The cell wall carries the history of the growth pattern, which could influence future behavior. One approach to study the establishment of the rod shape has been to physically constrain cells in polymer molds of different shapes and see how the cytoskeleton and cell growth patterns respond (Minc et al., 2009b; Terenna et al., 2008). These studies have shown that microtubule contact with the cell cortex can establish new growth zones at novel sites in a bent cell.

Here I took a different approach: removing the cell wall to create depolarized spheroplasts and then studying the recovery of the normal rod cell shape. Fission yeast, unlike budding yeast, can recover from complete cell-wall digestion in liquid media (Kobori *et al.*, 1989). Previous work on spheroplast recovery has focused primarily on the first few hours, when the cell wall initially regrows all around the entire round spheroplast (Osumi *et al.*, 1989; Osumi *et al.*, 1992). The initial cell wall regrowth is partly polarized and involves the polarization of actin (Takagi *et al.*,

2003). It is inhibited by cytochalasin D, which disrupts actin polymerization (Kobori *et al.*, 1989). Later, as cell wall recovery proceeds to cover the entire surface of the cell, actin becomes unpolarized (Takagi *et al.*, 2003). The spheroplast at this stage is round or ellipsoid, has regrown the cell wall, and is again resistant to rupture by osmotic stress.

This chapter focuses on the second growth organization phase, where the recovering spheroplasts re-establish a normally-shaped fission yeast growth zone de novo from the spheroplast. This system allows us to look at both the position and dimensions of the growth domain when it is newly formed and to determine the effects of microtubule disruption and the deletion of genes involved in growth organization on growth-zone formation.

Results:

Spheroplast growth zone formation

To understand how the cell regains its rod shape and forms a growth zone, I observed the later stages of spheroplast recovery. Between three and five hours after spheroplast formation (early recovery spheroplasts) the cell is completely encased in a cell wall that renders it resistant to osmotic shock. In these early recovery spheroplasts, actin patches can be found all over the cell (Takagi *et al.*, 2003), and the cells are round to ellipsoid in shape. This state persists during the first part of the time course shown in Figure 4.1A. Then cells start to grow in a polarized way, producing a growth zone that resembles the growth zone of

exponentially growing cells, as seen seven hours after spheroplast formation (Figure 4.1A, Figure 4.1B, late recovery spheroplasts). About 25% of cells form a second growth zone, initiating bipolar growth from the spheroplast.

To understand the cytoskeletal underpinnings of de novo growth zone formation, I looked in living cells at fluorescently tagged proteins that mark microtubules (Atb2-GFP (Tatebe *et al.*, 2001)) and actin patches (Crn1-GFP (Pelham and Chang, 2001)). The cytoskeleton appears depolarized in spheroplasts and is reorganized when the growth zone forms. In exponentially growing cells, microtubules are arranged in three to five bundles that are aligned with the long axis of the cell. In newly formed and early recovery spheroplasts, this order is disrupted, and microtubules are randomly arrayed throughout the cell (Figure 4.1B, 0-1h and 5-6h). In late recovery spheroplasts, coincident with growth zone formation, microtubules become aligned primarily along the long axis of the cell generated by the new polarized growth (Figure 4.1B, 7-8h). Similar to the behavior of the microtuble array, actin patches are initially randomly distributed within the newly formed spheroplast, and do not form a distinct polarized zone in the early recovery spheroplast. Only when the cell resumes polarized growth in the late recovery spheroplast are actin patches again enriched in the growth zone as in exponentially growing cells (Figure 4.1B). A more direct marker of growth, the β-glucan synthase Bgs4, also does not form a distinct patch in early recovery spheroplasts, but is relocalized to the cell tip in the newly formed growth zone in late recovery spheroplasts. Similarly, a GFP-tagged CRIB domain, which is a marker for activated Cdc42 (Tatebe *et al.*, 2008), is initially evenly distributed around the

perimeter of a newly formed spheroplast, remains widely distributed when the cell wall has formed in the early recovery spheroplast, and then localizes more tightly to the growth zone of a late recovery spheroplast.

These data show that the formation of a growth zone leading to the re-establishment of the rod shape in fission yeast involves the formation of a defined growth zone, which is accompanied by a major reorganization of the tubulin and actin cytoskeletons and cell wall production.

Microtubules are not required for spheroplast polarization

Since microtubules have been implicated in the formation of growth zones, and in the straight-line growth of cells, I investigated if a growth zone could be formed de novo in the absence of microtubules by incubating spheroplasts in carbendazim (MBC), which inhibits microtubule polymerization (Castagnetti *et al.*, 2010), and using Atb2-GFP to monitor microtubules. When cells were treated with high levels of MBC (50μg/mL) there were no full-length microtubules, though some short stubs remained, probably nucleated from the spindle pole body on the nucleus (Figure 4.2A). Even in the presence of these high levels of MBC, spheroplasts were able to polarize growth (Figure 4.2A), showing that full-length microtubules are not required for the establishment of a new growth zone.

Figure 4.1

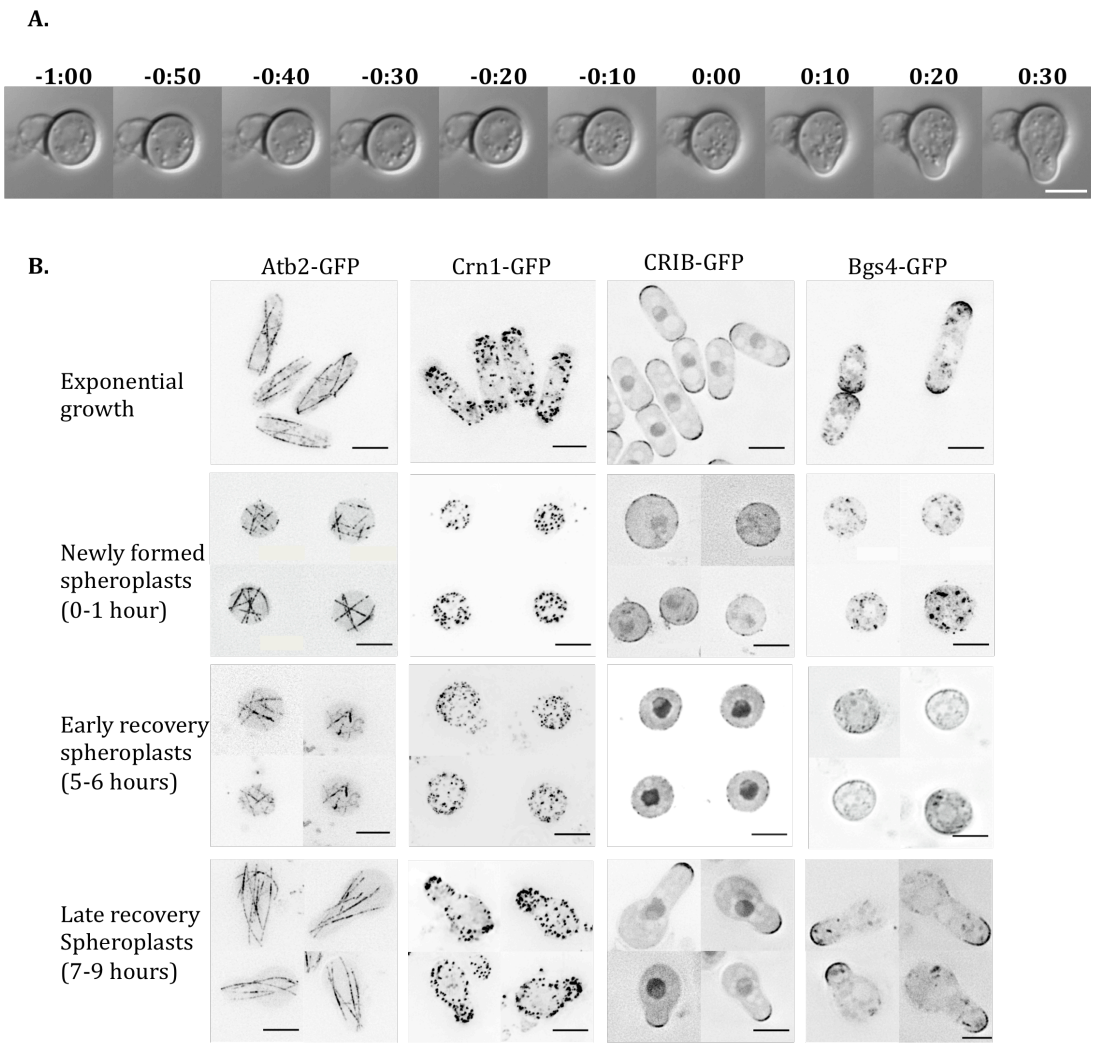

Figure 4.1: Depolarized spheroplasts can re-form a normal growth zone

A. Images from a time-lapse of a single recovering spheroplast forming a growth zone. Time is in hours:minutes from spheroplast polarization. DIC image, best focal plane for each timepoint from a Z-series of 6µm. **B.** Protein localization during spheroplast recovery; exponentially growing cells (top row) and cells at indicated times after spheroplast formation. All images show representative cells, and have been deconvolved, with inverted LUTs. For Atb2-GFP and Crn1-GFP the images are maximum projections of Z-series that spanned the cell width. For Bgs4-GFP and CRIB-GFP the images are of a single plane in the middle of the cell. Time is hours after spheroplast formation. Scale bars represent 5µm.

Although the microtubule array is not required to form a growth zone, the lack of microtubules influenced spheroplast regeneration, as was apparent in spheroplasts that exhibit bipolar growth, with two growth zones arising from the same rounded cell body. As spheroplasts advanced through recovery, bipolar spheroplasts were enriched in the population, probably because many cells had a delay in the initiation of bipolar growth. To enrich for bipolar cells without septation, I used a *cdc25-22* cell-cycle mutant, which arrests cells at the G2/M transition in the cell cycle. The cells continue polarized growth, but do not advance through septation (Fantes, 1979). The locations of the two growth zones relative to one another can be expressed as the angle that results from two lines drawn from each growth zone to the middle of the cell (Figure 4.2C). Usually the two growth zones of a bipolar spheroplast are opposite one another (180°) on the round or ellipsoidal spheroplast body, but the angle formed between the two growth zones varied widely when cells were treated with MBC (Figure 4.2B, 4.2C).

The growth-zone-angle defects that are apparent when cells are treated with MBC were even more extreme in untreated *tea1Δ* cells (Figure 4.2C). Tea1 is a tip-localized protein that is delivered by microtubules and is important for cell growth in a straight line (Mata and Nurse, 1997). These results show that microtubules are not required for the establishment of a new polarized growth zone but they are important for establishing the proper localization of a second growth zone to ensure that cells grow in a straight line. This influence of microtubules on the organization of bipolar growth may be due to the delivery of the protein Tea1, or another protein that interacts with Tea1, since *tea1Δ* has a similar effect on the angle of bipolar growth as microtubule disruption.

Figure 4.2

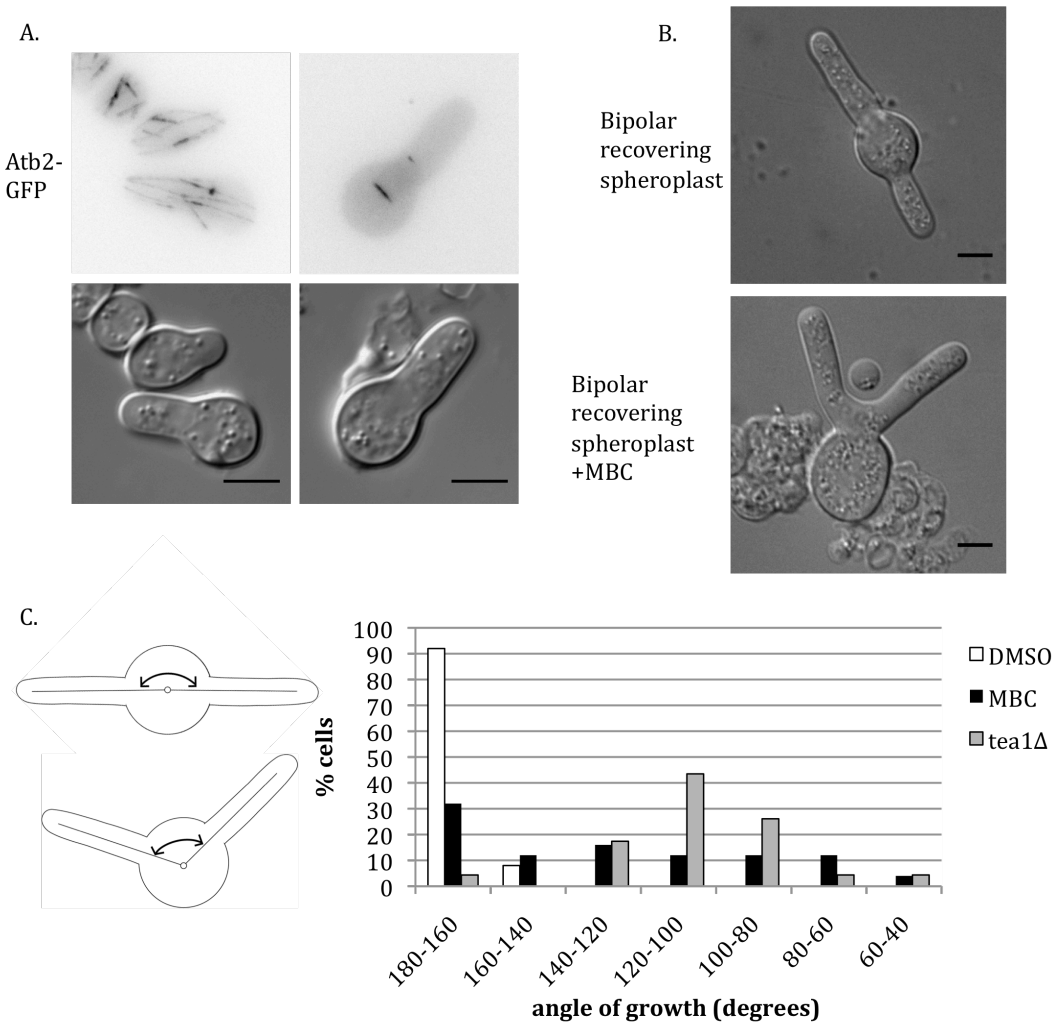

Figure 4.2: Microtubules are not required for growth zone formation, but they influence the angle of bipolar growth. A. Treatment with 50µM MBC depolymerizes microtubules in recovering spheroplasts. MTs are marked with Atb2-GFP; images are Z-projections of the max. fluorescence of the middle 3µm of the cell, inverted LUT, 8 hours post-spheroplast formation. **B.** Recovering spheroplasts that have initiated bipolar growth. Cell-cycle-blocked *cdc25-22* cells, 11 hours after spheroplast formation, treated with either 50µM MBC or DMSO (control). **C.** Distribution of the angles formed between the two growth zones in bipolar cells. Diagrams indicate how growth zone angle was measured (heavy double-headed arrow). At least 25 bipolar cells were measured for each condition. Scale bar represents 5micron.

Mutations and overall cell size can influence growth zone size

When fission yeast is growing exponentially, cell width remains essentially constant throughout the cell cycle. Recovering spheroplasts have a greater variation in overall cell size, since cells vary in size at spheroplast formation and the time needed to establish polarized growth varies widely. I used this variation in cell size to look at the relationship between the size of the growth zone and the size of the spheroplast cell body. Assessing cell growth during time-lapse experiments of spheroplast recovery, as in Figure 4.1A, shows that once a growth zone has formed most of the cell's growth is directed toward its linear extension. This observation makes it reasonable to compare growth zone width and spheroplast cell-body volume in spheroplasts that have already polarized growth because the cell body remains essentially constant after polarization. To limit the influence of cell-cycle progression, these experiments comparing cell width were also performed in a *cdc25-22* background. The volume of the body of the spheroplast had a weak positive correlation with the width of the growth zone that had formed from that spheroplast (Figure 4.3), but a large change in the volume of the cell body resulted in only a small change in the width of the growth zone. When the width of the growth zone is plotted against another linear dimension, such as the width of the cell body, then the relationship between the two variables is stronger. But if the effect of cell body size on growth zone width is based on total protein content then the proper comparison is to cell volume, not cell body width.

I next spheroplasted the temperature sensitive Pak1 mutant *orb2-34*. This mutant recovered from spheroplasting with a wider growth zone than wild-type cells (the average width of an *orb2-34 cdc25-22* spheroplast growth zone is 5.9μm±0.8 and the average width of a *cdc25-22* spheroplast growth zone is 4.5μm±0.5). Analysis of the correlation between cell-body volume and growth zone width in this mutant showed that the size of the cell body still influenced the width of the growth zone, but cell widths were shifted towards wider growth zones across the whole range of cell-body sizes (Figure 4.3).

I draw three conclusions from these observations. The first is that growth-zone size is relatively constant regardless of cell volume—a large change in cell volume results in only a small change in growth zone width. The second is that, although the effect is small, a large cell has a larger growth zone, suggesting that cell size has some influence on the width of the newly formed growth zone. The third conclusion is that the size of the newly formed growth zone can also be influenced by a gene, in this case *pak1,* that influences the width in a normally growing cell.

Figure 4.3

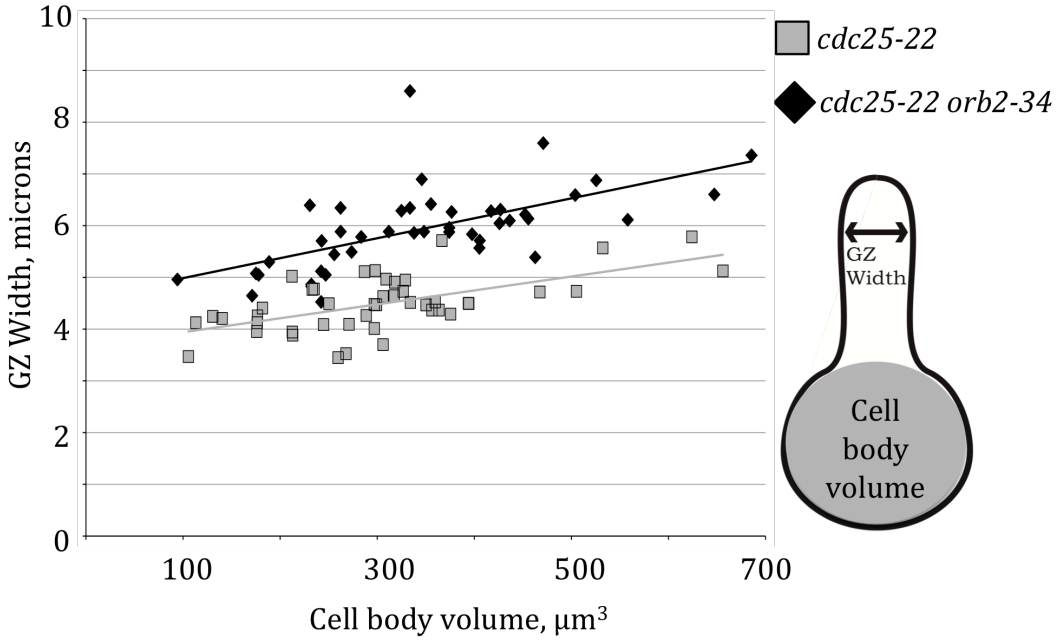

Figure 4.3: Growth zone size is also influenced by cell size. Scatter plot of growth zone (GZ) width vs. cell body volume, measured 11 hours after spheroplasting. Cell body volume is calculated from the diameter of the round part of the spheroplast.

The Cdc42 pathway affects the width of a growth zone formed de novo

Given the small range of growth zone sizes shown in a wide range of cell body sizes, I investigated how growth zone size in recovering spheroplasts compared with cell width in growing cells. I found that in polarized spheroplasts, the newly formed growth zone is the same width as a growing control cell (Figure 4.4A). The width does not depend on microtubules, as growth zones that formed in the presence of MBC were still of wild-type width (Figure 4.4A).

As described in Chapter 2 and other studies (Das *et al.*, 2007), there are several deletion mutants that are wider than wild-type during exponential growth. To determine if the same genes also influence the size of the newly formed growth zones I compared the widths of late recovery spheroplasts' growth zones in wide mutants and wild-type cells. I focused on the deletion mutants of three genes that are closely related to the control of the small GTPase Cdc42: the genes encoding the GAP *rga4,* the GEF *scd1*, and the scaffold *scd2*. Each of these deletion mutants was able to form a growth zone from a spheroplast, indicating that the genes are not required for growth polarization. In each case the new growth zone was wider than in wild-type cells, just as these deletion mutants are wider in exponential growth (Figure 4.4B, 4.4C). Therefore I conclude that the Cdc42 pathway determines the size of a growth zone in spheroplasts, which have no history of a specific cell width derived from the cell wall.

Figure 4.4

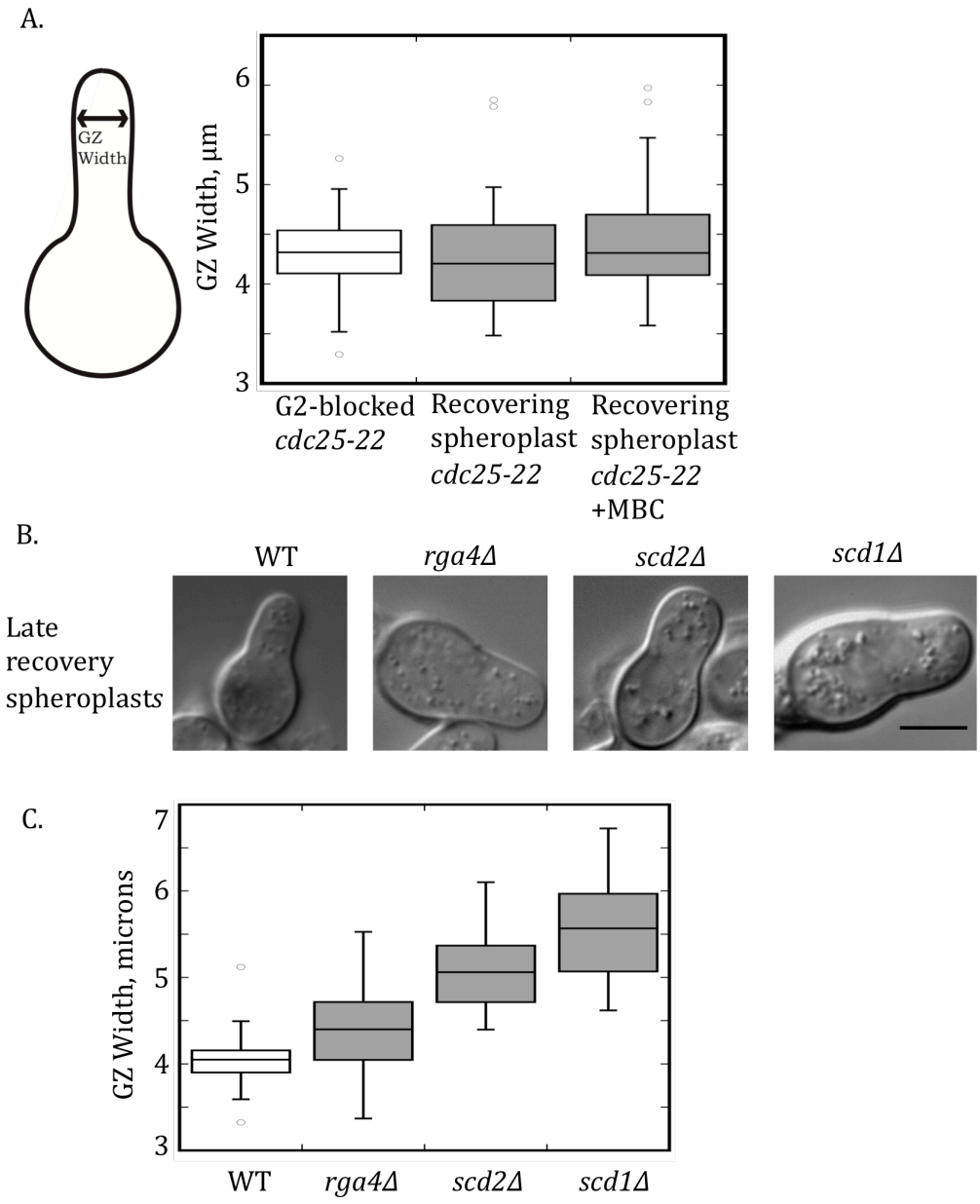

Figure 4.4: Spheroplasts can recover with growth zones of wild-type width.
A. Growth zone widths. All cells are *cdc25-22*, blocked in G2 during spheroplast recovery, or blocked as a control culture, 11 hours after spheroplast formation. **B.** Recovering spheroplasts from wild-type cells and indicated deletion mutants. DIC microscopy. Scale bar is 5 microns. **C.** Box-and-whiskers plots of recovering spheroplast growth zone widths. Images and measurements were taken 8 hours after spheroplast formation.

Spore germination tubes are the same width as wild-type growth zones, and may be controlled by the same genes

I next investigated de novo growth in a system with even less evidence of cell history. When spores form after meiosis, each spore membrane is newly formed, and so will not carry marks of previous polarized growth (Nakamura *et al.*, 2008). When these spores are exposed to growth conditions they germinate and begin polarized growth with a germination tube. The width of the wild-type germination tube, 3.84μm ±0.25, is very similar to the width of an exponentially growing cell, 3.88μm ±0.15. To look at whether germination tube width and growth zone width are controlled by the same genes, I generated a homozygous diploid of the archetypical wide mutant *scd2Δ*. This homozygous diploid was then induced to sporulate, and germinating spores were photographed and measured (Figure 4.5A, B). In these germinating spores the *scd2Δ* cells produced a wider germination tube. This provides more evidence that the mechanism establishing the width of a growth zone is cell intrinsic, and does not depend on history, and that the genes that control cell width during normal cell growth also control de novo growth zone size.

Figure 4.5

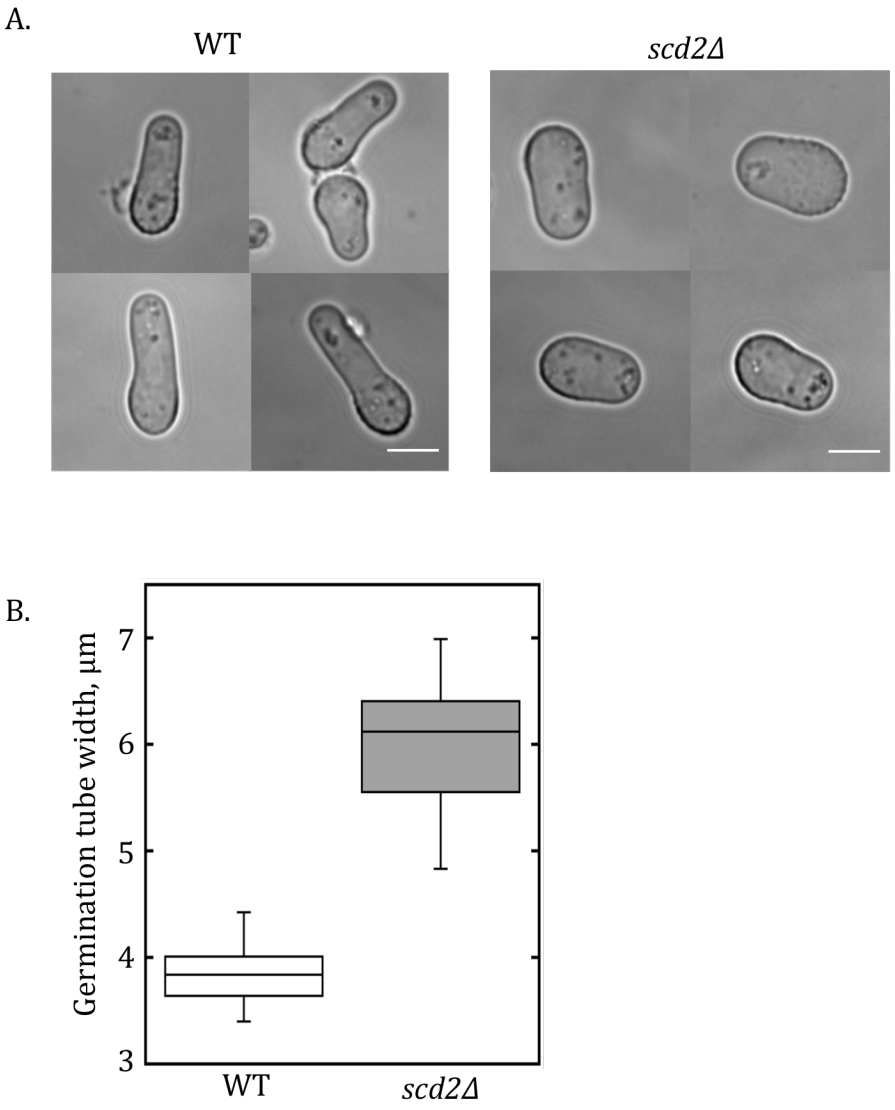

Figure 4.5: Spore germination tubes are the same width as wild-type growth zones, and may be controlled by the same genes

A. Germinating spores, brightfield. **B.** Box-and-whiskers plots of germination tube widths. Scale bars represent 5microns.

Cdc42 regulators do not carry the memory of the growth zone through spheroplasting.

Since the regulators of Cdc42 are important for establishing the width of the growth zone in recovering spheroplasts and exponentially growing cells (Chapter 2), I investigated how they were localized during spheroplast formation and recovery. These proteins localize to the growth zone in the exponentially growing cell, and so might carry the shape and size of the growth zone through spheroplast formation and recovery by forming a persistent patch. This was not the case: Scd1-3GFP, Scd2-3GFP, and Rga4-3GFP were depolarized in newly formed spheroplasts, and did not carry their characteristic localizations through spheroplasting (Figure 4.6, newly formed spheroplasts). Even after the cell wall has regrown, as in early recovery spheroplasts, these proteins were not organized in a patch defining a growth zone. But when the new growth zone forms and the cell returns to linear extension their localization was restored to a patch at the new growth zone (Figure 4.6, late recovery spheroplasts).

Figure 4.6

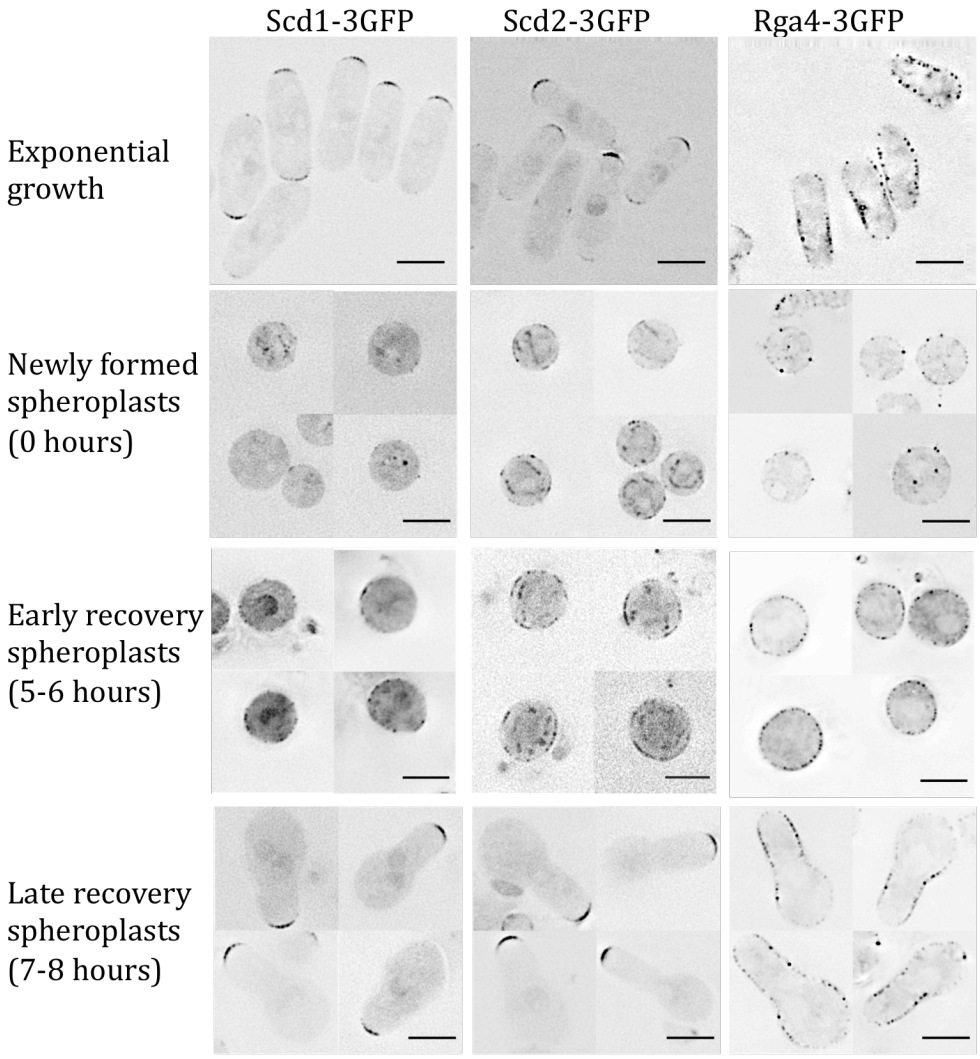

Figure 4.6: Cdc42 regulators do not carry the memory of the growth zone through spheroplasting. Protein localization during spheroplast recovery; images taken of exponentially growing cells (top row) and at indicated times after spheroplast formation. All images show single, middle planes from Z-stacks of representative cells, and have been deconvolved, with inverted look-up tables. Scale bars represent 5 microns.

Scd2 polarizes before growth begins in the new spheroplast

To explore how the new polarized growth zone forms, I used time-lapse imaging of Scd2 and Rga4, two proteins that are involved in the specification of the size of the growth zone. Scd2-3GFP localizes to the growth zone in exponentially growing cells. In recovering spheroplasts this protein formed a distinct patch before cells had formed a growth zone (Figure 4.7). This patch appeared and was eventually stabilized in the same location where the growth zone ultimately formed. I observed this patch formation leading directly to growth in time-lapse series of all six Scd2-3GFP cells that polarized during time-lapse imaging, and in an additional nine cells in the two-color time-lapse series with Scd2-mCherry. In an exponentially growing cell, the shape of the cell could direct growth proteins to the cell tip, thus determining their localizations. But since Scd2 can form a protein patch in a round spheroplast, its localization is not completely dependent on the shape of the cell.

Figure 4.7

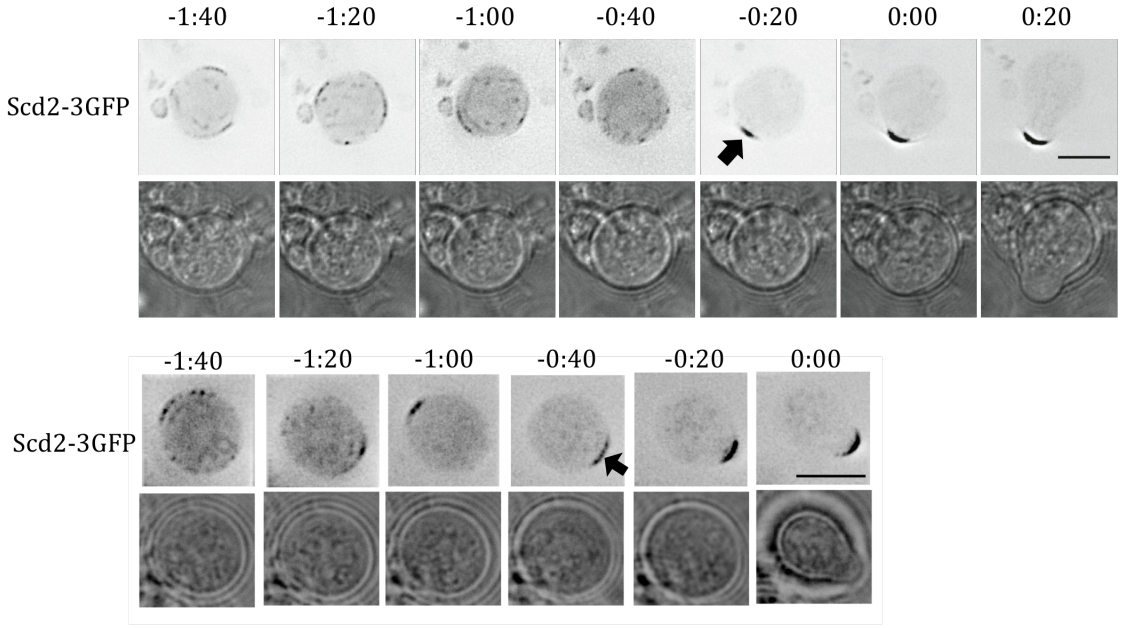

Figure 4.7: Scd2 polarizes before cell shape changes. Two time-lapse series of Scd2-3GFP in two spheroplasts as they undergo the transition to polarized growth. The black arrows indicate the appearance of a bright patch of Scd2-3GFP before the shape of the spheroplast has changed. Fluorescence images are deconvolved single planes, best fluorescent signal, with inverted LUTs. Time is in hours:minutes from spheroplast polarization, and the scale bars represent 5 microns.

Rga4 is cleared as the growth zone forms

Rga4-3GFP, which localizes to the sides of normally growing cells, was found throughout the surface of early recovery spheroplasts, but its localization changed as growth began. As the cells changed shape, Rga4-3GFP was lost from the new growth zones (Figure 4.8). This clearing of Rga4 from the growth zone was observed in 12 of the 15 cells filmed. In these experiments the time resolution, particularly for tracking when growth begins, was not sufficient to determine if Rga4 is cleared from the area before or after that site begins growing. In Figures 4.7 and 4.8, the initial polarization of growth is considered to be time zero, to make comparisons between cells easier. Spheroplasts vary widely in when they begin polarized growth, and these time-lapse experiments span several hours. I do not know what causes the variation in polarization time. When cells are spheroplasted they will be at different phases of the cell cycle, which could account for some of the variation. But it also may be that some stage of recovery involves a stochastic delay.

Figure 4.8

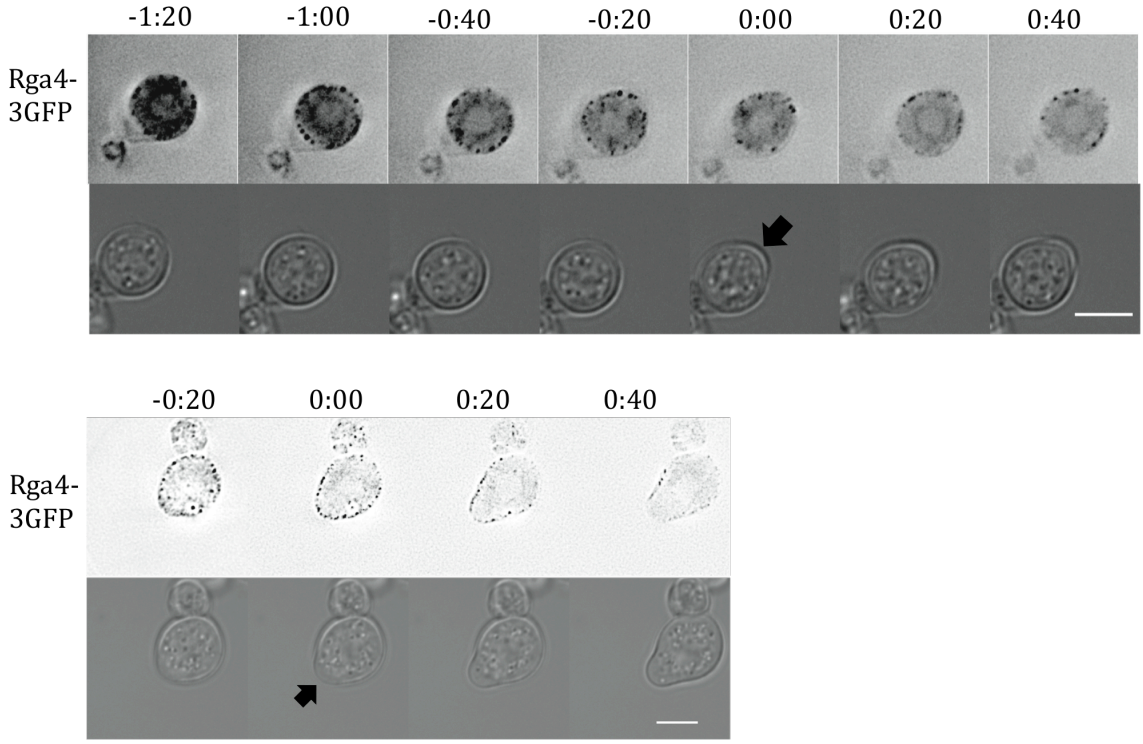

Figure 4.8: Rga4 is excluded as the growth zone forms. Two time-lapse series of Rga4-3GFP in spheroplasts as they undergoes the transition to polarized growth. Arrows indicate the location of polarized growth. Fluorescence images are deconvolved, LUT inverted, single planes, best fluorescent signal. Time is in hours:minutes from spheroplast polarization, and the scale bars represent 5 microns.

Scd2 organizes into a patch before Rga4 is excluded

The time-lapse imaging of Rga4 and Scd2 in recovering spheroplasts led us to ask which of these components of growth zone specification organized first in the recovering spheroplast. Rga4 and Scd2 both contribute to the genetic control of cell width and localize to mutually exclusive zones in the cell, but the genesis of these zones is unknown. These two proteins can localize independently of one another, as neither is delocalized in the deletion of the other (Figure 3.1). I have proposed that these two mutually exclusive domains are independently established, and together set the width of the cell, but it is unknown how these domains form.

To investigate the order of recruitment I simultaneously monitored the localization of Rga4-3GFP and Scd2-mCherry in recovering spheroplasts that had both proteins fluorescently tagged. The mCherry fluorophore bleached rapidly in these experiments, but by combining data from the first time point where a distinct Scd2 patch is visible with time-lapse imaging to determine the eventual location of the growth zone I can correlate Scd2 patch formation, Rga4 localization, and growth zone formation. I was able to extract data for fifteen double-labeled cells that polarized during the time-lapse. In twelve of these cells Scd2-mCherry formed a patch before the Rga4-3GFP localization had significantly changed, and in the remaining three it was not possible to determine which proteins' localization changed first. Three cells from these experiments are shown in Figure 4.9. Since Scd2 forms a patch, and then Rga4 is excluded as growth begins, it provides evidence that the localization of Rga4 to cell sides in exponentially growing cells is mediated by exclusion from the growth zone.

Figure 4.9

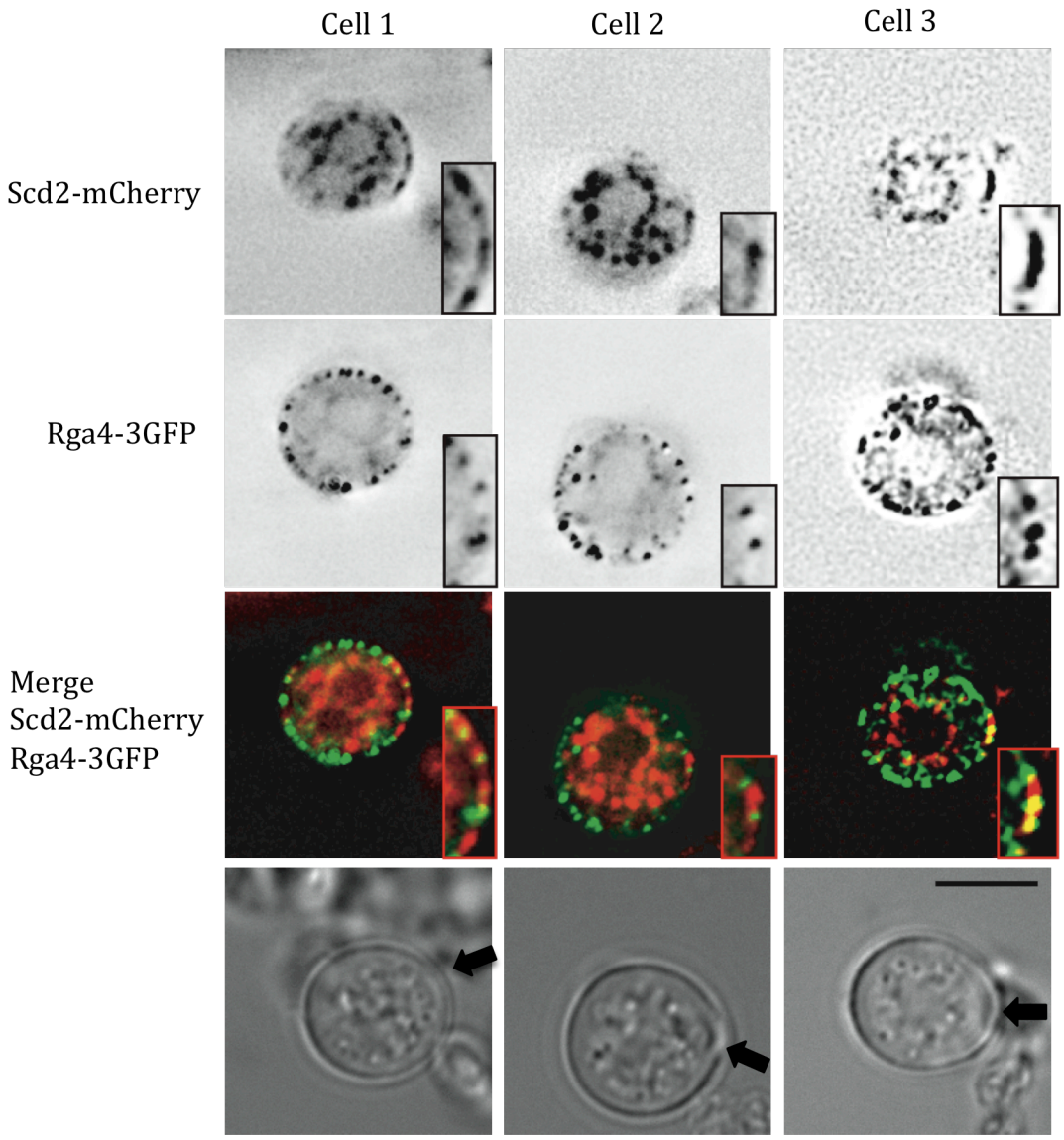

Figure 4.9: Scd2 organizes into a patch before Rga4 is excluded. Early recovery spheroplasts before polarized growth begins. Images are from the same time-point and Z-section for three different cells. Boxed inset shows a 2x magnification of the area of the Scd2-mCherry patch. Arrow on the brightfield image shows the ultimate location of polarized growth, as determined by time-lapse for each of these cells. Fluorescent images are single planes, inverted and deconvolved. Merge images are not inverted; green channel is Rga4-3GFP, red channel is Scd2-mCherry. Scale bar represents 5 microns.

Discussion:

Spheroplasts form a growth zone de novo

The study of cell shape determination in fission yeast has been limited by the fact that it is difficult to determine the role of the cell wall and cell history, since the cell is always surrounded by the cell wall, growth is stably polarized, and the cells are already rod-shaped. In this study I circumvented that problem by studying the regeneration of spheroplasts, which are apparently depolarized cells that form a new growth zone de novo.

The new growth zones formed from spheroplasts resemble normal cell tips in diameter, and their diameter is controlled by the same genes that control the width of normal vegetatively growing cells. Microtubules are not required for growth zone formation, but they do direct growth in a straight line, as seen in recovering spheroplasts that form a second growth zone and become bipolar.

Spheroplasts shed light on how tip-localized proteins are directed to form their distinctive patches at the cell tips. Because the shape of a normally growing cell does not change during the cell cycle, it has been difficult to say whether those proteins are specifically localized to domains at the ends of the cell because of the pre-existing shape of the cell, or whether they would form those domains intrinsically. Our data show that selected proteins are completely delocalized when a spheroplast is formed, and remain delocalized even after cell wall formation in a round spheroplast. But, when the spheroplast forms a new distinct growth zone, these proteins become localized to that new growth zone. I followed the localization

of the tip-localized protein Scd2 by time-lapse, and showed that it forms a defined, stable protein patch within spheroplasts that do not yet have a distinct growth zones, and are still spherical. This indicates that these proteins can self-assemble into a growth zone in a cell that does not have defined ends. Furthermore, in these time-lapse analyses the new growth zone forms at the location of the Scd2 protein patch, potentially indicating a role for Cdc42 activation in forming the new growth zone.

Growth zone formation is a problem distinct from symmetry breaking

In this chapter I describe a fission yeast system that has allowed me to look at how the cell re-forms a distinct growth zone of the correct size and shape rather than the symmetry-breaking event directly analogous to budding yeast bud-site selection. Since the cell wall is removed initially, I do not have the landmarks from past growth locations in newly formed spheroplasts, and so it is difficult to determine if the cell begins growth in a new randomly selected location. But by looking at newly formed spheroplasts (Figures 4.1B and 4.6A) I have shown that the proteins that usually localize to the cell tip and contribute to tip growth are delocalized, and that their localization is restored when the growth zone re-forms. I have focused on the size and shape of the newly formed growth zone, irrespective of its relative location on the cell.

The contribution of the cytoskeleton to growth zone formation

Microtubules and actin both contribute to growth organization in fission yeast (Hayles and Nurse, 2001). It has been previously shown that actin is associated with initial cell wall formation (Takagi *et al.*, 2003), and that actin polymerization is required for recovery from spheroplasting (Kobori *et al.*, 1989). In contrast to actin, microtubules are not required for spheroplast recovery, since inhibition of microtubule polymerization did not prevent recovery from spheroplasting (Figure 4.2A). After MBC treatment, short microtubules are visible, so I cannot absolutely exclude that these stubs play a role in spheroplast recovery. But microtubules, and Tea1, are required to organize growth in a straight line, and this requirement is evident when microtubules are disrupted: When two growth zones form on the same spheroplast in the presence of MBC they are not arranged opposite from one another (Figure 4.2). These results comport well with published data about the role of Tea1 and microtubules in establishing new growth zones. Deletion mutants of *tea1* occasionally form supernumerary growth zones at the cell center (Mata and Nurse, 1997). It has been shown that a growth zone is normally inhibited from forming adjacent to an existing growth zone, but that inhibition is reduced in *tea1Δ* cells (Castagnetti *et al.*, 2007). Such a loss of inhibition may allow growth zones to form closer together in bipolar spheroplasts as well. Tea1 depends on microtubules for its localization to cell ends, and so the effects of inhibiting microtubule polymerization may be due to the resulting mislocalization of Tea1 (Mata and Nurse, 1997).

Growth zone size is reestablished in a recovering spheroplast

I have shown here that a growth zone that forms from a spheroplast is the same width as the growth zone of a normal cell, and that both are controlled by the same genes. Even spores, which cannot carry any positional history, form a germination tube of the same width as a normal cell, and the width of that germination tube can be affected by at least one of the genes that renders normally growing cells wide. These results, taken together with the results of a genetic screen for wide mutants (Chapter 2), show that cell width is a genetically encoded trait that does not depend on the history of the original cell shape or the cell wall, and that the same genetic pathways control cell width in exponentially growing cells, recovering spheroplasts, and most probably germinating spores.

Scd2 polarization and subsequent growth lead to Rga4's exclusion from the newly formed growth zone

Since the fission yeast cell always has geometrically defined cell tips, the tip-localized proteins could be directed to the cell tips by the shape of the cell. Spheroplasts allowed us to monitor protein localization in differently shaped cells. Through time-lapse imaging I showed that Scd2 can form a distinct patch in a cell that does not have a tip. This means that the protein does not depend on the shape of the cell for its localization to a patch. Once this patch formed, the growth zone formed at that location on the spheroplast, so Scd2 may be part of a mechanism that organizes the growth zone. This is reminiscent of the process of symmetry breaking in budding yeast, a process that has been well studied, (Irazoqui *et al.*, 2003; Slaughter *et al.*, 2009a). The stochastic

activation of Cdc42 is important, and the scaffold Bem1, which is a homolog of Scd2, is involved in the stabilization of activated Cdc42 (Kozubowski *et al.*, 2008). This system, and its relevance to spheroplast polarization, will be addressed in greater detail in Chapter 5.

The molecular basis for Rga4 localization to cell sides in exponentially growing cells is unknown, so I was interested in how it is established as the growth zone forms. Time-lapse imaging revealed that Rga4 is initially found throughout the spheroplast cortex, but is cleared from the site of growth as growth begins.

Comparing the localization of Rga4 and Scd2 in the same recovering spheroplast allowed me to assign a more specific temporal order to growth zone formation. When the first patch of Scd2 forms, Rga4 has not yet changed localization (Figure 4.9). Growth begins at the location of the Scd2 patch, and the time-lapse series of Rga4 (Figure 4.8) show that Rga4 must then be cleared from the growth zone. This initial organization of Scd2 followed by exclusion of Rga4 could indicate that Rga4 is excluded from areas of active cell growth. The exclusion does not occur via Scd2 itself, since Rga4's localization to the cell sides is maintained in the *scd2Δ* mutant.

Chapter 5: Discussion

The major conclusions of my thesis work can be summarized as follows:

- Spatial regulation of Cdc42 activation is a major determinant of cell width.
- The GAP Rga4 and the GEF Scd1 influence cell width through Cdc42 regulation in parallel, independent, spatially separated pathways.
- Wide mutants are still polarized, and localize growth to the cell tips, but the distribution of activated Cdc42 at cell tips is altered.
- The localization of Scd1 to cell tips and Rga4 to the cell cortex is important for their roles in determining the width of the cell.
- A growth zone that forms de novo from a depolarized spheroplast is indistinguishable from one in an exponentially growing cell, and Cdc42 regulators control its width.
- Spheroplast growth zone formation is preceded by the localized enrichment of Scd2 into a patch, followed by growth initiation and Rga4 exclusion from the growth zone.

These conclusions have led me to propose two models to integrate my results. The first model, Figure 5.1, describes how the size of the cell tip might be determined, and the second, Figure 5.2, describes how zones of growth activation and inhibition might be established de novo in the spheroplast.

Activated Cdc42 localization directs growth potential

S*chizosaccharomyces pombe* grows as a rod-shaped cell with a near-constant width throughout its vegetative growth cycle. This rod shape may help the cell divide in the proper location (Almonacid *et al.*, 2009) and correctly segregate DNA between the daughter cells (Ge *et al.*, 2005). The cell wall defines the cell shape and must be remodeled as growth occurs. The sexual cycle results in the production of round spores that germinate to form new rod-shaped cells. My results show that many of the same components specify both how the width of the cell is kept constant during vegetative growth and how a growth zone of proper width is newly established, and these results can be synthesized with the published work to support models that specify fission yeast growth zone formation and size determination. The basic model centers around the spatial control of the small GTPase Cdc42 because of the strong enrichment for Cdc42 regulators among the wide mutants identified in the unbiased screen for cell width mutants (Figure 2.2). Cdc42 is a major regulator growth polarization in many different cell types, and the basic principles of how its activation affects cell shape may be generally applicable. But, as described in Chapter 1, several other pathways are also important for controlling cell growth in fission yeast.

Model: Activated Cdc42 directs cellular growth potential

Based on my results, I propose a model for how the spatial pattern of Cdc42 activation determines the width of the cell. The model is predicated on the idea that each cell has a certain amount of growth potential, which persists regardless of whether the cell's morphology is altered. There is good support for the idea that the growth rate of a cell is not primarily dictated by its morphology. It has been demonstrated for bacteria and budding yeast that most of the cell's energy and protein production goes towards making ribosomes (Nomura, 1999). The rate of ribosome production is closely tied to the growth rate in a variety of nutrient conditions for budding yeast (Brauer *et al.*, 2008), and eukaryotic translation initiation factor mutants in fission yeast show a drastic reduction in growth rate while maintaining normal morphology (Akiyoshi *et al.*, 2001). The wide mutants isolated here only modestly affected growth rates, and the modest increases in generation time are not correlated with the increases in cell width. This suggests that the overall growth depends more on ribosome and protein production than on morphology, although this can be true only so long as growth is possible in an unrestricted way somewhere on the cell surface. When growth is disrupted altogether, as it is in the lethal *cdc42Δ* mutant, cells are small, round, and dense. It has been argued that these cells still have growth potential, and they are producing material to enlarge the cell, but they are unable to incorporate that material because the loss of Cdc42 blocks cell growth (Miller and Johnson, 1994).

In this model, when the cell is growing normally, its growth potential is directed to specific areas on the surface of the cell, the growth zones. When growth

is not as directed, it continues but is distributed more evenly across the cell cortex. This model proposes that activated Cdc42 directs the distribution of growth, which then determines the shape of the cell.

In wild-type cells, activated Cdc42 directs growth at the cell tips via interactions with downstream effectors. The activated fraction of Cdc42 is concentrated at cell tips, and at the cell center during septation (Tatebe *et al.*, 2008). This localized activation is strongest at the center of the tip of the cell and is reduced towards the cell sides (Figure 3.5). If this distribution of Cdc42 directs growth, then it could establish or reinforce the shape of the cell tip, as diagrammed in Figure 5.1. The localized activation of Cdc42 at cell tips is largely dependent on Scd1 and Scd2, as shown by the localization of CRIB-GFP in *scd1Δ* and *scd2Δ* cells (Figures 3.4C, 3.5). In both mutants the maximal peak of activation at the cell tip is lowered, changing the distribution of activated Cdc42 and the absolute amount. The activated Cdc42 is less focused, which results in a more even distribution of growth, which results in a wider cell.

Also in support of this model is the observation that Scd1 targeting to the cell tip is crucial for the control of cell width. In the *scd2Δ* mutant, overexpressing Scd1 does not restore the normal growth zone width, but redirecting Scd1 to the cell tips does (Figure 3.7). Scd1 is the primary cell-tip GEF and so its localization is a major determinant of tip-centered Cdc42 activation, and this model argues that the Scd1-related phenotypes could be explained by its effect on the distribution of activated Cdc42.

Rga4 localizes to cell sides, and I propose that its primary role there is to sharpen the edges of this distribution of activated Cdc42 (Figure 3.5C). This has a much stronger effect on the shape of the cell when the tip-growth-direction system is disrupted, as in the *scd2Δ* and *scd1Δ* mutants. Thus, when edge definition is also disrupted, as in the *scd2Δ rga4Δ* and *scd1Δ rga4Δ* mutants, the effect on morphology is more severe, since both double mutants are much wider than any of the single mutants (Figure 2.4). When Rga4 is overexpressed the protein still localizes to cell sides, but its localization extends further up the cell sides, and results in a narrower cell tip (Das *et al.*, 2007). The model presented below proposes that the tip is narrower because the GAP deactivates Cdc42 at the edge of the cell tip, acting as a boundary and preventing growth there, which results in the growth potential becoming more focused in the center of the cell tip.

Figure 5.1

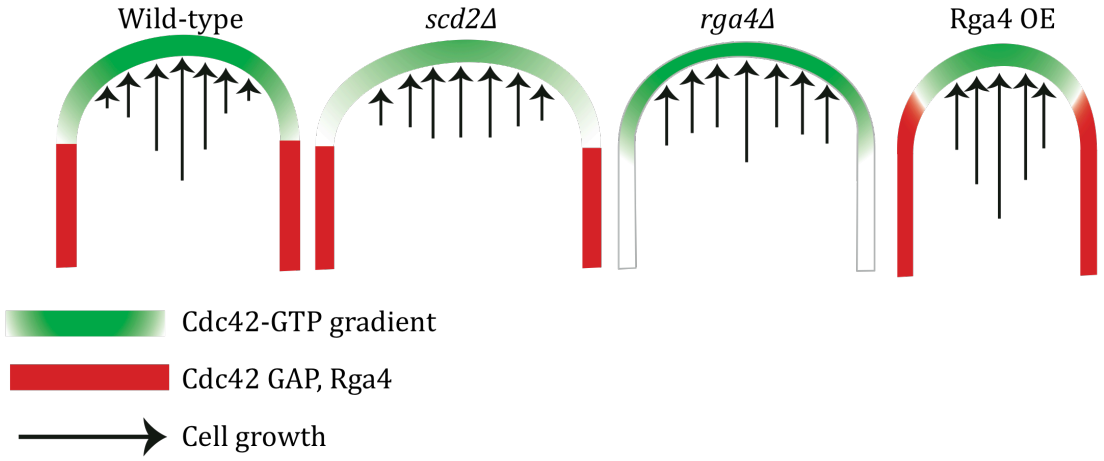

Figure 5.1 Activated Cdc42 directs cellular growth potential. This model of cell tips shows how altering the distribution of activated Cdc42 would result in wider cells, as described in the text. The green gradient represents the localization of Cdc42-GTP, similar to the CRIB-GFP localization I have reported. The red cell sides represent the localization of Rga4. Arrows represent cell growth, and their length indicates how much relative growth would take place at each location on the cell tip. Activated Cdc42 directs where cell growth will take place within the cell tip. When activated Cdc42 is most concentrated in the center of the cell tip growth is concentrated there and the cell tip has its normal shape and width. When the concentration of activated Cdc42—and growth—towards the center is reduced, such as in the *scd2Δ* mutant represented here, growth is more evenly distributed, and the cell tip is flatter and wider. When the edge definition by Rga4 is absent, Cdc42 extends further towards the edges of the cell, the cell grows more at the edges of the cell tip, and the tip of the cell is wider, though growth is still more concentrated at the center of the tip. When Rga4 is overexpressed it extends further up the cell sides, reducing Cdc42 activation—and therefore growth— at the edges of the cell tip. The resulting cell tip is narrower.

Cdc42 growth direction model has similarities to the hyphoid model

Hyphal cells grow by persistant polarization at the hyphal tip, which is shaped very similarly to the fission yeast cell tip. Hyphae grow very fast, and their growth is driven by a steady supply of vesicles from the Spitzenkörper. As discussed in the introduction, the hyphoid model of hyphal morphogenesis postulates that the location of the Spitzenkörper can determine the width and direction of the hypha simply by its location. In the hyphoid model, the Spitzenkörper acts as a non-directed vesicle supply center, spewing vesicles in all directions, and wherever those vesicles land the cell grows (Reynaga-Pena *et al.*, 1997). In fast growing hyphae, it is located at the apex of the cell tip, and so the apex of the cell tip grows fastest, and areas of the cell farther away grow more slowly. This positioning alone can determine the width of the cell tip (Crampin *et al.*, 2005). A Spitzenkörper has not been detected in fission yeast despite labeling of the membrane trafficking pathway with FM4-64 (Gachet and Hyams, 2005), and so it is unlikely that the width of the fission yeast cell is determined the same way. But the pattern of cell wall expansion in this model is very similar to the pattern I have proposed, so some of the guiding principles may apply (Gierz and Bartnicki-Garcia, 2001). Tip growth requires a steep, localized gradient of exocytosis, and many different mechanisms might yield that gradient (Harold, 2002).

Cdc42 activation organizes a new growth zone

The above model for how localized Cdc42 activation controls cell width does not explain how the tip-localized domain of Cdc42 activation forms, or how the edge

definition of Rga4 becomes localized to the cell sides. In each daughter cell these domains are already established, and are reinforced by cellular geometry. To explain growth zone establishment we need to turn to cells that are depolarized, such as spheroplasts. The challenge of establishing a new growth zone is also faced by germinating spores, but it is difficult to track protein localization by microscopy in spores since their protein levels are low and they have thick spore-specific cell walls. The data presented here show that de novo growth zone formation in the spheroplast is a good model for the formation of the cell tip because the new growth zone shares many characteristics of a cell tip. The width of a growth zone formed from a spheroplast, the germination tube, and a non-spheroplasted cell are all very similar (Figures 4.4 and 4.5). Deletion mutants that are wide in exponential growth are similarly wide when they form a de novo growth zone from a spheroplast (Figure 4.4), and the proteins that localize to the cell tip in exponentially growing cells localize to the newly formed growth zone when cells recover from spheroplasting (Figure 4.1 and 4.6).

Model: Stochastic growth initiation organizes zones of growth activation and inhibition

The growth zone is re-formed from an apparently depolarized cell. The width of the growth zone is not simply carried through the spheroplasting process by the localization of the fluorescently tagged growth-control proteins that I have studied. Scd1, Scd2, Rga4, actin patches (Crn1), microtubules (Atb2), and the cell-wall-synthesis enzyme (1,3)β-D-glucan synthase Bgs4 are all depolarized in newly formed spheroplasts (Figures 4.1 and 4.6). But we cannot say with certainty that

spheroplasts are completely depolarized cells because there may be a protein or structure that remains polarized and directs growth in the cell.

Time-lapse imaging of Scd2-3GFP shows that the protein will often form several small patches in different locations or a single patch that moves around before a patch of protein is stabilized and enlarged (as seen in Figure 4.7, early time points). In recovering spheroplasts, Scd2-mCherry appears to form a patch while Rga4-3GFP is still localized throughout the cell cortex (Figure 4.9). I hypothesize that when Cdc42, Scd2, and Scd1 form a patch, Cdc42 will be activated in this location, which stimulates actin-cable formation via For3 (Martin *et al.*, 2007) and creates a positive feedback loop of protein delivery, complex formation, and activation. This stabilized patch then directs the formation of the new growth zone. From the time-lapse imaging of Rga4-3GFP we know that Rga4 is cleared from the growth zone as growth begins (Figure 4.8). These data suggest that growth polarization at the site of the Scd2 patch is actively excluding Rga4, and that the growth zone clears Rga4, as shown in the model of growth zone establishment in Figure 5.2. This model assumes that Rga4 is stably distributed throughout the cell cortex unless it is actively removed, an assumption that is supported by preliminary FRAP and time-lapse imaging data for Rga4-GFP (data not shown). When growth begins at one location Rga4 could be recycled off the cell cortex in the area of the new growth zone, possibly by the endocytosis that accompanies growth in fission yeast (Gachet and Hyams, 2005). This creates a small hole in the localization of Rga4, and that hole is stably maintained by growth at that site. Rga4 builds up

outside the growth zone, and its localization depends on the rate of removal from the growth zone.

This model explains how a growth zone and an Rga4 exclusion area might form in a recovering spheroplast, but it does not fully explain the localization of Rga4 in exponentially growing cells. In monopolar cells Rga4 is not found at either the growing or the non-growing tip of the cell. The exclusion from the non-growing end depends on the polarity kinase Pom1 (Tatebe *et al.*, 2008). Pom1 localizes to both ends of the cell, is enriched at the non-growing end (Bahler and Pringle, 1998), and physically interacts with Rga4 (Tatebe *et al.*, 2008). In the *pom1Δ* mutant Rga4 is still excluded from the growing end, but it is no longer excluded from the non-growing end. Exclusion from non-growing tips is Pom1-dependent, but exclusion from areas of growth is Pom1-independent, so the mechanism of Rga4 exclusion from the spheroplast growth zone may be the Pom1-independent mechanism. It is not known how Pom1 dynamically localizes within the spheroplast, or whether the exclusion of Rga4 from the new growth zone would be altered in the *pom1Δ* mutant, but this model proposes that Rga4 exclusion from the spheroplast growth zone is driven by growth directly and is Pom1-independent.

Although there is a correlation between Scd2 recruitment to and Rga4 clearance from the growth zone, Rga4's exclusion does not depend on Scd2 directly. In *scd2Δ* cells Rga4 is still enriched on the cell sides (Figure 3.1A). The model proposes that some underlying aspect of cell growth, rather than Scd2 itself, is responsible for Rga4's exclusion from the newly formed growth zone.

Figure 5.2

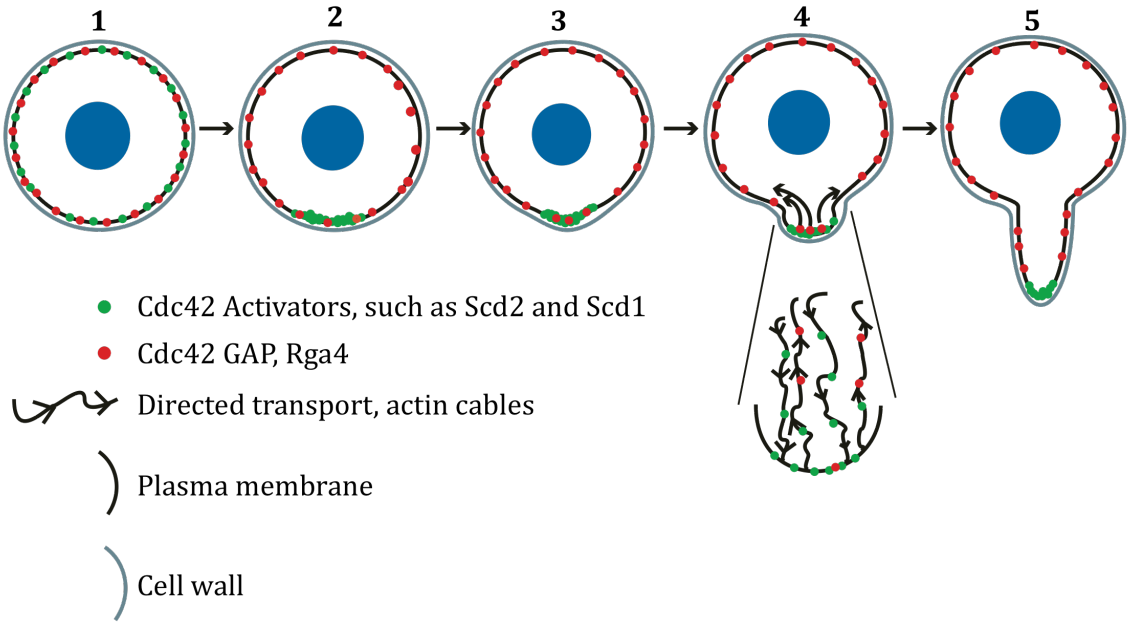

Figure 5.2: Stochastic growth initiation organizes zones of growth activation and inhibition. This model of growth zone formation shows how the GAP Rga4 could be cleared from the newly formed growth zone. Stage 1: After spheroplast formation and cell wall regrowth Rga4, Scd2, and other cell polarity proteins are located throughout the cell cortex. Stage 2: A patch of Scd2, and probably Scd1 and activated Cdc42, forms on the plasma membrane. Rga4 localization is unchanged. Stage 3: Growth begins at the location of the Scd2 patch while some Rga4 remains there. Stage 4: As growth proceeds, and transport to and from the site of growth increases, Rga4 is passively cleared. Zoomed view of Stage 4: Endocytosis and transport from the cell tip by actin cables could deplete otherwise stably localized Rga4. The arrowheads on the cables show the direction of transport. Since Cdc42, Scd2, and Scd1 are actively transported to the cell tip they will be enriched as growth proceeds, even if they are also carried away from the tip non-selectively by endocytosis. Stage 5: This passive depletion results in the characteristic localization of Rga4 and activated Cdc42 in an established growth zone.

Spheroplast polarization may share mechanistic features with symmetry breaking in budding yeast

The self-reinforcing Cdc42 activation and growth, coupled with Rga4 exclusion from the growth zone, may create a stable two-state system, similar to those postulated by reaction-diffusion mechanisms. As described in the introduction, two different experimentally based models for Cdc42 polarization have been proposed to explain budding yeast symmetry breaking. One model depends on a positive feedback loop in which actin cables deliver Cdc42 and its activators to the incipient site of polarization, and then activated Cdc42 stimulates actin-cable formation from that site, resulting in more Cdc42 delivery (Wedlich-Soldner *et al.*, 2003). A second model does not depend on actin transport, but depends instead on the scaffold Bem1 to recruit and stabilize Cdc42 and the GEF Cdc24, and also depends on Cdc42 cycling between the active and inactive states (Irazoqui *et al.*, 2003).

Further work has integrated these two models: Actin transport forms a fast-feedback loop that is not very stable, and intermolecular interactions with Bem1 forms a more stable but slower feedback loop. These two redundant loops in principle provide both quick responsiveness and stable and robust polarity (Slaughter *et al.*, 2009b). As outlined in the introduction, many of the proteins involved in Cdc42 regulation are highly conserved between budding yeast and fission yeast, so these models may be applicable to fission yeast spheroplast recovery, and provide testable hypotheses for how polarization within fission yeast might occur.

In an activator-inhibitor model, a homogeneous two-component system made up of an activator and an inhibitor can resolve into distinct, stable peaks of activation surrounded by inhibition (Sick *et al.*, 2006). The budding yeast models discussed above do not incorporate an inhibitor or take the negative regulation of Cdc42 activity by GAPs into account. This is because the GAPs do not function analogously in budding yeast. Of the three known Cdc42 GAPs, only one plays a significant role in budding, and that GAP localizes to the previous bud site and prevents re-budding at that site (Tong *et al.*, 2007). If fission yeast spheroplast polarization is a symmetry-breaking event, then Rga4 could play a role in the efficient establishment of an activated Cdc42 patch. It is not essential, since *rga4Δ* cells can polarize after spheroplasting (Figure 4.4B), but it may affect the rate of polarization and obviously affects the size of the resulting growth zone.

Orb6 and Gef1 also influence the distribution of activated Cdc42

As described in the introduction, several different protein pathways are important for fission yeast cell morphology. These pathways interact with the localized Cdc42 activation system described here, and they include several proteins that also affect the activation and localization of Cdc42. The other known Cdc42 GEF, Gef1, is partially redundant with Scd1 and localizes to cell tips and the cell septum (Coll *et al.*, 2003; Hirota *et al.*, 2003). That localization depends on the essential NDR kinase Orb6 (Das *et al.*, 2009), which is also localized to cell tips (Wiley *et al.*, 2003). Orb6 loss-of-function mutants are nearly spherical, with Gef1, activated Cdc42, and For3 mislocalized to the cell sides. Orb6 influences Cdc42

activation through Gef1, since deletion of *gef1* restores tip-localized Cdc42 activation in Orb6 loss-of-function mutants (Das *et al.*, 2009).

Several lines of evidence indicate that Orb6-localized Gef1 activation of Cdc42 acts in parallel to the Scd1/Scd2/Rga4 system described in this model. An Orb6 loss-of-function mutant does not affect the localization of Scd1 or Rga4 (Das *et al.*, 2009). Deletions of *gef1* and *scd1* are synthetically lethal (Coll *et al.*, 2003), and deletion of *rga4* in an Orb6 loss-of-function background exacerbates the *orb6-25* temperature-sensitive loss of polarity (Das *et al.*, 2009) . Though *gef1Δ* is not wide, it is synthetically wide with *rga4Δ* (Figure 2.4). It is likely that the weak CRIB-GFP localization to cell tips in *scd1Δ* cells (Figure 3.4) is due to Cdc42 activation at cell tips by Gef1. I have not investigated the localization of Gef1 or Orb6 in spheroplasts, and it would be interesting to see if this parallel pathway plays a role in spheroplast recovery.

Domains of GAP inhibition and GEF activation of Cdc42 may be broadly conserved.

The small GTPase Cdc42 and its regulation by GEFs and GAPs are conserved from yeasts to humans. There are metazoan parallels for the role of GAPs and GEFs in determining Cdc42 localization, and perhaps their role in controlling cellular dimensions. In *C. elegans* development, at the single-cell stage, the GAP CHIN-1 is required for the polarized distribution of Cdc42 on the membrane, and CHIN-1 is localized to the end of the embryo opposite activated Cdc42 (Kumfer et al., 2010). In the eight-cell *C. elegans* embryo the GAP PAC-1 is restricted to inner surfaces of the

embryo and is required for the exclusion of Cdc42 from those inner surfaces, even though the embryo is properly formed at that point (Anderson et al., 2008). Like the GEF Scd1 and the scaffold Scd2, the Cdc42 GEF βPIX is important in fibroblasts for the formation of leading-edge protrusions after wound healing, and the scaffold Scrib mediates βPIX localization to the leading edge (Osmani et al., 2006). In hippocampal neurons the atypical Cdc42 GEF Zizmin1 promotes dendrite outgrowth, and Zizmin knock-down causes short dendrites. The effect on dendrite length depends on GEF activity: A catalytically inactive GEF results in short dendrites (Kuramoto *et al.*, 2009).

These parallels with metazoan cells show that a system of a GEF, a scaffold, and a GAP controlling the localization of Cdc42 activation—and therefore growth—is conserved in a range of eukaryotic organisms, and so our model for determining the size of cellular growth zones in fission yeast may also be relevant to metazoan cells.

Future directions:

The models proposed above, taken with the results presented in this thesis, raise specific, testable questions about how the size and shape of a growth zone are determined. These questions are beyond the scope of the present project, but they would allow further development of the models I have proposed for the distribution of growth and the establishment of a de novo growth zone.

How is the distribution of activated Cdc42 translated into growth?

I have observed several situations in which alterations of Cdc42 activation correlate with alterations in growth patterns, and I have proposed that the distribution of activated Cdc42 determines the shape of the tip of the cell. The retargeting of Scd1 to the cell tips in *scd2Δ* corrected the width of the cell and restored tip localization of the effector kinase Pak1 to the cell tip. But this experiment did not determine which aspects of the distribution specifically determine cell width. Analysis of the distribution of activated Cdc42 in other retargeting experiments, such as targeting either Scd1 or activated Cdc42 to the cell sides, and Rga4 specifically to the cell tips, would provide a way to alter and measure the distribution of Cdc42 directly while observing the changes to the cell shape. Overexpression of constitutively activated Cdc42 causes cells to become more rounded (Miller and Johnson, 1994). Under the model proposed here this would be due to non-targeted localization of activated Cdc42. These manipulations of cell shape and Cdc42 activation would clarify which aspects of the distribution of Cdc42 expression actually determine the shape of the cell: Is the peak intensity of activation important? Or is the shape of the distribution more influential?

How is the growth zone restricted?

The experiments presented here provide evidence that Rga4 exclusion from the growth zone follows Scd2's localization to the growth zone. In the model, I propose that the growth process removes Rga4 in a passive manner from the cell tips. But this is not the only mechanism determining Rga4 localization, because Rga4

is excluded from the growing and non-growing tips of exponentially growing cells. Exclusion from the non-growing tip, but not the growing tip, depends on Pom1, which is evidence for a Pom1-dependent and Pom1-independent mechanism acting in Rga4 localization. To understand how growth changes Rga4 localization more directly, one would need to test Rga4 localization in a *pom1Δ* mutant in spheroplast recovering spheroplasts and non-growing cells.

It is unknown if Rga4 resides in the plasma membrane or the endoplasmic reticulum. The fission yeast cortical ER lies just beneath the cell membrane, and it can be difficult to distinguish the two by light microscopy. A recent study in fission yeast characterized several proteins that shape the ER, which are homologues to well-studied membrane-curvature proteins in budding yeast (Voeltz *et al.*, 2006; Zhang *et al.*, 2010). Deletion mutants are viable, but the cortical ER becomes partially dissociated from the lateral cortex (Zhang *et al.*, 2010). Examining Rga4 localization in these mutants would help determine the role that the ER plays in its localization.

If Rga4 is located in the plasma membrane, Rga4 could selectively partition to cell sides due to differences in lipid composition between cell sides and cell tips. The plasma membrane at the cell tip is enriched for sterols relative to the cell sides (Wachtler *et al.*, 2003). These sterol-rich regions can be disrupted, and if Rga4 depends on differential lipid localization for its exclusion from cell tips then the disruption of sterol localization would change Rga4's localization too.

What other pathways are important in cell width control?

In addition to the Cdc42-related mutants that I studied, the screen identified four other wide mutants that have not been associated with Cdc42 regulation. Some basic characterization of these mutants would expand our understanding of how cell width is determined. These mutants could act either outside of Cdc42 regulation or by indirectly affecting Cdc42 activation. For each mutant one would analyze the actin and microtubule cytoskeletons and the distribution of activated Cdc42 using the CRIB domain.

In particular, the width defect of *myo52Δ* could potentially inform my model for how cell width is determined. Myo52 is a type V myosin (Win *et al.*, 2001), and is thought to transport proteins on actin cables (Motegi *et al.*, 2001). The model I have proposed for spheroplast polarization and growth zone formation control invokes active transport on actin cables (Figure 5.2), and I have presented data that Scd1 and Scd2 depend on actin for their localization. To determine if *myo52Δ* is also altering Cdc42 activation indirectly, through transport defects, one could investigate the localization of Rga4-, Scd1-, Scd2-, and CRIB-GFP in this mutant in exponentially growing cells and spheroplasts.

The width defect of *asl1Δ*, which was the only deletion mutant corrected by sorbitol, could provide insight into Cdc42-independent cell width control. Asl1 is not well characterized, though it has been identified as one of six proteins covalently bound to the cell wall (de Groot *et al.*, 2007). This localization, especially in view of the fact that the *asl1Δ* width defect could be corrected by sorbitol, suggests that the

deletion mutant has an altered cell wall. To further investigate one could analyze the cell wall structure and composition, and screen for other proteins that interact physically. The other covalently bound cell wall protein might interact with Asl1, either physically or genetically.

How is de novo growth localized?

The spheroplast recovery experiments have not revealed whether the site of growth zone formation is truly random. Time-lapse imaging of Scd2-3GFP has provided a framework for future investigations of initial growth polarization. Additional time-lapse experiments with more closely spaced time points within a narrow window in the transition between the early- and late-recovery spheroplat stages would allow proper description of patch formation and the localization of other polarity proteins during polarization. If polarized patch formation is the first step toward formation of a new growth zone, then understanding that process will illuminate how a location is chosen for polarized growth. It would also be interesting to compare the localization of Scd2 and Tea1, since Tea1 localization could be established prior to Scd2 localization in a wild-type spheroplast, though neither protein is absolutely required for spheroplast recovery.

Another cellular structure also could be directing growth to one location. The spindle pole body is a microtubule-organizing center found adjacent to the nuclear envelope (Ding *et al.*, 1997), and could direct growth localization. Two-color time-lapse imaging of a spindle pole body component and Scd2-GFP in recovering spheroplasts could test the role of the spindle pole body in growth-site selection. In

budding yeast, eisosomes form static structures in the plasma membrane (Walther *et al.*, 2006), and one of the homologous proteins forms stable filamentous structures in the fission yeast plasma membrane (James Moseley, unpublished data). These structures, which are excluded from cell ends, could retain their organization through spheroplast formation and form domains in the spheroplast membrane.

Conclusion: Wide mutants and spheroplast studies illuminate different aspects of the same problem

This project was designed to illuminate how the cell specifies the width of the growth zone. I approached the question through three major sets of experiments: First, I identified deletion mutants with altered cell width. Second, through genetic interaction, localization, and retargeting I determined that a subset of the proteins that determine cell width act locally to control Cdc42 activation. Third, I used spheroplasts to determine how growth zones formed de novo, and showed that the same genes that control cell width in vegetative cells influence the width of a de novo growth zone. The spheroplast experiments also provided insight into how zones of Cdc42 activation and inhibition form. The data from these complementary studies, combined with published work, have led to models for how cell growth is directed and established that are broadly applicable due to the broad evolutionary conservation of polarity and growth mechanisms.

Chapter 6: Materials and Methods

Yeast strains were grown as previously described (Moreno et al., 1991). For all experiments cells were grown in Edinburgh Minimal Media (EMM) with supplements at 32° C, unless otherwise specified. For microscopy with fluorescent proteins, media was sterilized by filtration to reduce auto-fluorescence. Fission yeast strains were transformed using the long lithium acetate protocol (Forsburg and Rhind, 2006).

Near-genome-wide screen for width mutants

To screen the deletion collection, I used an early version of the *S. pombe* haploid collection of systemic gene deletions. This version of the collection is known as the beta version and is derived from heterozygous diploid deletions that covered 85% of the fission yeast genome. The collection includes only viable haploid deletions, constructed as described (Kim *et al.*, 2010). A senior scientist in the lab, Dr. Jacqueline Hayles, initially characterized the haploid deletions by observing and noting growth phenotypes under the microscope on agar plates. I used her characterizations to choose 97 potentially wide mutants and 41 potentially thin mutants for further screening. For the images from the plate microscope in Figure 2.1B images were taken on a Zeiss Axioscop 40 microscope with a Nikon CF Plan 50x objective (numerical aperture .55) and a Minolta Dimage A1 camera with a 5.0 megapixel sensor.

For secondary screening, potential wide mutants were grown and measured in hydroxyurea (HU). Cells were grown for 5 hours in EMM4S + 11mM HU (Sigma)

from a 1M stock freshly prepared in dH_2O. Potentially thin mutants were grown in exponential culture. For exponential-phase growth measurements, cells were grown in liquid culture in exponential-phase growth for at least two generations and then photographed live. For cell-width measurements and DIC photographs, cells were imaged in Metamorph (MDS Analytical Technologies) using an epifluorescence microscope (Axioplan 2, Carl Zeiss, Inc.) equipped with a CoolSNAP HQ camera (Roper Scientific), and analyzed in ImageJ (Abramoff et al., 2004). A compilation of representative images for each potential wide mutant can be found in Appendix 1. A searchable digital version is available on the Nurse Lab Server. Width measurements were made from brightfield photographs using the line tool in ImageJ. Cell width was measured on the cell body, approximately two microns from the cell tip on brightfield images. At least 40 cells were measured for each strain.

Tertiary screening was performed by growth of the 26 haploid deletions that were wide or narrow in the secondary screen. Cells were grown in exponential culture, photographed, and 100 cells were measured for each mutant. Growth rates and other morphological defects were assessed; all width mutants had a growth rate within 30% of the wild-type growth rate and did not show other major morphological defects.

Genetic characterization of wide mutants and strain construction

All strains characterized in this study are listed in the strain table, Table 6.1. Deletion strain genotypes were verified by colony PCR across the kanamycin-resistance cassette. The *scd1Δ* strain from the collection did not appear to be

completely deleted, so this strain was reconstructed. The deletion of *scd1* and GFP-tagging of other proteins was performed by homologous recombination as described (Bahler and Jian-Qiu Wu, 1998). Strains expressing GFP-, mCherry-, and 3xGFP- tagged proteins were analyzed to ensure that growth rate, cell size, and cell width were all similar to wild-type cells. All other strains were constructed by tetrad dissection, where applicable.

Cell width in sorbitol (Table 2.2) was assessed by measuring cells that were growing exponentially in EMM4S + 1.2M sorbitol for at least two generations. The % WT Width was calculated by dividing the width of the mutant strain grown in sorbitol by the width of the wild-type strain grown in sorbitol. The % Change in Sorbitol was calculated by dividing the width of each strain when grown in EMM4S + 1.2M sorbitol by the width of the strain when grown without sorbitol, and then subtracting that value from 1.

The deletion mutants *scd1Δ* and *scd2Δ* are sterile. To create all of the strains with these deletions, the mutants were complemented by transformation with a plasmid that contained the deleted gene under control of the high-level *nmt1* promoter. The plasmid also contained the selectable marker LEU2 and was maintained by growth on selective minimal media (EMM-leu). After crossing the strains and dissecting tetrads, the desired strain was selected based on antibiotic resistance or phenotype, such as the presence of a fluorescently tagged protein. The strain was then screened for plasmid loss by growth on selective plates. Strains that no longer grew on EMM-leu, and therefore had lost the complementing plasmid, were selected for further analyses.

Cell widths are represented in box-and-whiskers plots. In these plots, the box represents the middle two quartiles of the data. The median value is marked with a horizontal line across the box and the whiskers on the plot represent the outer quartiles of the distribution. If the range of the outer quartiles spans more than 1.5 times the size of the boxes then higher or lower values (outliers) are plotted as individual points. (Synergy, 2004)

Microscopy

Actin patches and cables were visualized by staining formaldehyde fixed cells with Alexa Fluor 488 phalloidin (Invitrogen) and imaging on a DeltaVision Spectris (Applied Precision) composed of an Olympus IX71 wide-field inverted fluorescence microscope, an Olympus UPlanSApo ×100, numerical aperture 1.4, oil-immersion objective, and a Photometrics CoolSNAP HQ camera (Roper Scientific). Images were captured and processed by iterative constrained deconvolution using SoftWoRx (Applied Precision), and analyzed in ImageJ. This microscope setup was used for all of the fluorescent-protein live-cell imaging, except in Figures 3.3A, 3.4A, 3.7A, and 3.10A, where the previously described Zeiss microscope was used, and images were not deconvolved. The imaging conditions for spheroplasts will be discussed below. For Figures 3.4C and 3.5 images were also not deconvolved. To stain growing cell wall, I added blankophor (Frank, 1991) to the media (MP Biomedicals; 1:100,000 dilution).

Images are displayed with an inverted look-up table for improved viewing and printing. The inversion of the look-up table was done in ImageJ using the “Invert

LUT" command, which subtracts the value of each pixel from the maximum possible value but does not alter the relative value of each point. (NIH, 2010)

For the CRIB-GFP and Pak1-mCherry line-scan analysis in Figures 3.5 and 3.8, a series of images were taken spanning the width of the cell, and images were calibrated using a uniform fluorescent field and the calibration software in SoftWoRx (Applied Precision). Line scans that are directly compared come from images gathered on the same day and under the same conditions, and calibrated with the same set of uniform fluorescence images. Line intensity was analyzed in ImageJ. The image plane in the Z-stack with the highest maximum intensity was chosen, and a segmented line was drawn from the center of the tip of the cell, following the cell edge, to approximately 1 micron past the edge of the tip. The line was 5 pixels wide, and drawn with a spline fit. The intensity profile of the line was then plotted, and then 50 of these profiles, aligned by cell centers, were averaged for each genotype. For the Pak1-mCherry analysis in figure 3.8C, the average value for each point in both expression conditions was normalized by subtracting the value for *scd2Δ* Pak1-mCherry from each point.

Fusion protein construction

Fusion proteins and the control proteins under the control of the *nmt41* promoter used in Figures 3.7, 3.8, and 3.9 were constructed as follows. To GFP tag *scd1* under the control of the *nmt41* promoter, the gene was amplified from the genome with primers that contained a Sal1 (F) and an Xma1 (R) site, column purified, and digested with those restriction enzymes. The vector pREP41 with a C-

terminal eGFP tag (Craven et al., 1998) was also digested with Sal1 and Xma1, followed by gel purification. The vector and PCR insert were ligated together to produce *nmt41P-scd1-GFP-nmt41T* (plasmid ARC2077). This construct was moved into the integration vector by PCR amplification with primers for the *nmt41* promoter and terminator containing restriction enzyme sites for Eag1 and Cla1, respectively, then ligation into pJK148 digested with the same enzymes creating plasmid ARC2078. The plasmid was then integrated into the *leu1* locus after digestion with Nru1 as described (Keeney and Boeke, 1994).

To make the For3N-Scd1 fusion, the plasmid ARC2077 was digested with Sal1 at the Scd1 N-terminus. The first 2106 nucleotides of *for3* were amplified out of the genome using primers with homology to the sequences flanking the Sal1 cut site, and then the PCR product and digested vectors were ligated using the In-Fusion PCR Cloning Kit (Clonetech) to produce *nmt41P-for3N-scd1-GFP-nmt41T* (plasmid ARC2079). This construct was subcloned into the integration vector pJK210 at the Eag1 site using the In-Fusion PCR Cloning Kit (Clonetech), as described above, to make plasmid ARC2080. This plasmid was then integrated at *ura4* after digestion with EcoRV (Keeney and Boeke, 1994).

To GFP-tag cytoRga4 under the control of the *nmt41* promoter, the gene was amplified from the genome of CA5544 (Tatebe et al., 2008) with primers that contained an Nde1 (F) and an Xma1 (R) site, column purified, and digested with those restriction enzymes. The vector pREP41 with a C-terminal eGFP tag (Craven et al., 1998) was also digested with Nde1 and Xma1, followed by gel purification. The vector and PCR insert were ligated together to produce *nmt41P-cytoRga4-GFP-*

nmt41T (plasmid ARC2081). This construct was moved into the integration vector by PCR amplification with primers for the *nmt41* promoter and terminator containing restriction enzyme sites for Eag1 and Cla1, respectively, then ligated into pJK148 digested with the same enzymes (to create plasmid ARC2082). This plasmid was integrated into the *leu1* locus after digestion with Nru1 as described (Keeney and Boeke, 1994).

To generate *nmt41P-blt1-cytoRga4-GFP-nmt41T*, Nde1 and BamHI sites were added between the *nmt41* promoter and *cytoRga4*, and the full-length genomic copy of *blt1* was amplified by PCR using primers that contained NdeI and BamHI sites, digested, and inserted into the *nmt41-cytoRga4* plasmid digested with the same enzymes. This created the plasmid ARC 2083. The construct was sub-cloned into pJK148, the *leu1* integration vector, as described for ARC 2081 to make ARC 2084. This plasmid was then integrated into the genome in the *leu1* locus after digestion with Nru1 as described (Keeney and Boeke, 1994).

To GFP-tag amino acids 622-760 of Rga4 under the control of the *nmt41* promoter, those nucleotides of the Rga4 gene were amplified from the genome with primers that contained an Nde1 (F) and an Xma1 (R) site, column purified, and digested with those restriction enzymes. The vector pREP41 with a C-terminal eGFP tag (Craven et al., 1998) was also digested with Nde1 and Xma1, followed by gel purification. The vector and PCR insert were ligated together to produce *nmt41P-Rga4 aa622-760-GFP-nmt41T* (plasmid ARC2084).

Other protocols

Genes under the control of the *nmt41* promoter were grown in the presence of 5μg/mL thiamine, then washed three times by filtration with EMM4S without thiamine, resuspended in EMM4S without thiamine, and grown for the number of hours noted in the text before the cells were measured and photographed.

Actin was disrupted by addition of either 10μM (low-level) or 100μM (high level) LatrunculinA (Sigma) from a 1mM stock. Microtubules were disrupted by treatment with carbendazim (Aldrich) at a final concentration of 50μg/mL, from a freshly made 1mg/mL stock in DMSO.

The levels of the induced fusion proteins were assessed by a standard Western blotting procedure. Proteins were extracted by rapid bead-beating. Western blots were probed with an anti-GFP antibody (Cristea et al., 2005) to assess fusion protein level and an anti-tubulin antibody to assess protein loading (anti-Tat1, gift of K. Gull).

Spheroplast generation

Spheroplasts were generated by protocol similar to that of Tagaki et al. (2003). Cells were grown in exponential culture in EMM4S to mid log phase, then washed twice in E-buffer + sorbitol (50mM sodium citrate, 100mM sodium phosphate buffer, +1.2M Sorbitol, pH 5.6), and resuspended in E-buffer + sorbitol. To form spheroplasts, cells were incubated at 37°C with 0.2mg/mL zymolyase 100T (Seikagaku Biobusiness) and 1.25mg/mL lysing enzymes from trichoderma

harzianum (Sigma). Cell wall digestion was monitored by estimating the percentage of spheroplasts under the microscope, and cells were washed in EMM4S+1.2M Sorbitol once more than 90% of cells appeared to be escaping the cell wall. It would take between ten and twenty minutes to reach this level of cell wall digestion. Cells were washed gently three times in EMM4S+1.2M Sorbitol, and then allowed to recover in the same media, shaking, at either 32°C or 36.5°C, as indicated in the text.

Spheroplast imaging

For time-lapse imaging, spheroplasts were mounted on agarose pads (1.4% agarose in filtered EMM4S or EMM4S +1.2M sorbitol). For time-lapse series greater than two hours, coverslips were sealed with VALAP (Vaseline, Lanolin, Paraffin; 1:1:1). For Figures 4.1A, 4.2, 4.3, 4.4, and 4.5 cells were imaged live using the Zeiss Axioplan microscope described above, and analyzed in ImageJ (National Institutes of Health). Width measurements were made from photographs using the line tool in ImageJ. Cell width was measured on the growth zone, near the tip of the cell. The angle of cell growth for bipolar cells was measured in ImageJ using the angle tool. For Figures 4.1B, 4.6, 4.7, 4.8, and 4.9, cells were imaged on the DeltaVision Spectris microscope described above (Applied Precision). Images were captured and, for figures 4.1B, 4.6, 4.7, and 4.9, processed by iterative constrained deconvolution using SoftWoRx (Applied Precision). Image analysis was done using ImageJ.

To compare the volume of the spheroplast to the width of the growth zone that formed from that spheroplast, the volume was estimated by measuring the diameter of the

round part of the recovering spheroplasts in photographs, using the line tool in image J, and then calculating the volume as though it were a sphere.

Diploid generation and spore germination

For spore germination, a homozygous h+/h+ diploid was generated by treatment with 20mg/mL MBC for 5 hours, followed by plating on YE4S plates containing 5 mg/l phloxin B (Sigma). Diploids were selected by increased cell size, and then transformed with the plasmid pON177 containing the mat1-M sequence (Styrkarsdottir et al., 1993). These cells were starved for nitrogen by growth in EMM-N to induce sporulation. Spores were collected by digesting the ascus wall, washed, and resuspended in rich media to induce germination. Germination was monitored, and germination tubes were imaged live 6 hours after return to rich media (YE4S).

Table 6.1 *Schizosaccharomyces pombe* strains used in this thesis

Strain number	Genotype	Source
PN556	*ade6-216 ura4-D18 leu1-32 h+*	Lab collection
PN10227	*ral2Δ::kanMX6 ade6-M216 ura4-D18 leu1-32 h+*	(Kim et al., 2010)
PN10720	*spy1Δ::kanMX6 ade6-M216 ura4-D18 leu1-32 h+*	(Kim et al., 2010)
PN10064	*rga4Δ::kanMX6 ade6-M216 ura4-D18 leu1-32 h90*	(Kim et al., 2010)
PN10224	*efc25Δ::kanMX6 ade6-M216 ura4-D18 leu1-32 h+*	(Kim et al., 2010)
PN10721	*asp1Δ::kanMX6 ade6-M216 ura4-D18 leu1-32 h+*	(Kim et al., 2010)
PN10267	*cpp1Δ::kanMX6 ade6-M216 ura4-D18 leu1-32 h+*	(Kim et al., 2010)
PN10722	*asl1Δ::kanMX6 ade6-M216 ura4-D18 leu1-32 h+*	(Kim et al., 2010)
PN10226	*scd2Δ::kanMX6 ade6-M216 ura4-D18 leu1-32 h+*	(Kim et al., 2010)
PN1653	*ras1Δ::ura4+ ade6-M210 leu1-32 ura4-D18 h90*	Lab collection
PN10225	*myo52Δ::kanMX6 ade6-M216 ura4-D18 leu1-32 h+*	(Kim et al., 2010)
PN10723	*scd1Δ::kanMX6 ade6-M210 ura4-D18 leu1-32 h+*	This study
PN 10724	*rga4Δ::kanMX6 scd2Δ::kanMX6 ade6-M216 ura4-D18 leu1-32 h*	This study
PN10725	*rga4Δ::kanMX6 scd1Δ::kanMX6 ura4-D18 leu1-32 h*	This study
PN10726	*scd1Δ::kanMX6 scd2Δ::kanMX6 ade6-M216 ura4-D18 leu1-32 h*	This study
PN10727	*rga4-3GFP::kanMX6 ura4-D18 leu1-32 ade6-M210 h+*	This study
PN10728	*scd2Δ::kanMX6 rga4-3GFP:kanMX6 ura4-D18 leu1-32 ade6-M216 h90*	This study
PN 10729	*scd1Δ::kanMX6 rga4-GFP ura4-D18 leu1-32 h-*	This study
PN10730	*scd2-3GFP::KanMX6 h+*	This study
PN10731	*rga4Δ::kanMX6 scd2-3GFP::kanMX6 leu1-32 ura4-D18 h-*	This study

PN10732	*scd1-3GFP::kanMX6 h+*	This study
PN10733	*rga4Δ::kanMX6 Scd1-3GFP::KanMX6 h+*	This study
PN10734	*scd1-3GFP::kanMX6 scd2Δ::kanMX6 ura4-D18 leu1-32 ade6-M216 h+*	This study
PN10735	*scd1Δ::kanMX6 scd2-3GFP::kanMX6 ura4-D18 leu1-32 h-*	This study
CA5931	*ura4-294::[P_{pak1}+:ScGIC2 CRIB domain-3xGFP:ura4+] leu1-32*	(Tatebe et al., 2008)
PN10737	*scd2Δ::kanMX6 ura4-294::[P_{pak1}+ScGic2:3XGFP:ura4+] leu1-32 h+*	This study
PN10738	*scd1Δ::kanMX6 ura4-294(P_{pak1}+:ScGic2:3XGFP:ura4+) leu1-32 ade6-M216 h+*	This study
PN10739	*scd2Δ::kanMX6 leu1-32::(nmt41-scd1-GFP::leu1+) ade6-M210 h+*	This study
PN10740	*scd2Δ::kanMX6 ura4-294::(nmt41-For3N-scd1-GFP::ura4+) leu1-32 ade6-M216 h+*	This study
CA5544	*rga4 Δaa622-760-GFP::ura4+ leu1-32 ura4-D18*	(Tatebe et al., 2008)
PN10742	*rga4Δ::kanMX6 ura4-D18 leu1-32::[nmt41-cytorga4-GFP:: leu1+]*	This study
PN10743	*rga4::kanMX6 ura4-D18 leu1-32::[nmt41-Blt1-cytorga4-GFP:: leu1+] h-*	This study
PN10753	*orb2-34-GFP::kanMX6 ade6-M210 leu1-32 h+*	This study
PN1002	*orb2-34 ade6-M216 leu1-32*	(Verde, 1995)
PN10754	*scd2::KanMX6 pak1-mCherry::natR leu1-32(nmt41P:scd1-GFP-nmt41T::leu1+)*	This study
PN10755	*scd2::kanMX6 pak1-mCherry ura-294::[nmt41:For3N-scd1-GFP::ura4+]*	This study

PN10756	*scd2::kanMX6 pak1-mCherry::natR*	This study
PN10757	*pak1-mCherry::natR h-*	This study
PN4635	*SV40-GFP-atb2-GFP::leu1+ leu1-32 ura4-D18 h-*	(Tatebe *et al.*, 2001)
PN4251	*crn1-GFP::kanMX6 ura4-D18 leu1-32 h+*	(Pelham and Chang, 2001)
PN10355	*bgs4Δ::ura4⁺ P_{bgs4^+}::GFP-bgs4⁺leu1-32 ura4-D18 hys3-D* h-	(Cortes *et al.*, 2005)
PN143	*cdc25-22 h-*	Lab collection
PN3053	*orb2-34 cdc25-22 h+*	(Verde *et al.*, 1995)
PN10758	*scd2::kanMX6/scd2::kanMX6 h+/h+* transformed with M factor plasmid pON177	This study
PN10759	*rga4-3GFP::kanMX6 scd2-mCherry::kanMX6*	This study

Appendix I
Screen for Stout Mutants

FDK25, PN4, WT

HU width: 4.17
Other Phenotypes: none
Gene function/sequence info: none

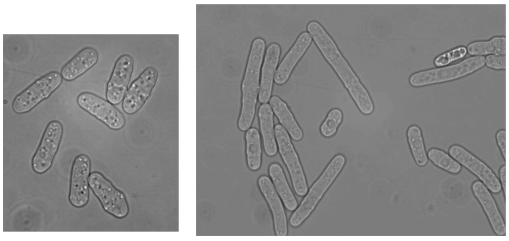

PN556, WT w/auxotrophies

HU width: 4.12
Other Phenotypes: none
Gene function/sequence info: This is probably the best control- it has the same auxotrophies as the deletion collection:ade6-M216 ura4-D18 leu1-32 h+

exponential HU

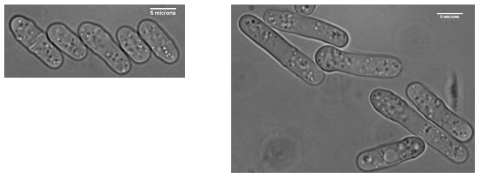

FDK32, for3

HU width: 4.57
Other Phenotypes: lumpy, irregular
Gene function/sequence info: formin

exponential HU

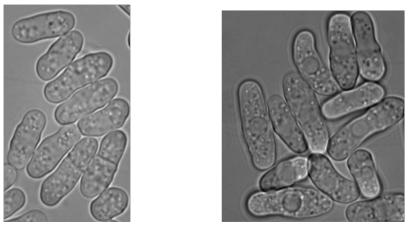

FDK38, PN10058, SPBC16H5.08c

HU width: 4.18
Other Phenotypes:
Gene function/sequence info: putative ABC-transporter (ATP-binding cassette). SC homolog is involved in ribosome biogenesis.

exponential HU

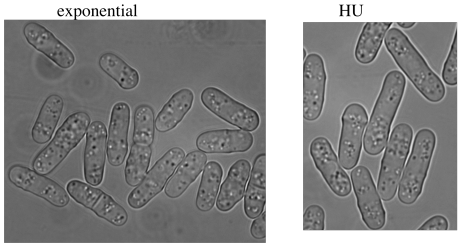

FDK39, PN10063, gyp10

HU width: 3.93
Other Phenotypes: some cells curved, lumpy
Gene function/sequence info: TBC domain containing family, GTPase activators of Rab-like small GTPases

exponential HU

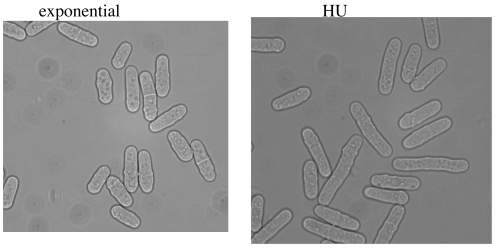

FDK40, PN10064, rga4

HU width: 4.99
Other Phenotypes:
Gene function/sequence info: rho gap.

exponential HU

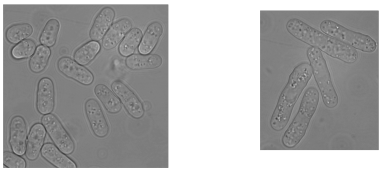

FDK41, PN10067, SPAC7D4.12c

HU width: 4.29
Other Phenotypes: some cells curved
Gene function/sequence info: predicted integral membrane protein.

exponential HU

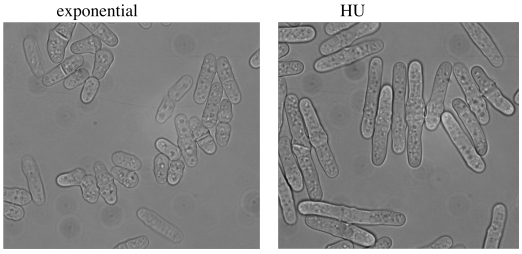

FDK42, PN10079, SPAC821.05

HU width: 5.1
Other Phenotypes: slow growing, does not elongate much in HU, misplaced cell wall patches.
Gene function/sequence info: almost no info. Low similarity to EIF3.

exponential HU

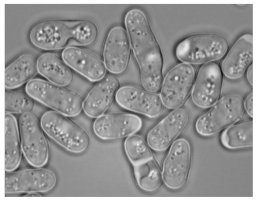

FDK43, PN10083, clp1

HU width: 3.99
Other Phenotypes:
Gene function/sequence info: a probable dual specificity phosphatase that inhibits cdc2

exponential HU

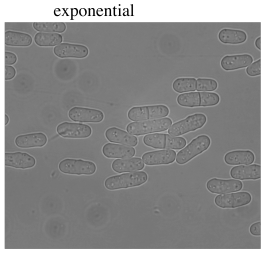
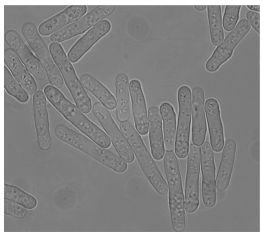

FDK44, PN10089, SPAC1B2.02c

HU width: 4.13
Other Phenotypes: cells look pretty good, but only grow well in YE4S
Gene function/sequence info: a probable dual specificity phosphatase that inhibits cdc2

exponential HU

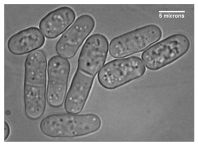
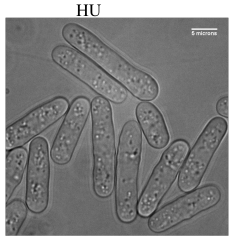

FDK45, PN10091, SPBC8D2.17

HU width: 4.49
Other Phenotypes:some curved cells, many swollen in the middle or at the end
Gene function/sequence info: probable alpha-1,2-galactosyltransferase.

exponential HU

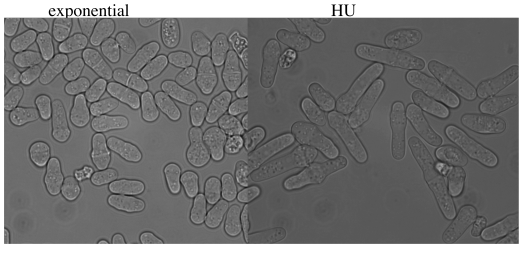

FDK47, PN10094, chr3/cfh1

HU width: 4.13
Other Phenotypes:
Gene function/sequence info: putative chitin synthase regulatory factor

exponential HU

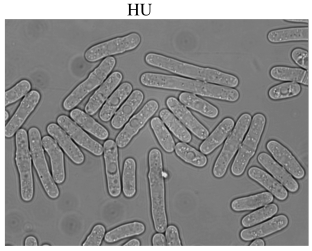

FDK48, PN10095, SPAC1071.02

HU width:4.29
Other Phenotypes: only grows well in YE4S
Gene function/sequence info: transcriptional regulation (predicted)

exponential HU

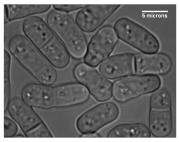
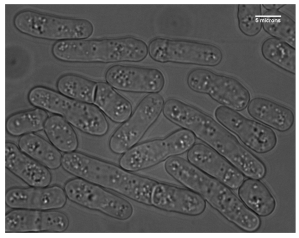

FDK49, PN10096, SPAC11E3.05

HU width:4.29
Other Phenotypes: only grows well in YE4S
Gene function/sequence info: contains 5 WD domains

exponential HU

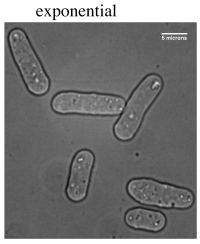

FDK50, PN10097, SPBC119.12

HU width: 4.10
Other Phenotypes: slightly elongated in exponential culture?
Gene function/sequence info: putative hydrophobic protein?

Exponential? HU

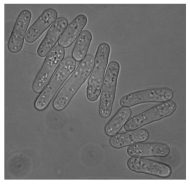
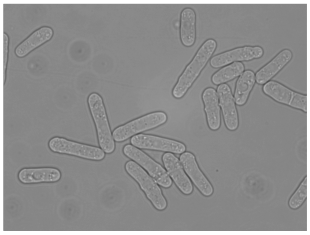

FDK51, PN10228, SPAC1782.05

HU width: 4.45
Other Phenotypes: large calcafluor staining caps
Gene function/sequence info: related to SC protein involved in rapamycin sensitivity

Exponential HU

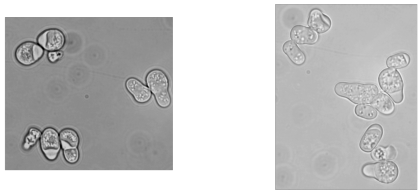

FDK52, PN10231, SPAC1071.06

HU width: 4.44
Other Phenotypes: some cells are quite swollen, some septation issues.
Gene function/sequence info: Low similarity to SC Arp9, not much else.

Exponential HU

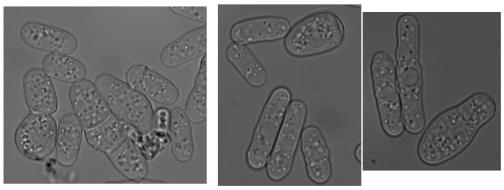

FDK53, PN10260, kin1

HU width: 4.81
Other Phenotypes: grows better in YE4S,
Gene function/sequence info: serine/threonine protein kinase, reported as rounded ends.

Exponential HU

FDK57, PN10265, SPAC8C9.11

HU width: 4.05
Other Phenotypes: some cells are quite swollen, some septation issues.
Gene function/sequence info: BolA-like protein family .

Exponential HU

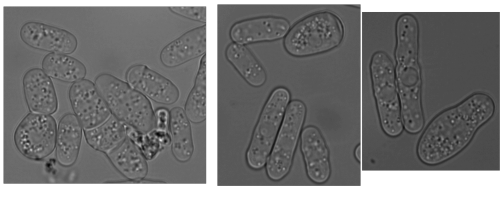

FDK58, PN10224, efc25

HU width:5.0
Other Phenotypes: cells are polarized, though this is published as orb.
Gene function/sequence info: GEF for Ras1

Exponential HU

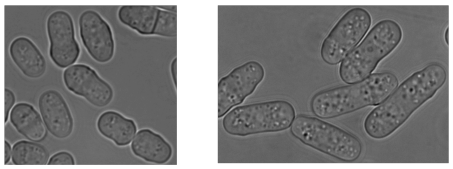

FDK59, PN10010, SPBC3E7.15c

HU width: 4.53
Other Phenotypes: many round or swollen cells, esp swollen in the center, cells are irregular.
Gene function/sequence info: predicted ceramide biosynthesis, secretion, GPI-anchored protein production.

Exponential HU

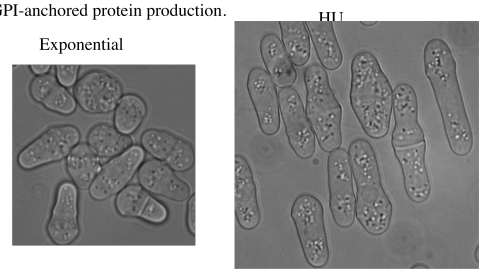

FDK60, PN10071, SPBC4F6.12

HU width: 4.31
Other Phenotypes: cells look pretty good. . .
Gene function/sequence info: LIM-domain containing.

Exponential HU

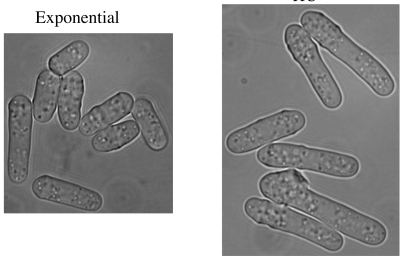

FDK61, PN10225, myo52

HU width: 4.94
Other Phenotypes: some cells can be irregular.
Gene function/sequence info:myo52 is pretty stout.

Exponential HU

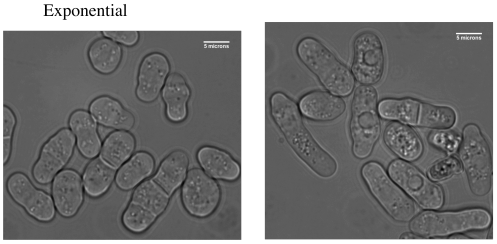

FDK62, PN10227, ral2

HU width: 4.78
Other Phenotypes: cells are somewhat lumpy and lemon shaped, look a bit wide.
Gene function/sequence info: Ras GEF

Exponential

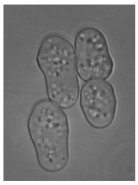

HU

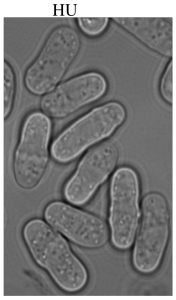

FDK63, PN10082, sat1

HU width: 4.41
Other Phenotypes: pretty wt looking.
Gene function/sequence info: an allele shows nitrogen starvation induced arrest in G2

Exponential

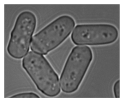

HU

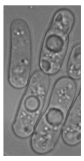

FDK64, PN10226, scd2/ral3

HU width: 5.5
Other Phenotypes: orbish, though most cells elongate in HU.
Gene function/sequence info: transfer of GTP-bound Cdc42p from the upstream activator Scd1p to the downstream effector Pak1p is facilitated by the scaffold protein Scd2p.

Exponential

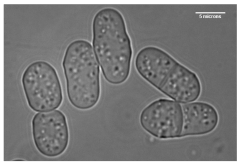

HU

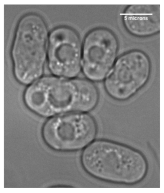

FDK65, 10073, scd1

HU width: 4.60
Other Phenotypes: only grows at 25C in YE4S
Gene function/sequence info: putative GEF for cdc42

Exponential

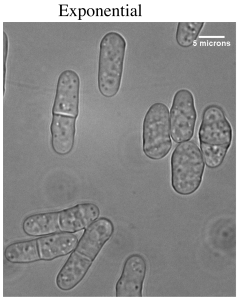

HU

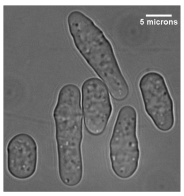

FDK66, PN10261, cta4

HU width: 5.65
Other Phenotypes: Some cells have swollen pieces, swollen ends. Grown in YE4S, does not grow in EMM
Gene function/sequence info: ATPase activity, Ca++ transport, ER localization

Exponential

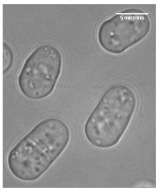

HU

FDK68, PN10059, pmr1

HU width: 4.81*--I did not measure totally round cells.
Other Phenotypes: more orbish in HU than exponential?
Gene function/sequence info:calcium transporting atp-ase

Exponential

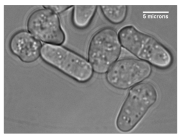

HU

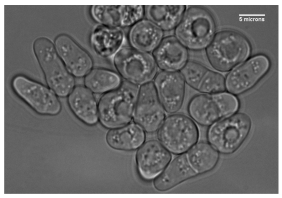

FDK69, 10267, cpp1

HU width: 4.70
Other Phenotypes: TS only grows at 25C, many orb cells, only measured those that elongated.
Gene function/sequence info: beta subunit of farnesyltransferase

Exponential

HU

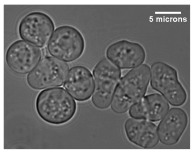

FDK72, PN10233, meu29

HU width: 4.29
Other Phenotypes: rounded at one end, almost looks like a recovering spheroplast
Gene function/sequence info: upregulated in meiosis. Contains a putative transmembrane domain

Exponential

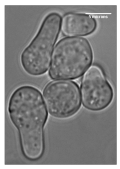

HU

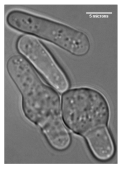

FDK73, PN10259, SPAC323.05c

HU width: 4.35
Other Phenotypes: some lumpy cells? But pretty Wtish.
Gene function/sequence info: almost no info. Some similarity to predicted SC methyltransferases

Exponential

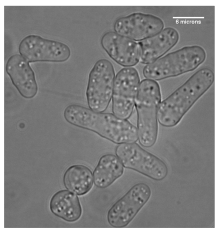

HU

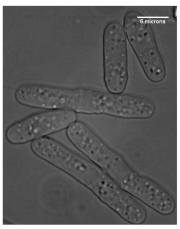

FDK74, PN10264, SPAC1071.04c

HU width: 4.20
Other Phenotypes: swollen middles, some cells quite small and don't elongate.
Gene function/sequence info: predicted signal peptidase subunit, two predicted transmembrane domains

Exponential

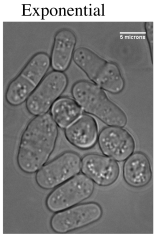

HU

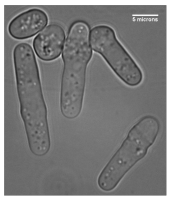

FDK75, PN10075, SPBC30B4.04c

HU width: 4.45
Other Phenotypes: lumpy/curvy
Gene function/sequence info: contains DNA binding domain.

Exponential

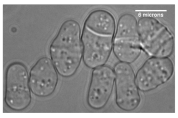

HU

FDK76, PN10076, set3

HU width: 4.08
Other Phenotypes: cells look pretty dang good.
Gene function/sequence info:contains a SET domain, implicated in histone methyltransferase.

Exponential

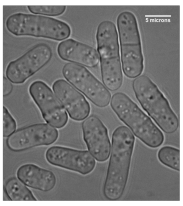

HU

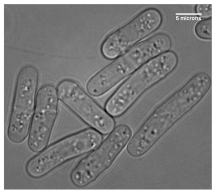

FDK77, PN10084, atp10

HU width: 4.29
Other Phenotypes: does not grow well in EMM. This is in YES.
Gene function/sequence info: related to proteins involved in mitochondrial ATPase complex assembly

Exponential

HU

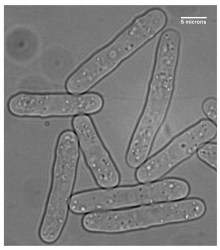

FDK78, PN10246, SPBC9B6.07

HU width: 4.23
Other Phenotypes: a bit curvy/lumpy.
Gene function/sequence info: predicted rRNA processing involvement

Exponential

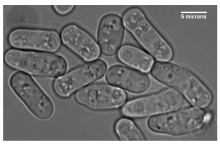

HU

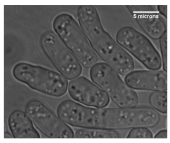

FDK79, PN10009, SPBC30B4.03c

HU width: 4.72
Other Phenotypes: Some funny blebbs in arrested cells.
Gene function/sequence info: no info

Exponential

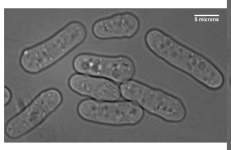

HU

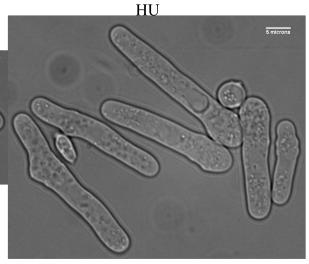

FDK81, PN10087, SPBC18H10.04c/sce3

HU width: 4.16
Other Phenotypes: bit lumpy?
Gene function/sequence info: similarity to eIF4B

Exponential

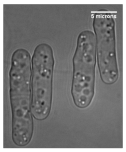

HU

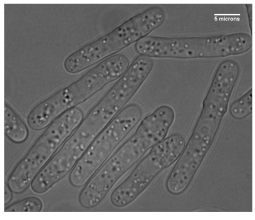

FDK82, PN10258, SPAC1F5.05c

HU width: 4.05
Other Phenotypes: lumpy, rounded in the exp culture, less so when blocked w/HU.
Gene function/sequence info: no info

Exponential

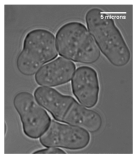

HU

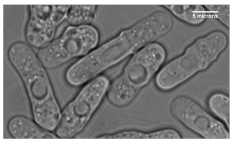

FDK84, h234, rdr1

HU width: 4.46
Other Phenotypes: occasional Ts in culture, rounded cells
Gene function/sequence info: RNA-directed RNA polymerase, involved in gene silencing.

Exponential

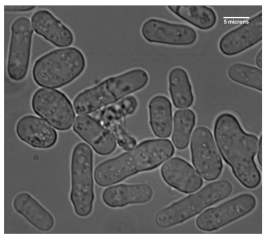

HU

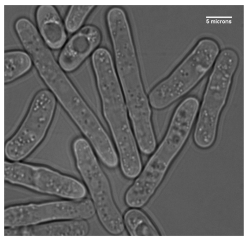

FDK85, w565, ubr1

HU width: 4.26
Other Phenotypes: cells look pretty normal
Gene function/sequence info: putative component of ubiquitin protein ligase

Exponential

HU

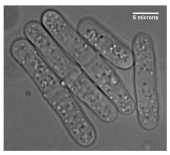

FDK86, s325,rga6

HU width: 4.50
Other Phenotypes: some curved cells
Gene function/sequence info: putative GAP for Rho1 family proteins

Exponential

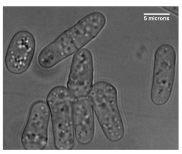

HU

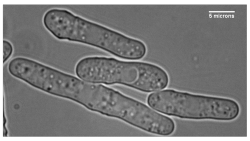

FDK87, s17, pom1

HU width: 4.09
Other Phenotypes: curved, irregular cells
Gene function/sequence info: protein kinase involved in morphogenesis

Exponential

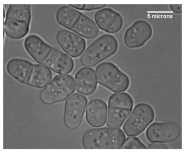

HU

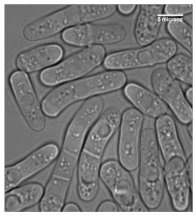

FDK88, p65, SPAC637.06

HU width: 4.08
Other Phenotypes: cells swollen at the bottoms, I usually measured away from that part- not as pronounced in HU
Gene function/sequence info: putative galactosyltransferase

Exponential

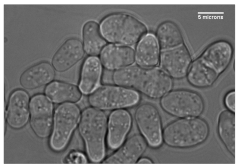

HU

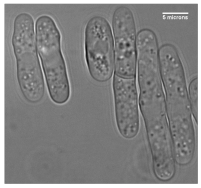

FDK89, h32, myo1

HU width: 5.01
Other Phenotypes: lumpy!
Gene function/sequence info: myosin I, activates arp2/3 complex

Exponential

HU

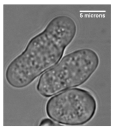

FDK90, p17, pek1

HU width: 4.32
Other Phenotypes: cells are slightly wide, but regularly shaped
Gene function/sequence info:protein kinase in MAPKKK cascade during cell wall morphogenesis.

Exponential

HU

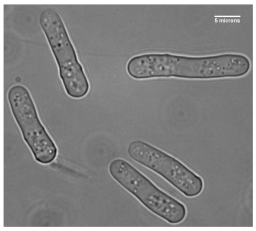

FDK91, p19, pmp1

HU width: 4.62
Other Phenotypes: many cells are swollen in the middle- I measured closer to the ends
Gene function/sequence info: protein phosphatase involved in chloride ion homeostasis

Exponential

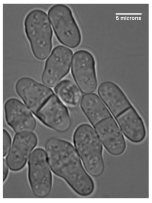

HU

FDK92, p170, mpr1/spy1

HU width: 4.72
Other Phenotypes:
Gene function/sequence info: protein kinase involved in stress response, upstream of mcs4

Exponential

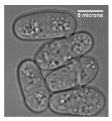

HU

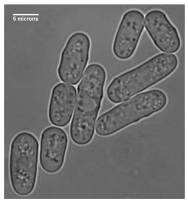

FDK93, s7, SPBC31F10.10c

HU width: 5.48 (many irregular, orb, or very large cells)
Other Phenotypes: many cells very irregular, some swollen, multiseptated
Gene function/sequence info: member of the MYND zinc finger family, induced in meiosis

Exponential

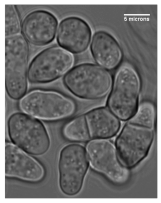

HU

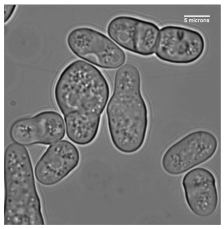

FDK94, w2418 ,rdi1

HU width: 4.22
Other Phenotypes: occasionally cells aren't totally straight
Gene function/sequence info: GTPase regulator, affects localization of rho4

Exponential

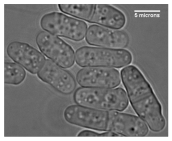

HU

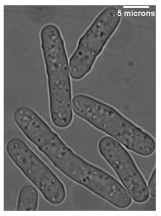

FDK95, SPAC1F5.05c

HU width: 4.80
Other Phenotypes: bit lumpy, much like myo52
Gene function/sequence info: sequence orphan

Exponential

HU

FDK96, w3399, alg5

HU width: 4.10
Other Phenotypes: looks pretty normal
Gene function/sequence info: probable glycosyl transferase

Exponential

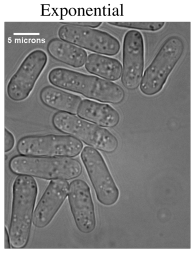

HU

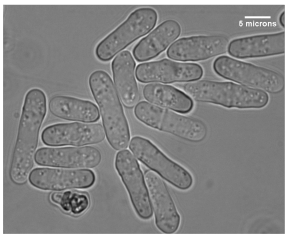

FDK97, w3248, alg6

HU width: 4.21
Other Phenotypes: rounded bottoms- measured near tips.
Gene function/sequence info:Putative alpha-1,3-glucosyltransferase involved in synthesis of the dolichol-linked, oligosaccharide precursor

Exponential

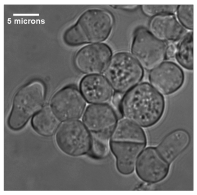

HU

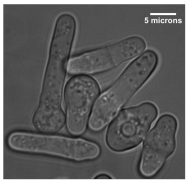

FDK98, w3273, gps2

HU width: 4.1
Other Phenotypes: rounded ends- which is growing?
Gene function/sequence info: defects in galactosylation of N-linked oligosaccharides

Exponential

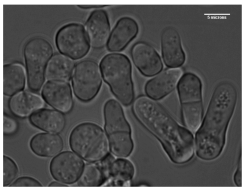

HU

FDK99, w778, pmc5

HU width: 3.95
Other Phenotypes: some curvy, swollen cells
Gene function/sequence info: component of the RNA pol II holoenzyme and mediator subcomplex

Exponential

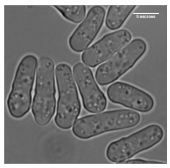

HU

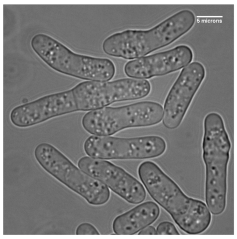

FDK101, h136, par1

HU width: 4.49
Other Phenotypes: lumpy
Gene function/sequence info: protein phosphatase PP2A, subunit B'

Exponential

HU

FDK102, p40, alp14

HU width: 4.12
Other Phenotypes: a bit lumpy/ swollen towards middle/ends.
Gene function/sequence info: kinetochore-associated protein required for spindle checkpoint, w/MT destabilizing proteins klp5 and klp6

Exponential

HU

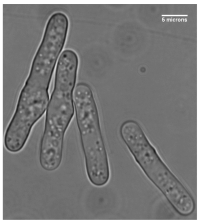

FDK103, c198, mal3

HU width: 3.73
Other Phenotypes: some cells curved
Gene function/sequence info: involved in MT organization and stability. Are these cells narrow?

Exponential

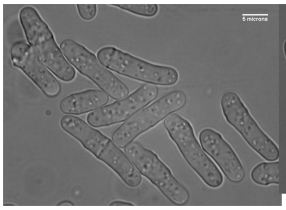

HU

FDK104, w3391, spn3

HU width: 4.02
Other Phenotypes: cells look pretty good. . .
Gene function/sequence info: member of GTP-binding cell division family, similar to SC cdc11

Exponential

HU

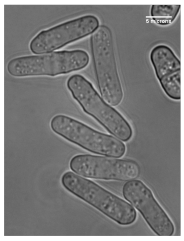

FDK106, w663, SPCC1919.15

HU width: 4.15
Other Phenotypes: cells septate and branch.
Gene function/sequence info:

Exponential

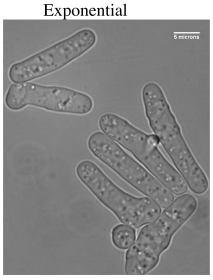

HU

FDK107, asp1, w3763

HU width: 4.96
Other Phenotypes: sone irregular/lumpy cells, not very elongated
Gene function/sequence info: interacts genetically with profilin, required for establishment and maintanance of polarized growth

Exponential

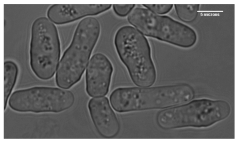

HU

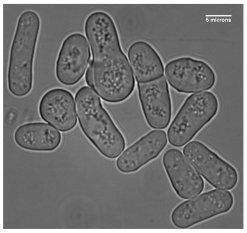

FDK109, y109, SPBC9B6.07

HU width: 4.26
Other Phenotypes: cells did not elongate very much
Gene function/sequence info: nop52 family, no other info.

Exponential

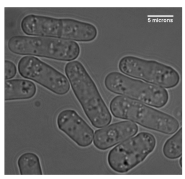

HU

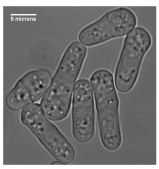

FDK110, w2982, SPBC19G7.16 (isw1)

HU width: 4.41
Other Phenotypes: some cells lumpy, some cells curved.
Gene function/sequence info: possible role in transcription regulation by homology to SC isw1.

Exponential

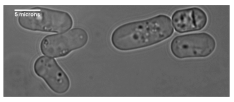

HU

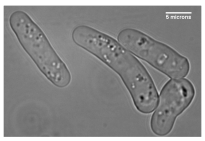

FDK111, w86, SPAC27F1.08, pdt1

HU width: 4.39
Other Phenotypes: these cells look pretty good- maybe a bit irregular when elongated
Gene function/sequence info: metal transporter for manganese regulation, mutant reported to loose polarity in media lacking manganese.

Exponential

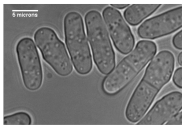

HU

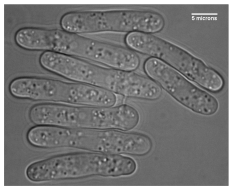

FDK112, x312, SPAC513.06c

HU width: 4.05
Other Phenotypes: cells look pretty good- a bit lumpy
Gene function/sequence info: member of the oxyreductase family?

Exponential

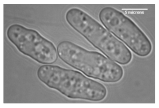

HU

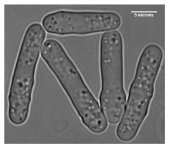

FDK113, w2418, rdi1 SPAC6F12.06

HU width: 4.41
Other Phenotypes: looks lumpy and wide, but varied.
Gene function/sequence info: Rho GDP-dissociation inhibitor activity

Exponential

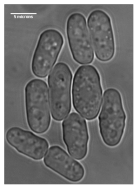

HU

FDK114, x464, wee1

HU width: 4.04
Other Phenotypes:
Gene function/sequence info: advanced progression into mitosis

Exponential

HU

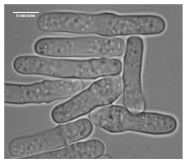

FDK115, x517, SPBC27.02c

HU width: 4.04
Other Phenotypes:
Gene function/sequence info: a member of the DASH complex, localizes to the kinetechore

Exponential

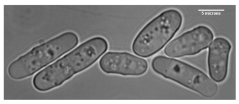

HU

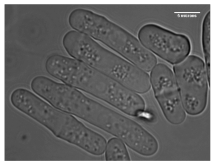

FDK116, x420, SPCC4F11.03c

HU width: 4.18
Other Phenotypes: a bit lumpy?
Gene function/sequence info: no info

Exponential

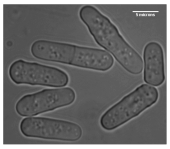

HU

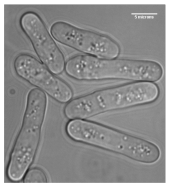

FDK117, w327, SPAC607.04

HU width: 4.30
Other Phenotypes: changes in diameter, swollen middle, etc
Gene function/sequence info: member of the inositol phosphate kinase family, by homology

Exponential

HU

FDK119, w1376, SPAC1006.03c

HU width: 4.36
Other Phenotypes: trifle elongated?
Gene function/sequence info: coiled-coil protein, unknown fxn

Exponential

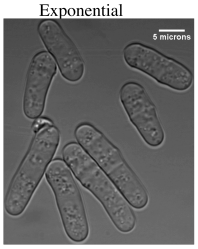

HU

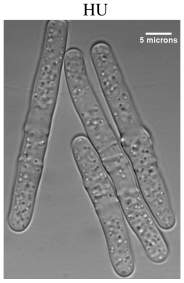

FDK120, s20, alp13

HU width: 4.40
Other Phenotypes: little lumpy
Gene function/sequence info: chromodomain, histone deacetylase

Exponential

HU

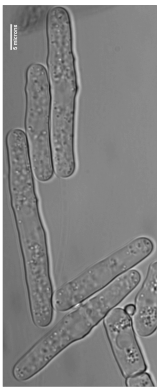

FDK123, SPAC13G6.10c

HU width: 4.65
Other Phenotypes: often swollen at one (non-growing?) end
Gene function/sequence info: unknown fxn

Exponential

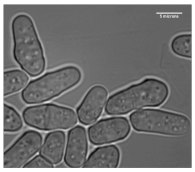

HU

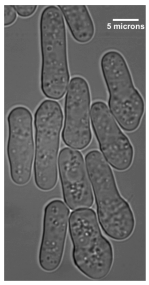

Rgs1

HU width: 4.05
Other phenotypes: bit irregular?
Gene Function: neg. regulates pheremone signaling during mating

exponential

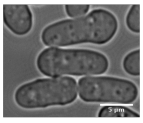

HU

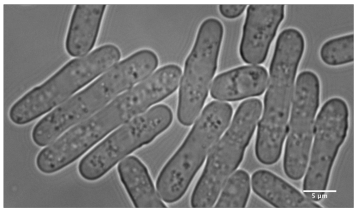

Tea1

HU width: 3.75
Other phenotypes: irregular and bent
Gene Function: marker of cell ends, may regulate MTs

exponential

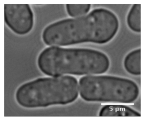

HU

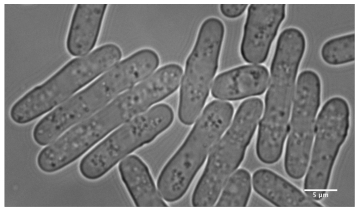

Fdk133, trm112

HU width: 3.73
Other Phenotypes: methyltransferase reg subunit

exponential

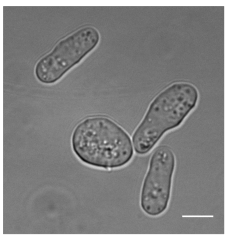

HU

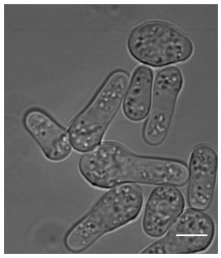

Fdk39, w2982, tea2

HU width: 3.92
Other Phenotypes: polarity protein

exponential

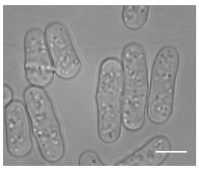

HU

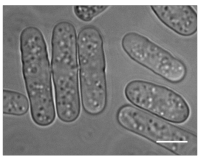

Fdk114, h111, SPCC794.11C

HU width: 4.03
Other Phenotypes: ent3 homolog

exponential

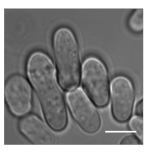

HU

Fdk131, p9, SPAC23H4.17c

HU width: 4.12
Sequence info: srb10
Other Phenotypes: elongated?

exponential

HU

Fdk106, w3874, brl1

HU width: 4.26
Sequence info: ubiquitin protein ligase
Other Phenotypes: elongated

exponential

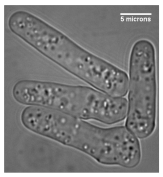

HU

Fdk128, x436, SPCC584.11c

HU width: 4.16
Sequence info: related to svf1
Other Phenotypes: elongated?

exponential

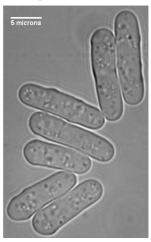

HU

Fdk130, w732, SPAC3H1.11

HU width: 4.34
Sequence info: hsr1, transcription factor
Other Phenotypes:

exponential

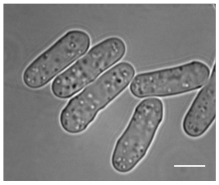

HU

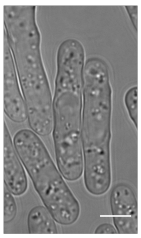

Fdk97, w747, cap1

HU width: 4.21
Sequence info:
Other Phenotypes: rounded, lumpy, irregular

exponential

HU

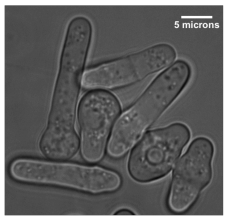

Fdk127, c86, SPAC2G11.07c

HU width: 4.35
Sequence info: ptc3
Other Phenotypes:

exponential

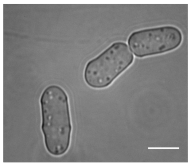

HU

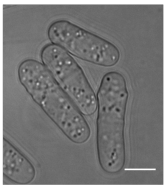

Fdk78, h30, vps1

HU width: 4.25
Sequence info:
Other Phenotypes: bent cells

exponential

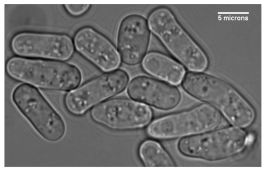

HU

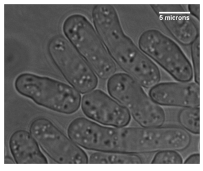

Fdk110, w2982, iws1

HU width: 4.41
Sequence info: transcription elongation factor
Other Phenotypes:

exponential

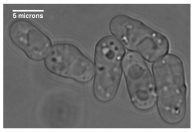

HU

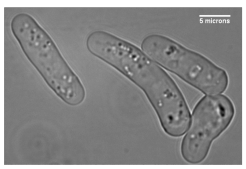

Fdk129, x156, SPCC63.02c

HU width: 4.53
Sequence info: alpha-amalyase homolog
Other Phenotypes: mixed elongated and diploid

exponential HU

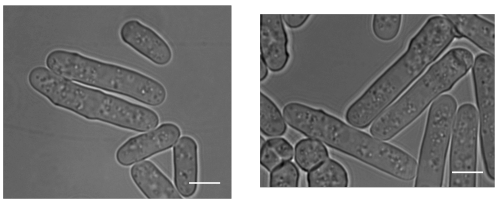

Fdk121, w623, pub1

HU width: 4.55
Sequence info: ubiquitin ligase
Other Phenotypes:

exponential HU

FDK46, PN10092, ogm1

HU width: 4.39
Other Phenotypes:also some cells curved or bent
Gene function/sequence info: uncharacterized mannosyltransferase, O-linkedglycosylation family.

exponential HU

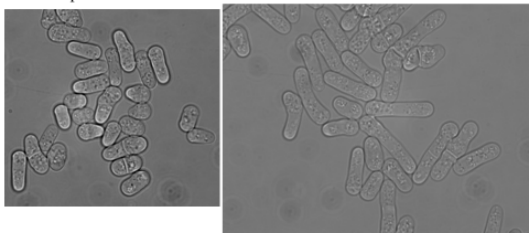

Fdk43, x200, pep3

HU width: 3.99
Other Phenotypes: ubiquitin protein ligase E3

exponential HU

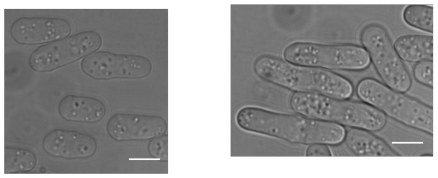

FDK126, SPAP27G11.06c

HU width: 4.57
Other Phenotypes: elongated?
Gene function/sequence info: high homology to clathrin adaptor

HU

Exponential

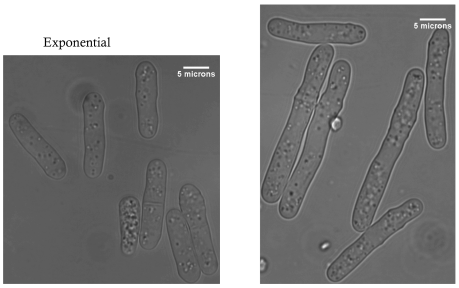

FDK118, s251, SPAC824.02

HU width: 4.78
Other Phenotypes:
Gene function/sequence info: Phosphatidylinositol deacylase activity

HU

Exponential

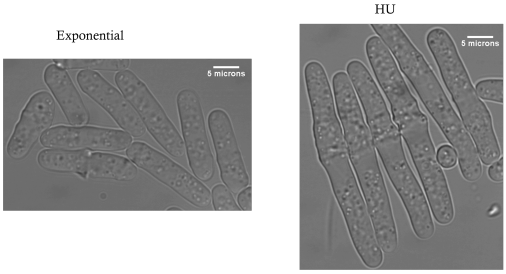

FDK83, y61, pab1

HU width:4.60
Other Phenotypes: some cells seem wide, others not.
Gene function/sequence info: Protein phosphatase type 2A, cell wall biogenesis.

Exponential

HU

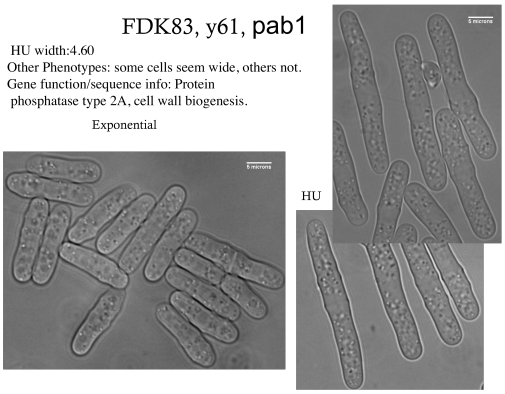

FDK80, PN10086, yak4

HU width: 5.05
Other Phenotypes: kind of wide
Gene function/sequence info: predicted role in transcription regulation. Homolog in Candida also effects morphology.

Exponential HU

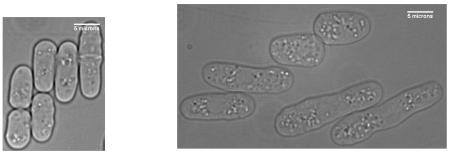

FDK71, PN10242, alm1

HU width: 4.28
Other Phenotypes:
Gene function/sequence info: slightly long. RD has shown involvement in spindle elongation and formation.

Exponential

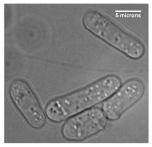

HU

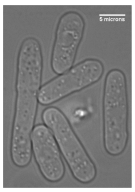

FDK67, PN10245, sec14/spo20

HU width: 4.39
Other Phenotypes: some long cell curve. Cells might stick together a lot?
Gene function/sequence info: phosphatidylinositol/phosphatidylcholine transfer protein, required for normal golgi secretory function, previously reported to be essential.

Exponential

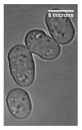

HU

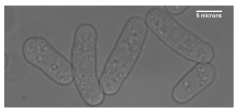

FDK70, PN10001, SPAC227.01c

HU width: 4.29
Other Phenotypes: swollen on one end
Gene function/sequence info: predicted g-protein coupled receptor, induced in late meiosis.

Exponential

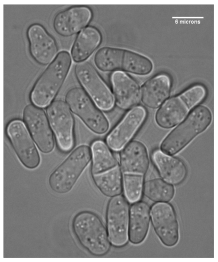

HU

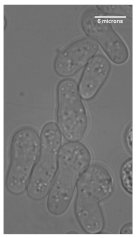

FDK46, PN10092, ogm1

HU width: 4.39
Other Phenotypes:also some cells curved or bent
Gene function/sequence info: uncharacterized mannosyltransferase, O-linkedglycosylation family.

exponential

HU

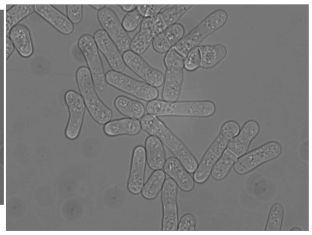

Abramoff, M., P. Magelhaes, and S. Ram. 2004. Image Processing with ImageJ. *Biophotonics International*. 11:36-42.

Adamo, J.E., J.J. Moskow, A.S. Gladfelter, D. Viterbo, D.J. Lew, and P.J. Brennwald. 2001. Yeast Cdc42 functions at a late step in exocytosis, specifically during polarized growth of the emerging bud. *J. Cell Biol.* 155:581-592.

Adams, A.E., and J.R. Pringle. 1984. Relationship of actin and tubulin distribution to bud growth in wild-type and morphogenetic-mutant Saccharomyces cerevisiae. *J Cell Biol*. 98:934-45.

Ahmad, F.J., H.C. Joshi, V.E. Centonze, and P.W. Baas. 1994. Inhibition of microtubule nucleation at the neuronal centrosome compromises axon growth. *Neuron*. 12:271-80.

Akiyoshi, Y., J. Clayton, L. Phan, M. Yamamoto, A.G. Hinnebusch, Y. Watanabe, and K. Asano. 2001. Fission yeast homolog of murine Int-6 protein, encoded by mouse mammary tumor virus integration site, is associated with the conserved core subunits of eukaryotic translation initiation factor 3. *J Biol Chem*. 276:10056-62.

Almonacid, M., J.B. Moseley, J. Janvore, A. Mayeux, V. Fraisier, P. Nurse, and A. Paoletti. 2009. Spatial control of cytokinesis by Cdr2 kinase and Mid1/anillin nuclear export. *Curr Biol*. 19:961-6.

Anderson, D.C., J.S. Gill, R.M. Cinalli, and J. Nance. 2008. Polarization of the C. elegans Embryo by RhoGAP-Mediated Exclusion of PAR-6 from Cell Contacts. *Science*. 320:1771-1774.

Aoyama, K., Y. Mitsubayashi, H. Aiba, and T. Mizuno. 2000. Spy1, a histidine-containing phosphotransfer signaling protein, regulates the fission yeast cell cycle through the Mcs4 response regulator. *J Bacteriol*. 182:4868-74.

Arellano, M., H. Cartagena-Lirola, M.A. Nasser Hajibagheri, A. Duran, and M. Henar Valdivieso. 2000. Proper ascospore maturation requires the chs1+ chitin synthase gene in Schizosaccharomyces pombe. *Mol Microbiol*. 35:79-89.

Arellano, M., A. Duran, and P. Perez. 1996. Rho1 GTPase activates the (1-3)-beta-D-glucan synthase and is involved in *Schizosaccharomyces pombe* morphogenesis. *EMBO*. 15:4584-4591.

Arellano, M., A. Duran, and P. Perez. 1997. Localisation of the Schizosaccharomyces pombe rho1p GTPase and its involvement in the organisation of the actin cytoskeleton. *J Cell Sci*. 110:2547-2555.

Attanapola, S.L., C.J. Alexander, and D.P. Mulvihill. 2009. Ste20-kinase-dependent TEDS-site phosphorylation modulates the dynamic localisation and endocytic function of the fission yeast class I myosin, Myo1. *J Cell Sci*. 122:3856-61.

Ayad-Durieux, Y., P. Knechtle, S. Goff, F. Dietrich, and P. Philippsen. 2000. A PAK-like protein kinase is required for maturation of young hyphae and septation in the filamentous ascomycete Ashbya gossypii. *J Cell Sci*. 113 Pt 24:4563-75.

Bahler, J., and M.S.L. Jian-Qiu Wu, Nirav G. Shah, Amos Mckenzie III, Alexander B. Steever, Achim Wach, Peter Philippsen, John R. Pringle,. 1998. Heterologous modules for efficient and versatile PCR-based gene targeting in *Schizosaccharomyces pombe*. *Yeast*. 14:943-951.

Bahler, J., and J.R. Pringle. 1998. Pom1p, a fission yeast protein kinase that provides positional information for both polarized growth and†cytokinesis. *Genes Dev.* 12:1356-1370.

Ballou, L., and C. Ballou. 1995. Schizosaccharomyces pombe mutants that are defective in glycoprotein galactosylation. *Proc Natl Acad Sci U S A*. 92:2790-4.

Ben-Shem, A., L. Jenner, G. Yusupova, and M. Yusupov. 2010. Crystal structure of the eukaryotic ribosome. *Science*. 330:1203-9.

Bender, A., and J.R. Pringle. 1989. Multicopy suppression of the cdc24 budding defect in yeast by CDC42 and three newly identified genes including the ras-related gene RSR1. *Proc Natl Acad Sci U S A*. 86:9976-80.

Bendezu, F.O., and S.G. Martin. 2011. Actin cables and the exocyst form two independent morphogenesis pathways in the fission yeast. *Mol Biol Cell*. 22:44-53.

Bieling, P., L. Laan, H. Schek, E.L. Munteanu, L. Sandblad, M. Dogterom, D. Brunner, and T. Surrey. 2007. Reconstitution of a microtubule plus-end tracking system in vitro. *Nature*. 450:1100-5.

Botstein, D., R.K. Chan, and C.H. Waddell. 1972. Genetics of bacteriophage P22. II. Gene order and gene function. *Virology*. 49:268-82.

Brauer, M.J., C. Huttenhower, E.M. Airoldi, R. Rosenstein, J.C. Matese, D. Gresham, V.M. Boer, O.G. Troyanskaya, and D. Botstein. 2008. Coordination of growth rate, cell cycle, stress response, and metabolic activity in yeast. *Mol Biol Cell*. 19:352-67.

Browning, H., J. Hayles, J. Mata, L. Aveline, P. Nurse, and J.R. McIntosh. 2000. Tea2p is a kinesin-like protein required to generate polarized growth in fission yeast. *J Cell Biol*. 151:15-28.

Brunner, D., and P. Nurse. 2000. CLIP170-like tip1p Spatially Organizes Microtubular Dynamics in Fission Yeast. *Cell*. 102:695-704.

Busch, K.E., and D. Brunner. 2004. The Microtubule Plus End-Tracking Proteins mal3p and tip1p Cooperate for Cell-End Targeting of Interphase Microtubules. *Curr Biol*. 14:548-559.

Bush, D.A., M. Horisberger, I. Horman, and P. Wursch. 1974. The wall structure of Schizosaccharomyces pombe. *J Gen Microbiol*. 81:199-206.

Butty, A.C., N. Perrinjaquet, A. Petit, M. Jaquenoud, J.E. Segall, K. Hofmann, C. Zwahlen, and M. Peter. 2002. A positive feedback loop stabilizes the guanine-nucleotide exchange factor Cdc24 at sites of polarization. *EMBO J*. 21:1565-76.

Calonge, T.M., M. Arellano, P.M. Coll, and P. Perez. 2003. Rga5p is a specific Rho1p GTPase-activating protein that regulates cell integrity in Schizosaccharomyces pombe. *Molecular MicroBiol*. 47:507-518.

Calonge, T.M., K. Nakano, M. Arellano, R. Arai, S. Katayama, T. Toda, I. Mabuchi, and P. Perez. 2000. Schizosaccharomyces pombe Rho2p GTPase Regulates Cell Wall alpha -Glucan Biosynthesis through the Protein Kinase Pck2p. *Mol. Biol. Cell*. 11:4393-4401.

Carazo-Salas, R.E., and P. Nurse. 2006. Self-organization of interphase microtubule arrays in fission yeast. *Nature Cell Biol*. 8:1102-1107.

Carnero, E., J.C. Ribas, B. Garcia, A. Duran, and Y. Sanchez. 2000. Schizosaccharomyces pombe ehs1p is involved in maintaining cell wall integrity and in calcium uptake. *Mol Gen Genet*. 264:173-83.

Caspar, D.L., and A. Klug. 1962. Physical principles in the construction of regular viruses. *Cold Spring Harb Symp Quant Biol*. 27:1-24.

Castagnetti, S., B. Novak, and P. Nurse. 2007. Microtubules offset growth site from the cell centre in fission yeast. *J Cell Sci*. 120:2205-2213.

Castagnetti, S., S. Oliferenko, and P. Nurse. 2010. Fission yeast cells undergo nuclear division in the absence of spindle microtubules. *PLoS Biol*. 8:e1000512.

Chang, E., G. Bartholomeusz, R. Pimental, J. Chen, H. Lai, L.-h.L. Wang, P. Yang, and S. Marcus. 1999. Direct Binding and In Vivo Regulation of the Fission Yeast p21-

Activated Kinase Shk1 by the SH3 Domain Protein Scd2. *Mol. Cell. Biol.* 19:8066-8074.

Chang, E.C., M. Barr, Y. Wang, V. Jung, H.-P. Xu, and M.H. Wigler. 1994. Cooperative interaction of S. pombe proteins required for mating and morphogenesis. *Cell*. 79:131-141.

Chang, F., and S.G. Martin. 2009. Shaping fission yeast with microtubules. *Cold Spring Harb Perspect Biol*. 1:a001347.

Chant, J., and I. Herskowitz. 1991. Genetic control of bud site selection in yeast by a set of gene products that constitute a morphogenetic pathway. *Cell*. 65:1203-12.

Coll, P.M., Y. Trillo, A. Ametzazurra, and P. Perez. 2003. Gef1p, a New Guanine Nucleotide Exchange Factor for Cdc42p, Regulates Polarity in Schizosaccharomyces pombe. *Mol. Biol. Cell*. 14:313-323.

Cortes, J.C.G., E. Carnero, J. Ishiguro, Y. Sanchez, A. Duran, and J.C. Ribas. 2005. The novel fission yeast (1,3) beta-D-glucan synthase catalytic subunit Bgs4p is essential during both cytokinesis and polarized growth. *J Cell Sci*. 118:157-174.

Crampin, H., K. Finley, M. Gerami-Nejad, H. Court, C. Gale, J. Berman, and P. Sudbery. 2005. Candida albicans hyphae have a Spitzenkorper that is distinct from the polarisome found in yeast and pseudohyphae. *J Cell Sci*. 118:2935-47.

Craven, R.A., D.J. Griffiths, K.S. Sheldrick, R.E. Randall, I.M. Hagan, and A.M. Carr. 1998. Vectors for the expression of tagged proteins in Schizosaccharomyces pombe. *Gene*. 221:59-68.

Cristea, I.M., R. Williams, B.T. Chait, and M.P. Rout. 2005. Fluorescent proteins as proteomic probes. *Mol Cell Proteomics*. 4:1933-41.

Das, M., D.J. Wiley, X. Chen, K. Shah, and F. Verde. 2009. The conserved NDR kinase Orb6 controls polarized cell growth by spatial regulation of the small GTPase Cdc42. *Curr Biol*. 19:1314-9.

Das, M., D.J. Wiley, S. Medina, H.A. Vincent, M. Larrea, A. Oriolo, and F. Verde. 2007. Regulation of Cell Diameter, For3p Localization, and Cell Symmetry by Fission Yeast Rho-GAP Rga4p. *Mol. Biol. Cell*. 18:2091-101.

de Groot, P.W., Q.Y. Yin, M. Weig, G.J. Sosinska, F.M. Klis, and C.G. de Koster. 2007. Mass spectrometric identification of covalently bound cell wall proteins from the fission yeast Schizosaccharomyces pombe. *Yeast*. 24:267-78.

de Medina-Redondo, M., Y. Arnaiz-Pita, C. Clavaud, T. Fontaine, F. del Rey, J.P. Latge, and C.R. Vazquez de Aldana. 2010. beta(1,3)-glucanosyl-transferase activity is essential for cell wall integrity and viability of Schizosaccharomyces pombe. *PLoS One*. 5:e14046.

Derivery, E., and A. Gautreau. 2010. Evolutionary conservation of the WASH complex, an actin polymerization machine involved in endosomal fission. *Commun Integr Biol*. 3:227-30.

Diamond, R.J., and A.H. Rose. 1970. Osmotic properties of spheroplasts from Saccharomyces cerevisiae grown at different temperatures. *J Bacteriol*. 102:311-9.

Dill, K.A., S.B. Ozkan, M.S. Shell, and T.R. Weikl. 2008. The protein folding problem. *Annu Rev Biophys*. 37:289-316.

Ding, R., R.R. West, D.M. Morphew, B.R. Oakley, and J.R. McIntosh. 1997. The spindle pole body of Schizosaccharomyces pombe enters and leaves the nuclear envelope as the cell cycle proceeds. *Mol Biol Cell*. 8:1461-79.

Dutcher, S.K. 2001. The tubulin fraternity: alpha to eta. *Curr Opin Cell Biol*. 13:49-54.

Endo, M., M. Shirouzu, and S. Yokoyama. 2003. The Cdc42 Binding and Scaffolding Activities of the Fission Yeast Adaptor Protein Scd2. *J. Biol. Chem.* 278:843-852.

Engel, B.D., W.B. Ludington, and W.F. Marshall. 2009. Intraflagellar transport particle size scales inversely with flagellar length: revisiting the balance-point length control model. *J Cell Biol*. 187:81-9.

Evangelista, M., D. Pruyne, D.C. Amberg, C. Boone, and A. Bretscher. 2002. Formins direct Arp2/3-independent actin filament assembly to polarize cell growth in yeast. *Nat Cell Biol*. 4:260-9.

Fantes, P. 1979. Epistatic gene interactions in the control of division in fission yeast. *Nature*. 279:428-30.

Feierbach, B., and F. Chang. 2001. Roles of the fission yeast formin for3p in cell polarity, actin cable formation and symmetric cell division. *Curr Biol*. 11:1656-1665.

Feierbach, B., F. Verde, and F. Chang. 2004. Regulation of a formin complex by the microtubule plus end protein tea1p. *J. Cell Biol.* 165:697-707.

Feoktistova, A., D. McCollum, R. Ohi, and K.L. Gould. 1999. Identification and Characterization of Schizosaccharomyces pombe asp1+, a Gene That

Interacts with Mutations in the Arp2/3 Complex and Actin. *Genetics*. 152:895-908.

Foethke, D., T. Makushok, D. Brunner, and F. Nedelec. 2009. Force- and length-dependent catastrophe activities explain interphase microtubule organization in fission yeast. *Mol Syst Biol*. 5:241.

Forsburg, S.L., and N. Rhind. 2006. Basic methods for fission yeast. *Yeast*. 23:173-83.

France, Y.E., C. Boyd, J. Coleman, and P.J. Novick. 2006. The polarity-establishment component Bem1p interacts with the exocyst complex through the Sec15p subunit. *J Cell Sci*. 119:876-888.

Frank, V. 1991. The use of some fluorescent stains for studying morphogenesis of micromycetes. *Folia Microbiol (Praha)*. 36:92-6.

Fukui, Y., S. Miyake, M. Satoh, and M. Yamamoto. 1989. Characterization of the *Schizosaccharomyces pombe* ral2 Gene Implicated in Activation of the ras1 gene product. *Molecular and Cellular Biol*. 9:5617-5622.

Fukui, Y., and M. Yamamoto. 1988. Isolation and characterization of Schizosaccharomyces pombe mutants phenotypically similar to ras1. *Mol Gen Genet*. 215:26-31.

Fuller, M.T., and J. King. 1982. Assembly in vitro of bacteriophage P22 procapsids from purified coat and scaffolding subunits. *J Mol Biol*. 156:633-65.

Gachet, Y., and J.S. Hyams. 2005. Endocytosis in fission yeast is spatially associated with the actin cytoskeleton during polarised cell growth and cytokinesis. *J Cell Sci*. 118:4231-4242.

Galkin, V.E., A. Orlova, G.F. Schroder, and E.H. Egelman. 2010. Structural polymorphism in F-actin. *Nat Struct Mol Biol*. 17:1318-23.

Galkin, V.E., M.S. VanLoock, A. Orlova, and E.H. Egelman. 2002. A new internal mode in F-actin helps explain the remarkable evolutionary conservation of actin's sequence and structure. *Curr Biol*. 12:570-5.

Galletta, B.J., and J.A. Cooper. 2009. Actin and endocytosis: mechanisms and phylogeny. *Curr Opin Cell Biol*. 21:20-7.

Garcia, P., I. Garcia, F. Marcos, G.R. de Garibay, and Y. Sanchez. 2009. Fission yeast rgf2p is a rho1p guanine nucleotide exchange factor required for spore wall maturation and for the maintenance of cell integrity in the absence of rgf1p. *Genetics*. 181:1321-34.

Garcia, P., V. Tajadura, I. Garcia, and Y. Sanchez. 2006. Rgf1p is a specific Rho1-GEF that coordinates cell polarization with cell wall biogenesis in fission yeast. *Mol Biol Cell*. 17:1620-31.

Ge, W., T.G. Chew, V. Wachtler, S.N. Naqvi, and M.K. Balasubramanian. 2005. The Novel Fission Yeast Protein Pal1p Interacts with Hip1-related Sla2p/End4p and Is Involved in Cellular Morphogenesis. *Mol. Biol. Cell*. 16:4124-4138.

Gierz, G., and S. Bartnicki-Garcia. 2001. A three-dimensional model of fungal morphogenesis based on the vesicle supply center concept. *J Theor Biol*. 208:151-64.

Glynn, J.M., R.J. Lustig, A. Berlin, and F. Chang. 2001. Role of bud6p and tea1p in the interaction between actin and microtubules for the establishment of cell polarity in fission yeast. *Curr Biol*. 11:836-845.

Gomis-Ruth, S., C.J. Wierenga, and F. Bradke. 2008. Plasticity of polarization: changing dendrites into axons in neurons integrated in neuronal circuits. *Curr Biol*. 18:992-1000.

Gotta, M., M.C. Abraham, and J. Ahringer. 2001. CDC-42 controls early cell polarity and spindle orientation in C. elegans. *Curr Biol*. 11:482-8.

Grote, E., C.M. Carr, and P.J. Novick. 2000. Ordering the final events in yeast exocytosis. *J Cell Biol*. 151:439-52.

Harmouch, N., A. Pichova, J. Coulon, E. Streiblova, and R. Bonaly. 1995. Changes in cell wall composition of deformed ras1- cells of Schizosaccharomyces pombe. *Folia Microbiol (Praha)*. 40:519-27.

Harold, F.M. 1990. To shape a cell: an inquiry into the causes of morphogenesis of microorganisms. *MicroBiol Review*. 54:381-431.

Harold, F.M. 2002. Force and compliance: rethinking morphogenesis in walled cells. *Fungal Genet Biol*. 37:271-82.

Hayles, J., and P. Nurse. 2001. A Journey Into Space. *Nature Cell Biol*. 2:647-656.

Hirata, D., K. Nakano, M. Fukui, H. Takenaka, T. Miyakawa, and I. Mabuchi. 1998. Genes that cause aberrant cell morphology by overexpression in fission yeast: a role of a small GTP-binding protein Rho2 in cell morphogenesis. *J Cell Sci*. 111 (Pt 2):149-59.

Hird, S.N., and J.G. White. 1993. Cortical and cytoplasmic flow polarity in early embryonic cells of Caenorhabditis elegans. *J Cell Biol*. 121:1343-55.

Hirota, K., K. Tanaka, K. Ohta, and M. Yamamoto. 2003. Gef1p and Scd1p, the Two GDP-GTP Exchange Factors for Cdc42p, Form a Ring Structure that Shrinks during Cytokinesis in Schizosaccharomyces pombe. *Mol. Biol. Cell*. 14:3617-3627.

Hochstenbach, F., F.M. Klis, H. van den Ende, E. van Donselaar, P.J. Peters, and R.D. Klausner. 1998. Identification of a putative alpha-glucan synthase essential for cell wall construction and morphogenesis in fission yeast. *Proc Natl Acad Sci U S A*. 95:9161-6.

Hsu, S.C., A.E. Ting, C.D. Hazuka, S. Davanger, J.W. Kenny, Y. Kee, and R.H. Scheller. 1996. The mammalian brain rsec6/8 complex. *Neuron*. 17:1209-19.

Huckaba, T.M., A.C. Gay, L.F. Pantalena, H.-C. Yang, and L.A. Pon. 2004. Live cell imaging of the assembly, disassembly, and actin cable-dependent movement of endosomes and actin patches in the budding yeast, Saccharomyces cerevisiae. *J. Cell Biol.* 167:519-530.

Iden, S., and J.G. Collard. 2008. Crosstalk between small GTPases and polarity proteins in cell polarization. *Nat Rev Mol Cell Biol*. 9:846-59.

Irazoqui, J.E., A.S. Gladfelter, and D.J. Lew. 2003. Scaffold-mediated symmetry breaking by Cdc42p. *Nature Cell Biol*. 5:1062-1070.

Ishiguro, J., A. Saitou, A. Duran, and J.C. Ribas. 1997. cps1+, a Schizosaccharomyces pombe gene homolog of Saccharomyces cerevisiae FKS genes whose mutation confers hypersensitivity to cyclosporin A and papulacandin B. *J Bacteriol*. 179:7653-62.

Ishijima, S.A., M. Konomi, T. Takagi, M. Sato, J. Ishiguro, and M. Osumi. 1999. Ultrastructure of cell wall of the cps8 actin mutant cell in Schizosaccharomyces pombe. *FEMS Microbiol Lett*. 180:31-7.

Jenkins, N., J.R. Saam, and S.E. Mango. 2006. CYK-4/GAP provides a localized cue to initiate anteroposterior polarity upon fertilization. *Science*. 313:1298-301.

Jorgensen, P., N.P. Edgington, B.L. Schneider, I. Rupes, M. Tyers, and B. Futcher. 2007. The size of the nucleus increases as yeast cells grow. *Mol Biol Cell*. 18:3523-32.

Kaksonen, M., Y. Sun, and D.G. Drubin. 2003. A Pathway for Association of Receptors, Adaptors, and Actin during Endocytic Internalization. *Cell*. 115:475-487.

Kaksonen, M., C.P. Toret, and D.G. Drubin. 2005. A Modular Design for the Clathrin- and Actin-Mediated Endocytosis Machinery. *Cell*. 123:305-320.

Kamasaki, T., R. Arai, M. Osumi, and I. Mabuchi. 2005. Directionality of F-actin cables changes during the fission yeast cell cycle. *Nature Cell Biol*. 7:916-917.

Kanai, M., K. Kume, K. Sakai, K. Nakamura, K. Leonhard, D.J. Wiley, F. Verde, T. Toda, and D. Hirata. 2005. Fission yeast MO25 protein is localized at SPB and septum and is essential for cell morphogenesis. *EMBO J*. 24:3012-3025.

Katsura, I. 1987. Determination of bacteriophage lambda tail length by a protein ruler. *Nature*. 327:73-5.

Katsura, I. 1990. Mechanism of length determination in bacteriophage lambda tails. *Adv Biophys*. 26:1-18.

Keeney, J.B., and J.D. Boeke. 1994. Efficient targeted integration at leu1-32 and ura4-294 in Schizosaccharomyces pombe. *Genetics*. 136:849-56.

Kim, D.U., J. Hayles, D. Kim, V. Wood, H.O. Park, M. Won, H.S. Yoo, T. Duhig, M. Nam, G. Palmer, S. Han, L. Jeffery, S.T. Baek, H. Lee, Y.S. Shim, M. Lee, L. Kim, K.S. Heo, E.J. Noh, A.R. Lee, Y.J. Jang, K.S. Chung, S.J. Choi, J.Y. Park, Y. Park, H.M. Kim, S.K. Park, H.J. Park, E.J. Kang, H.B. Kim, H.S. Kang, H.M. Park, K. Kim, K. Song, K.B. Song, P. Nurse, and K.L. Hoe. 2010. Analysis of a genome-wide set of gene deletions in the fission yeast Schizosaccharomyces pombe. *Nat Biotechnol*.

Kim, H., P. Yang, P. Catanuto, F. Verde, H. Lai, H. Du, F. Chang, and S. Marcus. 2003. The kelch repeat protein, Tea1, is a potential substrate target of the p21-activated kinase, Shk1, in the fission yeast, Schizosaccharomyces pombe. *J Biol Chem*. 278:30074-82.

Kim, H., P. Yang, Y. Qyang, H. Lai, H. Du, J.S. Henkel, K. Kumar, S. Bao, M. Liu, and S. Marcus. 2001. Genetic and Molecular Characterization of Skb15, a Highly Conserved Inhibitor of the Fission Yeast PAK, Shk1. *Molecular Cell*. 7:1095-1101.

Kobori, H., N. Yamada, A. Taki, and M. Osumi. 1989. Actin is associated with the formation of the cell wall in reverting protoplasts of the fission yeast Schizosaccharomyces pombe. *J Cell Sci*. 94:635-646.

Kohli, M., V. Galati, K. Boudier, R.W. Roberson, and P. Philippsen. 2008. Growth-speed-correlated localization of exocyst and polarisome components in growth zones of Ashbya gossypii hyphal tips. *J Cell Sci*. 121:3878-3889.

Kozma, R., S. Sarner, S. Ahmed, and L. Lim. 1997. Rho family GTPases and neuronal growth cone remodelling: relationship between increased complexity induced by Cdc42Hs, Rac1, and acetylcholine and collapse induced by RhoA and lysophosphatidic acid. *Mol Cell Biol*. 17:1201-11.

Kozubowski, L., K. Saito, J.M. Johnson, A.S. Howell, T.R. Zyla, and D.J. Lew. 2008. Symmetry-Breaking Polarization Driven by a Cdc42p GEF-PAK Complex. *Curr Biol*. 18:1719-1726.

Kressler, D., E. Hurt, and J. Bassler. 2010. Driving ribosome assembly. *Biochim Biophys Acta*. 1803:673-83.

Kumfer, K.T., S.J. Cook, J.M. Squirrell, K.W. Eliceiri, N. Peel, K.F. O'Connell, and J.G. White. 2010. CGEF-1 and CHIN-1 regulate CDC-42 activity during asymmetric division in the Caenorhabditis elegans embryo. *Mol Biol Cell*. 21:266-77.

Kuramoto, K., M. Negishi, and H. Katoh. 2009. Regulation of dendrite growth by the Cdc42 activator Zizimin1/Dock9 in hippocampal neurons. *J Neurosci Res*. 87:1794-805.

Levy, D.L., and R. Heald. 2010. Nuclear size is regulated by importin alpha and Ntf2 in Xenopus. *Cell*. 143:288-98.

Loo, T.-H., and M. Balasubramanian. 2008. Schizosaccharomyces pombe Pak-related protein, Pak1p/Orb2p, phosphorylates myosin regulatory light chain to inhibit cytokinesis. *J. Cell Biol.* 183:785-793.

Luo, L., Y.J. Liao, L.Y. Jan, and Y.N. Jan. 1994. Distinct morphogenetic functions of similar small GTPases: Drosophila Drac1 is involved in axonal outgrowth and myoblast fusion. *Genes Dev*. 8:1787-802.

Malho, R., N.D. Read, A.J. Trewavas, and M.S. Pais. 1995. Calcium Channel Activity during Pollen Tube Growth and Reorientation. *Plant Cell*. 7:1173-1184.

Marcus, S., A. Polverino, E. Chang, D. Robbins, M. Cobb, and M. Wigler. 1995. Shk1, a Homolog of the Saccharomyces cerevisiae Ste20 and Mammalian p65PAK Protein Kinases, is a Component of a Ras/Cdc42 Signaling Module in the Fission Yeast Schizosaccharomyces pombe. *Proc Natl Acad Sci U S A*. 92:6180-6184.

Marks, J., I.M. Hagan, and J.S. Hyams. 1986. Growth polarity and cytokinesis in fission yeast: the role of the cytoskeleton. *J Cell Sci*. 5:229-41.

Marshall, W.F., H. Qin, M. Rodrigo Brenni, and J.L. Rosenbaum. 2005. Flagellar length control system: testing a simple model based on intraflagellar transport and turnover. *Mol Biol Cell*. 16:270-8.

Marshall, W.F., and J.L. Rosenbaum. 2001. Intraflagellar transport balances continuous turnover of outer doublet microtubules: implications for flagellar length control. *J Cell Biol*. 155:405-14.

Martin, S.G., and M. Berthelot-Grosjean. 2009. Polar gradients of the DYRK-family kinase Pom1 couple cell length with the cell cycle. *Nature*. 459:852-6.

Martin, S.G., and F. Chang. 2006. Dynamics of the Formin For3p in Actin Cable Assembly. *Curr Biol*. 16:1161-1170.

Martin, S.G., W.H. McDonald, J.R. Yates III, and F. Chang. 2005. Tea4p Links Microtubule Plus Ends with the Formin For3p in the Establishment of Cell Polarity. *Developmental Cell*. 8:479-491.

Martin, S.G., S.A. Rincon, R. Basu, P. Perez, and F. Chang. 2007. Regulation of the Formin for3p by cdc42p and bud6p. *Mol. Biol. Cell*. 18:4155-4167.

Martin, V., B. Garcia, E. Carnero, A. Duran, and Y. Sanchez. 2003. Bgs3p, a putative 1,3-beta-glucan synthase subunit, is required for cell wall assembly in Schizosaccharomyces pombe. *Eukaryot Cell*. 2:159-69.

Mata, J., and P. Nurse. 1997. tea1 and the Microtubular Cytoskeleton Are Important for Generating Global Spatial Order within the Fission Yeast Cell. *Cell*. 89:939-949.

Mendoza, M., S. Redemann, and D. Brunner. 2005. The fission yeast MO25 protein functions in polar growth and cell separation. *European Journal of Cell Biol*. 84:915-926.

Merla, A., and D.I. Johnson. 2000. The Cdc42p GTPase is targeted to the site of cell division in the fission yeast Schizosaccharomyces pombe. *Eur J Cell Biol*. 79:469-77.

Miller, P.J., and D.I. Johnson. 1994. Cdc42 GTPase is involved in controlling polarized cell growth in *Schizosaccharomyces pombe*. *Molecular and Cellular Biol*. 14:1075-1083.

Minc, N., A. Boudaoud, and F. Chang. 2009a. Mechanical Forces of Fission Yeast Growth. *Curr Biol*. 19:1096-101.

Minc, N., S.V. Bratman, R. Basu, and F. Chang. 2009b. Establishing new sites of polarization by microtubules. *Curr Biol*. 19:83-94.

Minc, N., and F. Chang. 2010. Electrical Control of Cell Polarization in the Fission Yeast Schizosaccharomyces pombe. *Curr Biol*. 20:710-6.

Moody, M.F. 1999. Geometry of phage head construction. *J Mol Biol*. 293:401-33.

Moreno, S., A. Klar, and P. Nurse. 1991. Molecular genetic analysis of fission yeast Schizosaccharomyces pombe. *Methods Enzymol*. 194:795-823.

Moseley, J.B., and B.L. Goode. 2006. The Yeast Actin Cytoskeleton: from Cellular Function to Biochemical Mechanism. *Microbiol. Mol. Biol. Rev.* 70:605-645.

Moseley, J.B., A. Mayeux, A. Paoletti, and P. Nurse. 2009. A spatial gradient coordinates cell size and mitotic entry in fission yeast. *Nature*. 459:857-60.

Motegi, F., R. Arai, and I. Mabuchi. 2001. Identification of Two Type V Myosins in Fission Yeast, One of Which Functions in Polarized Cell Growth and Moves Rapidly in the Cell. *Mol. Biol. Cell*. 12:1367-1380.

Motegi, F., and A. Sugimoto. 2006. Sequential functioning of the ECT-2 RhoGEF, RHO-1 and CDC-42 establishes cell polarity in Caenorhabditis elegans embryos. *Nat Cell Biol*. 8:978-85.

Mulugu, S., W. Bai, P.C. Fridy, R.J. Bastidas, J.C. Otto, D.E. Dollins, T.A. Haystead, A.A. Ribeiro, and J.D. York. 2007. A Conserved Family of Enzymes That Phosphorylate Inositol Hexakisphosphate. *Science*. 316:106-109.

Munro, E., J. Nance, and J.R. Priess. 2004. Cortical flows powered by asymmetrical contraction transport PAR proteins to establish and maintain anterior-posterior polarity in the early C. elegans embryo. *Dev Cell*. 7:413-24.

Murakoshi, H., H. Wang, and R. Yasuda. 2011. Local, persistent activation of Rho GTPases during plasticity of single dendritic spines. *Nature*. 472:100-4.

Nakamura, T., H. Asakawa, Y. Nakase, J. Kashiwazaki, Y. Hiraoka, and C. Shimoda. 2008. Live observation of forespore membrane formation in fission yeast. *Mol Biol Cell*. 19:3544-53.

Nakano, K., J. Imai, R. Arai, A. Toh-e, Y. Matsui, and I. Mabuchi. 2002. The small GTPase Rho3 and the diaphanous/formin For3 function in polarized cell growth in fission yeast. *J Cell Sci*. 115:4629-4639.

Nakano, K., T. Mutoh, and I. Mabuchi. 2001. Characterization of GTPase-activating proteins for the function of the Rho-family small GTPases in the fission yeast Schizosaccharomyces pombe. *Genes to Cells*. 6:1031-1042.

Nakano, K., M. Toya, A. Yoneda, Y. Asami, A. Yamashita, N. Kamasawa, M. Osumi, and M. Yamamoto. 2011. Pob1 Ensures Cylindrical Cell Shape by Coupling Two Distinct Rho Signaling Events during Secretory Vesicle Targeting. *Traffic*. 12:726-39.

Nance, J., and J.A. Zallen. 2011. Elaborating polarity: PAR proteins and the cytoskeleton. *Development*. 138:799-809.

Necas, O. 1971. Cell wall synthesis in yeast protoplasts. *Bacteriol Rev*. 35:149-70.

Neumann, F.R., and P. Nurse. 2007. Nuclear size control in fission yeast. *J Cell Biol*. 179:593-600.

Niccoli, T., and P. Nurse. 2002. Different mechanisms of cell polarisation in vegetative and shmooing growth in fission yeast. *J Cell Sci*. 115:1651-62.

NIH. 2010. http://imagejdocu.tudor.lu/doku.php?id=gui:image:lookup_tables. Vol. 2011. NIH ImageJ Documentation Wiki.

Nobes, C.D., and A. Hall. 1995. Rho, rac, and cdc42 GTPases regulate the assembly of multimolecular focal complexes associated with actin stress fibers, lamellipodia, and filopodia. *Cell*. 81:53-62.

Nomura, M. 1999. Regulation of ribosome biosynthesis in Escherichia coli and Saccharomyces cerevisiae: diversity and common principles. *J Bacteriol*. 181:6857-64.

Onken, B., H. Wiener, M.R. Philips, and E.C. Chang. 2006. Compartmentalized signaling of Ras in fission yeast. *Proc Natl Acad Sci U S A*. 103:9045-9050.

Osmani, N., N. Vitale, J.P. Borg, and S. Etienne-Manneville. 2006. Scrib controls Cdc42 localization and activity to promote cell polarization during astrocyte migration. *Curr Biol*. 16:2395-405.

Osumi, M. 1998. The Ultrastructure of Yeast: Cell Wall Structure and Formation. *Micon*. 29:207-233.

Osumi, M., N. Yamada, H. Kobori, A. Taki, N. Naito, M. Baba, and T. Nagatani. 1989. Cell wall formation in regenerating protoplasts of Schizosaccharomyces pombe: study by high resolution, low voltage scanning electron microscopy. *J Electron Microsc (Tokyo)*. 38:457-68.

Osumi, M., N. Yamada, H. Kobori, and H. Yaguchi. 1992. Observations of Colloidal Gold Particles on the surface of yeast protoplasts with UHR-LVSEM. *Journal of Electron Microsc.* 41:392-396.

Ottilie, S., P.J. Miller, D.I. Johnson, C.L. Creasy, M.A. Sells, S. Bagrodia, S.L. Forsburg, and J. Chernoff. 1995. Fission yeast pak1+ encodes a protein kinase that interacts with Cdc42p and is involved in the control of cell polarity and mating. *EMBO J*. 14:5908-19.

Paavilainen, V.O., E. Bertling, S. Falck, and P. Lappalainen. 2004. Regulation of cytoskeletal dynamics by actin-monomer-binding proteins. *Trends Cell Biol*. 14:386-94.

Papadaki, P., V. Pizon, B. Onken, and E.C. Chang. 2002. Two Ras Pathways in Fission Yeast Are Differentially Regulated by Two Ras Guanine Nucleotide Exchange Factors. *Mol. Cell. Biol.* 22:4598-4606.

Pelham, R.J., and F. Chang. 2001. Role of actin polymerization and actin cables in actin-patch movement in Schizosaccharomyces pombe. *Nature Cell Biol*. 3:235-244.

Penkett, C.J., J.A. Morris, V. Wood, and J. Bahler. 2006. YOGY: a web-based, integrated database to retrieve protein orthologs and associated Gene Ontology terms. *Nucleic Acids Res*. 34:W330-4.

Perez, P., and S.A. Rincon. 2010. Rho GTPases: regulation of cell polarity and growth in yeasts. *Biochem J*. 426:243-53.

Piel, M., and P.T. Tran. 2009. Cell shape and cell division in fission yeast. *Curr Biol*. 19:R823-7.

Pierson, E.S., D.D. Miller, D.A. Callaham, A.M. Shipley, B.A. Rivers, M. Cresti, and P.K. Hepler. 1994. Pollen tube growth is coupled to the extracellular calcium ion flux and the intracellular calcium gradient: effect of BAPTA-type buffers and hypertonic media. *Plant Cell*. 6:1815-28.

Pohlmann, J., and U. Fleig. 2010. Asp1, a conserved 1/3 inositol polyphosphate kinase, regulates the dimorphic switch in S. pombe. *Mol Cell Biol*. 30:4535-47.

Ponting, C.P. 1996. Novel domains in NADPH oxidase subunits, sorting nexins, and PtdIns 3-kinases: binding partners of SH3 domains? *Protein Sci*. 5:2353-7.

Pruyne, D., and A. Bretscher. 2000. Polarization of cell growth in yeast. I. Establishment and maintenance of polarity states. *J Cell Sci*. 113:365-375.

Qyang, Y., P. Yang, H. Du, H. Lai, H. Kim, and S. Marcus. 2002. The p21-activated kinase, Shk1, is required for proper regulation of microtubule dynamics in the fission yeast, Schizosaccharomyces pombe. *Molecular MicroBiol*. 44:325-334.

Rafelski, S.M., and W.F. Marshall. 2008. Building the cell: design principles of cellular architecture. *Nat Rev Mol Cell Biol*. 9:593-602.

Reynaga-Pena, C.G., G. Gierz, and S. Bartnicki-Garcia. 1997. Analysis of the role of the Spitzenkorper in fungal morphogenesis by computer simulation of apical branching in Aspergillus niger. *Proc Natl Acad Sci U S A*. 94:9096-101.

Ribas, J.C., M. Diaz, A. Duran, and P. Perez. 1991. Isolation and characterization of Schizosaccharomyces pombe mutants defective in cell wall (1-3)beta-D-glucan. *J Bacteriol*. 173:3456-62.

Ridley, A.J., and A. Hall. 1992. The small GTP-binding protein rho regulates the assembly of focal adhesions and actin stress fibers in response to growth factors. *Cell*. 70:389-99.

Ridley, A.J., H.F. Paterson, C.L. Johnston, D. Diekmann, and A. Hall. 1992. The small GTP-binding protein rac regulates growth factor-induced membrane ruffling. *Cell*. 70:401-10.

Rincon, S., P.M. Coll, and P. Perez. 2007. Spatial regulation of Cdc42 during cytokinesis. *Cell Cycle*. 6:1687-91.

Rincon, S.A., Y. Ye, M.A. Villar-Tajadura, B. Santos, S.G. Martin, and P. Perez. 2009. Pob1 participates in the Cdc42 regulation of fission yeast actin cytoskeleton. *Mol Biol Cell*. 20:4390-9.

Roberts, P.J., N. Mitin, P.J. Keller, E.J. Chenette, J.P. Madigan, R.O. Currin, A.D. Cox, O. Wilson, P. Kirschmeier, and C.J. Der. 2008. Rho Family GTPase modification and dependence on CAAX motif-signaled posttranslational modification. *J Biol Chem*. 283:25150-63.

Santos, B., J. Gutierrez, T.M. Calonge, and P. Perez. 2003. Novel Rho GTPase Involved in Cytokinesis and Cell Wall Integrity in the Fission Yeast Schizosaccharomyces pombe. *Eukaryotic Cell*. 2:521-533.

Santos, B., A.B. Martin-Cuadrado, C.R. Vazquez de Aldana, F. del Rey, and P. Perez. 2005. Rho4 GTPase Is Involved in Secretion of Glucanases during Fission Yeast Cytokinesis. *Eukaryotic Cell*. 4:1639-1645.

Sawin, K.E., M.A. Nasser Hajibagheri, and P. Nurse. 1999. Mis-specification of cortical identity in a fission yeast PAK mutant. *Curr Biol.* 9:1335-1338.

Sawin, K.E., and H.A. Snaith. 2004. Role of microtubules and tea1p in establishment and maintenance of fission yeast cell polarity. *J Cell Sci*. 117:689-700.

Schmitz, H.P., A. Kaufmann, M. Kohli, P.P. Laissue, and P. Philippsen. 2006. From function to shape: a novel role of a formin in morphogenesis of the fungus Ashbya gossypii. *Mol Biol Cell*. 17:130-45.

Schott, D.H., R.N. Collins, and A. Bretscher. 2002. Secretory vesicle transport velocity in living cells depends on the myosin-V lever arm length. *J Cell Biol*. 156:35-9.

Shimada, Y., M.P. Gulli, and M. Peter. 2000. Nuclear sequestration of the exchange factor Cdc24 by Far1 regulates cell polarity during yeast mating. *Nat Cell Biol*. 2:117-24.

Sick, S., S. Reinker, J. Timmer, and T. Schlake. 2006. WNT and DKK determine hair follicle spacing through a reaction-diffusion mechanism. *Science*. 314:1447-50.

Sirotkin, V., C.C. Beltzner, J.-B. Marchand, and T.D. Pollard. 2005. Interactions of WASp, myosin-I, and verprolin with Arp2/3 complex during actin patch assembly in fission yeast. *J. Cell Biol.* 170:637-648.

Sirotkin, V., J. Berro, K. Macmillan, L. Zhao, and T.D. Pollard. 2010. Quantitative analysis of the mechanism of endocytic actin patch assembly and disassembly in fission yeast. *Mol Biol Cell*. 21:2894-904.

Slaughter, B.D., A. Das, J.W. Schwartz, B. Rubinstein, and R. Li. 2009a. Dual modes of cdc42 recycling fine-tune polarized morphogenesis. *Dev Cell*. 17:823-35.

Slaughter, B.D., S.E. Smith, and R. Li. 2009b. Symmetry breaking in the life cycle of the budding yeast. *Cold Spring Harb Perspect Biol*. 1:a003384.

Snaith, H.A., I. Samejima, and K.E. Sawin. 2005. Multistep and multimode cortical anchoring of tea1p at cell tips in fission yeast. *EMBO*. 24:3690-3699.

Snaith, H.A., and K.E. Sawin. 2003. Fission yeast mod5p regulates polarized growth through anchoring of tea1p at cell tips. *Nature.* 423:647-651.

Snyder, M., S. Gehrung, and B.D. Page. 1991. Studies concerning the temporal and genetic control of cell polarity in Saccharomyces cerevisiae. *J Cell Biol*. 114:515-32.

Styrkarsdottir, U., R. Egel, and O. Nielsen. 1993. The smt-0 mutation which abolishes mating-type switching in fission yeast is a deletion. *Curr Genet*. 23:184-6.

Sudbery, P., N. Gow, and J. Berman. 2004. The distinct morphogenic states of Candida albicans. *Trends Microbiol*. 12:317-24.

Synergy, S. 2004. KaleidaGraph Graphing and Data Analysis Software Manual. Synergy Software, Reading, PA.

Tajadura, V., B. Garcia, I. Garcia, P. Garcia, and Y. Sanchez. 2004. Schizosaccharomyces pombe Rgf3p is a specific Rho1 GEF that regulates cell wall beta-glucan biosynthesis through the GTPase Rho1p. *J Cell Sci*. 117:6163-74.

Takagi, T., S.A. Ishijima, H. Ochi, and M. Osumi. 2003. Ultrastructure and behavior of actin cytoskeleton during cell wall formation in the fission yeast Schizosaccharomyces pombe. *J Electron Microsc (Tokyo)*. 52:161-174.

Tatebe, H., G. Goshima, K. Takeda, T. Nakagawa, K. Kinoshita, and M. Yanagida. 2001. Fission yeast living mitosis visualized by GFP-tagged gene products. *Micron*. 32:67-74.

Tatebe, H., K. Nakano, R. Maximo, and K. Shiozaki. 2008. Pom1 DYRK Regulates Localization of the Rga4 GAP to Ensure Bipolar Activation of Cdc42 in Fission Yeast. *Curr Biol*. 18:322-330.

TerBush, D.R., and P. Novick. 1995. Sec6, Sec8, and Sec15 are components of a multisubunit complex which localizes to small bud tips in Saccharomyces cerevisiae. *J Cell Biol*. 130:299-312.

Terenna, C.R., T. Makushok, G. Velve-Casquillas, D. Baigl, Y. Chen, M. Bornens, A. Paoletti, M. Piel, and P.T. Tran. 2008. Physical Mechanisms Redirecting Cell Polarity and Cell Shape in Fission Yeast. *Curr Biol*. 18:1748-1753.

Ti, S.C., and T.D. Pollard. 2011. Purification of actin from fission yeast Schizosaccharomyces pombe and characterization of functional differences from muscle actin. *J Biol Chem*. 286:5784-92.

Ting, A.E., C.D. Hazuka, S.C. Hsu, M.D. Kirk, A.J. Bean, and R.H. Scheller. 1995. rSec6 and rSec8, mammalian homologs of yeast proteins essential for secretion. *Proc Natl Acad Sci U S A*. 92:9613-7.

Titus, M.A. 1997. Motor proteins: myosin V--the multi-purpose transport motor. *Curr Biol*. 7:R301-4.

Tong, Z., X.-D. Gao, A.S. Howell, I. Bose, D.J. Lew, and E. Bi. 2007. Adjacent positioning of cellular structures enabled by a Cdc42 GTPase-activating protein mediated zone of inhibition. *J. Cell Biol.* 179:1375-1384.

Tran, P.T., L. Marsh, V. Doye, S. Inoue, and F. Chang. 2001. A mechanism for nuclear positioning in fission yeast based on microtubule pushing. *J Cell Biol*. 153:397-411.

Tratner, I., A. Fourticq-Esqueoute, J. Tillit, and G. Baldacci. 1997. Cloning and characterization of the S. pombe gene efc25+, a new putative guanine nucleotide exchange factor. *Gene*. 193:203-10.

Tu, H., and M. Wigler. 1999. Genetic evidence for Pak1 autoinhibition and its release by Cdc42. *Mol Cell Biol*. 19:602-11.

Utsugi, T., M. Minemura, A. Hirata, M. Abe, D. Watanabe, and Y. Ohya. 2002. Movement of yeast 1,3-beta-glucan synthase is essential for uniform cell wall synthesis. *Genes Cells*. 7:1-9.

Verde, F., J. Mata, and P. Nurse. 1995. Fission yeast cell morphogenesis: identification of new genes and analysis of their role during the cell cycle. *J. Cell Biol.* 131:1529-1538.

Verde, F., D.J. Wiley, and P. Nurse. 1998. Fission yeast orb6, a ser/thr protein kinase related to mammalian rho kinase and myotonic dystrophy kinase, is required for maintenance of cell polarity and coordinates cell morphogenesis with the cell cycle. *Proc Natl Acad Sci U S A*. 95:7526-7531.

Vidali, L., S.T. McKenna, and P.K. Hepler. 2001. Actin polymerization is essential for pollen tube growth. *Mol Biol Cell*. 12:2534-45.

Villar-Tajadura, M.A., P.M. Coll, M. Madrid, J. Cansado, B. Santos, and P. Perez. 2008. Rga2 is a Rho2 GAP that regulates morphogenesis and cell integrity in S. pombe. *Mol Microbiol*. 70:867-81.

Voeltz, G.K., W.A. Prinz, Y. Shibata, J.M. Rist, and T.A. Rapoport. 2006. A class of membrane proteins shaping the tubular endoplasmic reticulum. *Cell*. 124:573-86.

Wachtler, V., S. Rajagopalan, and M.K. Balasubramanian. 2003. Sterol-rich plasma membrane domains in the fission yeast Schizosaccharomyces pombe. *J Cell Sci*. 116:867-874.

Walther, T.C., J.H. Brickner, P.S. Aguilar, S. Bernales, C. Pantoja, and P. Walter. 2006. Eisosomes mark static sites of endocytosis. *Nature*. 439:998-1003.

Wang, H., X. Tang, and M.K. Balasubramanian. 2003. Rho3p regulates cell separation by modulating exocyst function in Schizosaccharomyces pombe. *Genetics*. 164:1323-31.

Wang, Y., H.P. Xu, M. Riggs, L. Rodgers, and M. Wigler. 1991. byr2, a Schizosaccharomyces pombe gene encoding a protein kinase capable of partial suppression of the ras1 mutant phenotype. *Mol Cell Biol*. 11:3554-63.

Weber, T., B.V. Zemelman, J.A. McNew, B. Westermann, M. Gmachl, F. Parlati, T.H. Sollner, and J.E. Rothman. 1998. SNAREpins: minimal machinery for membrane fusion. *Cell*. 92:759-72.

Wedlich-Soldner, R., S. Altschuler, L. Wu, and R. Li. 2003. Spontaneous Cell Polarization Through Actomyosin-Based Delivery of the Cdc42 GTPase. *Science*. 299:1231-1235.

Wheatley, E., and K. Rittinger. 2005. Interactions between Cdc42 and the scaffold protein Scd2: requirement of SH3 domains for GTPase binding. *Biochem J*. 388:177-84.

Wiley, D.J., S. Marcus, G. D'urso, and F. Verde. 2003. Control of Cell Polarity in Fission Yeast by Association of Orb6p Kinase with the Highly Conserved Protein Methyltransferase Skb1p. *J. Biol. Chem.* 278:25256-25263.

Win, T., Y. Gachet, D. Mulvihill, K. May, and J. Hyams. 2001. Two type V myosins with non-overlapping functions in the fission yeast Schizosaccharomyces pombe: Myo52 is concerned with growth polarity and cytokinesis, Myo51 is a component of the cytokinetic actin ring. *J Cell Sci*. 114:69-79.

Wu, H., C. Turner, J. Gardner, B. Temple, and P. Brennwald. 2010. The Exo70 subunit of the exocyst is an effector for both Cdc42 and Rho3 function in polarized exocytosis. *Mol Biol Cell*. 21:430-42.

Yang, P., S. Kansra, R.A. Pimental, M. Gilbreth, and S. Marcus. 1998. Cloning and Characterization of shk2, a Gene Encoding a Novel p21-activated Protein Kinase from Fission Yeast. *J. Biol. Chem.* 273:18481-18489.

Yang, P., Y. Qyang, G. Bartholomeusz, X. Zhou, and S. Marcus. 2003. The Novel Rho GTPase-activating Protein Family Protein, Rga8, Provides a Potential Link between Cdc42/p21-activated Kinase and Rho Signaling Pathways in the Fission Yeast, Schizosaccharomyces pombe. *J. Biol. Chem.* 278:48821-48830.

Yang, W., J. Urano, and F. Tamanoi. 2000. Protein Farnesylation Is Critical for Maintaining Normal Cell Morphology and Canavanine Resistance in Schizosaccharomyces pombe. *J. Biol. Chem.* 275:429-438.

Zhang, D., A. Vjestica, and S. Oliferenko. 2010. The cortical ER network limits the permissive zone for actomyosin ring assembly. *Curr Biol*. 20:1029-34.

Zhang, X., K. Orlando, B. He, F. Xi, J. Zhang, A. Zajac, and W. Guo. 2008. Membrane association and functional regulation of Sec3 by phospholipids and Cdc42. *J Cell Biol*. 180:145-58.

Ziman, M., D. Preuss, J. Mulholland, J.M. O'Brien, D. Botstein, and D.I. Johnson. 1993. Subcellular localization of Cdc42p, a Saccharomyces cerevisiae GTP-binding protein involved in the control of cell polarity. *Mol Biol Cell*. 4:1307-16.

Zwilling, D., A. Cypionka, W.H. Pohl, D. Fasshauer, P.J. Walla, M.C. Wahl, and R. Jahn. 2007. Early endosomal SNAREs form a structurally conserved SNARE complex and fuse liposomes with multiple topologies. *EMBO J*. 26:9-18.